Olfactory neurogenesis during tissue maintenance and repair

Dissertation
for the award of the degree

"Doctor rerum naturalium"

of the Georg-August-Universität Göttingen

within the doctoral program *"Molecular Physiology of the Brain"*
of the Georg-August University School of Science (GAUSS)

submitted by

Katarina Dittrich

from Altdöbern,

Germany

Göttingen *2018*

Thesis Committee

Prof. Dr. Ivan Manzini

Department of Animal Physiology and Molecular Biomedicine

Justus-Liebig-University, Gießen

Prof. Dr. Thomas Dresbach

Department of Anatomy and Embryology

Georg-August-University, Göttingen

Dr. Kristine Henningfeld

Department of Developmental Biochemistry,

Georg-August-University, Göttingen

Members of the Examination Board

Referee: Prof. Dr. Ivan Manzini

Department of Animal Physiology and Biomedicine

Justus-Liebig-University, Gießen

2nd Referee: Prof. Dr. Thomas Dresbach

Department of Anatomy and Embryology

Georg-August-University, Göttingen

Further members of the Examination Board

Prof. Dr. Michael Hörner

Department of Cellular Neurobiology

Georg-August-University, Göttingen

Prof. Dr. Ralf Heinrich

Department of Molecular Neuropharmacology of Behavior

Georg-August-University, Göttingen

Ph.D. Camin Dean

Department of Trans-synaptic Signaling

Georg-August-University, Göttingen

Date of oral examination: May 31th, 2018

Affidavit

Herewith I declare, that I prepared the Dissertation
"Olfactory neurogenesis during tissue maintenance and repair"
on my own and with no other sources and aids than quoted.

_____ Gießen, March 29th 2018

Katarina Dittrich

Für André Dittrich

Table of content

Tables

List of Figures

Abbreviations

AA-Mix	amino acid mixture
2-MeSADP	2-methylthio-adenosine-5'-diphosphate
2-MeSATP	2-methylthio-adenosine-5'-triphosphate
AN	adult nose
AOB	accessory olfactory bulb
ATP	adenosine-5'-triphosphate
BC	basal cell
BCL	basal cell layer
Biocytin	ε-biotinoyl-L-lysine
BDNF	brain-derived neurotrophic factor
BMP	bone morphogenetic protein
cAMP	cyclic adenosine monophosphate
CNTF	ciliary neurotrophic factor
DAPI	4′,6-diamidin-2-phenylindol
DEPC	diethyl pyrocarbonate
Dp	dorsal-posterior part of the telencephalon
FGF	fibroblast growth factor
FGFα	fibroblast growth factor α
FPR	formyl peptide receptor
$G\alpha_i$	Gi alpha subunit
$G\alpha_0$	G0 alpha subunit
GCD	guanylyl cyclase receptor
GDNF	glial cell-derived neurotrophic factor
GG	Grueneberg ganglion
Hb	habenula
HT	hypothalamus
LB	larval bulb
LB2DAT	larval bulb 2 days after transection
LB1WAT	larval bulb 1 week after transection
LB7WAT	larval bulb 7 weeks after transection
LN	larval nose
LN2DAT	larval nose 2 days after transection

LN1WAT	larval nose one week after transection
LN7WAT	larval nose 7 weeks after transectionb
LN200AA	larval nose 200µM amino acid exposure for 5 hours
LN1000AA	larval nose 1000µM amino acid exposure for 5 hours
LPC	larval PC
LVNO	larval VNO
MC	middle cavity
MeBr	methyl bromide
MOE	main olfactory epithelium
MS-222	ethyl-3-aminobenzoate-methanesulfonate
NG	necklace glomeruli
NGS	normal goat serum
OB	olfactory bulb
OE	olfactory epithelium
OEC	olfactory ensheating cell
ON	olfactory nerve
OO	olfactory organ
OR	OR type olfactory receptor
ORN	olfactory receptor neuron
ORNL	olfactory receptor neuronal layer
PCA	principal component analysis
PGC	periglomerular cell
PI	propidium iodide
PBS	phosphate buffered saline
PBST	phosphate buffered saline with tween 20
PC	principal cavity
SC	supporting cell
SCL	supporting cell layer
SO	septal organ of Masera
TAAR	trace amine associated receptor
TE	telencephalon
TRPC2	transient receptor potential channel, subfamily 2, member 2
V1R	vomeronasal type-1 receptor
V2R	vomeronasal type-2 receptor
VNO	vomeronasal organ

VRN	vomeronasal receptor neuron
Vv	ventral nucleus of the ventral telencephalon
$ZnSO_4$	zinc sulfate

Abstract

During metamorphosis, the African clawed frog *Xenopus laevis* undergoes a fundamental transformation from a fully aquatic larva to a secondarily aquatic adult. This extensive habitat change requires major adaptations including alterations of the olfactory system. Larval *Xenopus laevis* has a subdivided olfactory organ consisting of two sensory epithelia lining the principal cavity (PC) and the vomeronasal organ (VNO). The main olfactory epithelium of the PC is specialized for sensing water-borne odors. During metamorphosis, this epithelium is remodeled into the adult "air nose". An additional third olfactory epithelium, the adult "water nose", forms in the newly developing middle cavity (MC). As a result of this rearrangement the postmetamorphotic adult frog has a tripartite olfactory organ consisting of MC, PC and the VNO. In the course of this thesis, I performed a stage by stage investigation of anatomical changes in the *Xenopus* olfactory organ and monitored apoptotic cell death and stem cell proliferation in all olfactory epithelia during metamorphosis. I observed a massive cell death in the sensory epithelium of the PC, suggesting that the majority of olfactory receptor neurons (ORNs) present in larvae is replaced during metamorphosis. The highest rate of stem cell proliferation in the PC and VNO was observed before the start of extensive apoptosis within these sensory epithelia. During the formation of the sensory epithelium lining the MC only few cells are sorted out. Supporting cells are relocated from the PC to the MC, whereas ORNs of this newly formed epithelium are developed *de novo*. In addition to the turnover of different cell types during metamorphosis, the olfactory epithelia of *Xenopus laevis* are able to recover after a substantial injury. I analyzed neuronal regeneration after mechanically or chemically induced injuries of the olfactory organ. I found that $ZnSO_4$ irrigation of the olfactory epithelia leads to massive cell death of olfactory receptor neurons and supporting cells of the PC within one day, followed by a rapid regeneration within five days. A mechanical lesion by bilateral transection of the olfactory nerves causes a massive cell death of ORNs within the first three days after treatment, followed by low number of apoptotic cells after seven days. This thorough investigation of morphological changes also sets the basis for analysis of molecular changes using RNA-sequencing.

In conclusion, the experiments conducted in the course of this thesis contribute to a deeper understanding of morphological changes of the olfactory organ during metamorphosis and

regeneration. The study forms the basis to further investigate the processes of neurogenesis during olfactory tissue maintenance and under regenerative conditions.

Zusammenfassung

Während der Metamorphose durchläuft der Krallenfrosch *Xenopus laevis* eine grundlegende Transformation von einer vollständig aquatischen Larve zu einem sekundär aquatischen Frosch. Diese umfangreiche Veränderung des Lebensraums erfordert große Anpassungen, einschließlich des Geruchssystems. Die *Xenopus laevis* Larve hat ein unterteiltes Riechorgan, das aus zwei sensorischen Epithelien besteht, die die Haupthöhle (PC) und das Vomeronasalorgan (VNO) auskleiden. Das olfaktorische Hauptepithel von der PC ist darauf spezialisiert, wasserlösliche Geruchsstoffe zu erkennen. Während der Metamorphose wird dieses Epithel in die adulte "Luftnase" umstrukturiert, während in der neu entstehenden mittleren Höhle (MC) ein drittes sensorisches Riechepithel, funktionell als adulte "Wassernase", gebildet wird. Nach der Metamorphose hat der Frosch ein in drei Teile untergliedertes Riechorgan bestehend aus der MC, der PC und dem VNO. Ich führte eine Stadien bezogene Untersuchung der anatomischer Veränderungen im Riechorgan von *Xenopus* durch und analysierte den apoptotischen Zelltod und die Zellproliferation in allen olfaktorischen Epithelien während der Metamorphose. Ich beobachtete ein massives Zellsterben im sensorischen Epithel der PC, was darauf hindeutet, dass die Mehrheit der olfaktorischen Rezeptorneurone der Larve während der Metamorphose ersetzt wird. Zusätzlich wurde die höchste Proliferationsrate vor Beginn der hohen Apoptoserate innerhalb der sensorischen Epithelien von der PC und dem VNO beobachtet. Meine Ergebnisse zeigen, dass während der Bildung des dritten sensorischen Epithels, das die MC auskleidet, nur wenige Zellen aussortiert werden. Während der Bildung der MC werden Stützzellen, jedoch keine olfaktorischen Rezeptorneurone, von der PC zur MC verlagert, was darauf hindeutet, dass alle olfaktorischen Rezeptorneurone dieses neu gebildeten Epithels *de novo* entwickelt werden. Neben dem physiologischen Zellumsatz während der Metamorphose kann sich das olfaktorische Epithel von *Xenopus laevis* nach einer starken Verletzung wieder regenerieren. Ich analysierte anatomische Veränderungen nach einer mechanischen oder chemischen Verletzung des Riechorgans. Ich fand heraus, dass eine chemische Reizung der Geruchsepithelien durch eine $ZnSO_4$-Behandlung innerhalb eines Tages zu einem massiven Zelltod von Geruchsrezeptor-Neuronen und Stützzellen der PC führt, gefolgt von einer schnellen Regeneration innerhalb von fünf Tagen. Eine mechanische Läsion, die durch eine

bilaterale Durchtrennung der Riechnerven verursacht wird, führt innerhalb der ersten drei Tage nach der Behandlung zu einem massiven Zelltod. Sieben Tage nach der eingeführten Läsion konnte nur eine geringe Anzahl von apoptotischen Zellen festgestellt werden. Diese umfassende Studie von morphologischen Veränderungen bildet die Grundlage für die Analyse von molekularen Veränderungen durch eine RNA-Sequenzierung.

Zusammenfassend tragen die hier durchgeführten Ergebnisse zu einem besseren Verständnis der morphologischen Veränderungen während der Metamorphose und unter regenerativen Prozessen bei. Diese Studie bildet daher die Grundlage, für das Verständnis der Neurogenese während der Aufrechterhaltung des olfaktorischen Gewebes und unter regenerativen Bedingungen.

Publication information

Parts of the results are published at the peer-reviewed journal " The Journal of Comparative Neurology".

Note that part of the Figures (Figure 12, Figure 13, Figure 14, Figure 15, Figure 16, Figure 18 and Figure 19) and table 2 used for my thesis are identical with Figures of the published manuscript. Some passages of 3.1; 3.2; 3.3; 3.4 and 4.1 are identical to parts of the manuscript.

<u>Publications:</u>

Dittrich Katarina, Kuttler Joshua, Hassenklöver Thomas and Manzini Ivan.
Metamorphic remodeling of the olfactory organ of the African clawed frog, *Xenopus laevis*. J Comp Neurol 524:986-98, 2016

Hawkins Sara Joy, Weiss Lukas, Offner Thomas, Dittrich Katarina, Hassenklöver Thomas and Manzini Ivan. 2017. Functional reintegration of sensory neurons and transitional dendritic reduction of mitral/tufted cells during injury-induced recovery of the larval *Xenopus* olfactory circuit. Front Cell Neurosci 11:380. doi: 10.3389/fncel.2017.00380

1. Introduction

1.1 Evolutionary background of olfaction

Olfaction is an ancient sense and it is essential for the survival of the individual animal and the species in general (Manzini and Korsching, 2011). Many species rely on olfaction in order to recognize and discriminate between a large variety of odors (for instance about 10.000 odors in humans; Mombaerts, 2004b). Most animals use olfactory information in order to asses food palatability and to initiate food intake (Rolls, 2005; Yeomans, 2006). Additionally, the sense of smell influences reproductive functions like sexual and maternal behaviors, social behaviors like recognition of conspecifics and predators, as well as emotional responses like fear and pleasure (Schulz and Tapp, 1973; Nimmermark, 2004; Takahashi *et al.*, 2005). In humans the importance of the sense of smell often becomes obvious only after its loss.

1.2 Organization of the vertebrate olfactory system

The olfactory system of vertebrates is a well suited model to study the lifelong turnover of neurons as well as neuronal recovery after an injury. This is due to the fact that the olfactory epithelium is capable of newly generating neurons throughout whole life of an individual animal (Murdoch and Roskams, 2007). The peripheral location of the olfactory organ makes it easy by accessible for diverse manipulations and therefore, renders it suitable to study regenerative processes after an injury. In order to study the regenerative capacity of the olfactory organ, it is of fundamental importance to know how the organ is structured and how its anatomy and morphology changes during development.

1.2.1 Organization of the mammalian olfactory system

The rodent olfactory organ consists of separated subsystems: the main olfactory system, the accessory olfactory system, the septal organ of Masera, the Grueneberg ganglion and the trigeminal system (see Figure1).
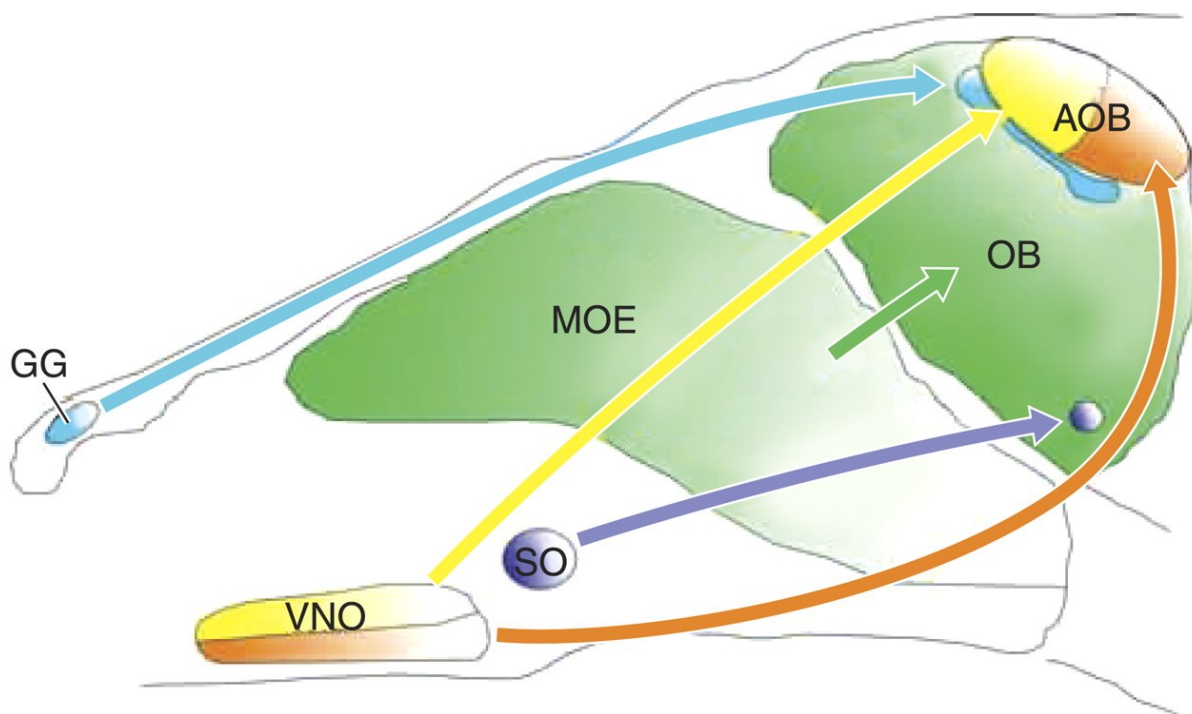
Figure 1. Projections of sensory neurons to the olfactory bulb

Olfactory receptor neurons of the main olfactory epithelium (MOE) send their axons to the main olfactory bulb (MOB) whereas vomeronasal receptor neurons of the vomeronasal organ (VNO) send their axons to the accessory olfactory bulb (AOB). Neurons of the septal organ of Masera (SO) project to the posterior ventromedial MOB and the Grueneberg ganglion project to necklace glomeruli (NG), which are located in the MOB (Tirindelli *et al.*, 2009).

Figure 1 was adapted from Tirindelli et al. 2009

The main olfactory system consists of the main olfactory epithelium and the main olfactory bulb. Additionally, there is the vomeronasal organ (VNO) and the accessory olfactory bulb (Figure 1) which are thought to be important for pheromone recognition and processing (Munger *et al.,* 2009; Liberles *et al.,* 2014). The olfactory epithelia contain three main cell types:

1. The proliferative basal cells are the stem cells of the olfactory epithelia. They are located in the basal part of the epithelium, close to the basal lamina. These cells replace dying olfactory receptor neurons (ORNs) and give rise to new supporting cells (Ronett and Moon, 2002). The basal cells therefore play an essential role in the maintenance of the sense of smell during lifelong turnover and acute injury.

2. The somata of the non-neuronal supporting cells are located in a tightly arranged columnar layer in the apical part of the epithelia. Supporting cells extend thin prolongations through the whole width of the sensory epithelium (Hassenklöver *et al.,* 2008), terminating on the basal lamina. Supporting cells have glia-like functions: they insulate ORNs (Breipohl *et al.,* 1974; Getchell and Getchell,1992), phagocyte dead cells (Suzuki *et al.,* 1996), detoxify noxious substances (Lazard *et al.,* 1991) and are also thought to take part in intraepithelial signaling pathway (Hegg and Lucero, 2006; Hassenklöver *et al.,* 2008).

3. ORNs have a bipolar morphology. They extend a single dendrite to the apical surface of the olfactory epithelium that terminates in a knob-like structure, which bears either cilia or microvilli (Ma, 2010; Munger *et al.,* 2009). These highly specialized structures are the site of olfactory transduction (Schild and Restrepo, 1998).
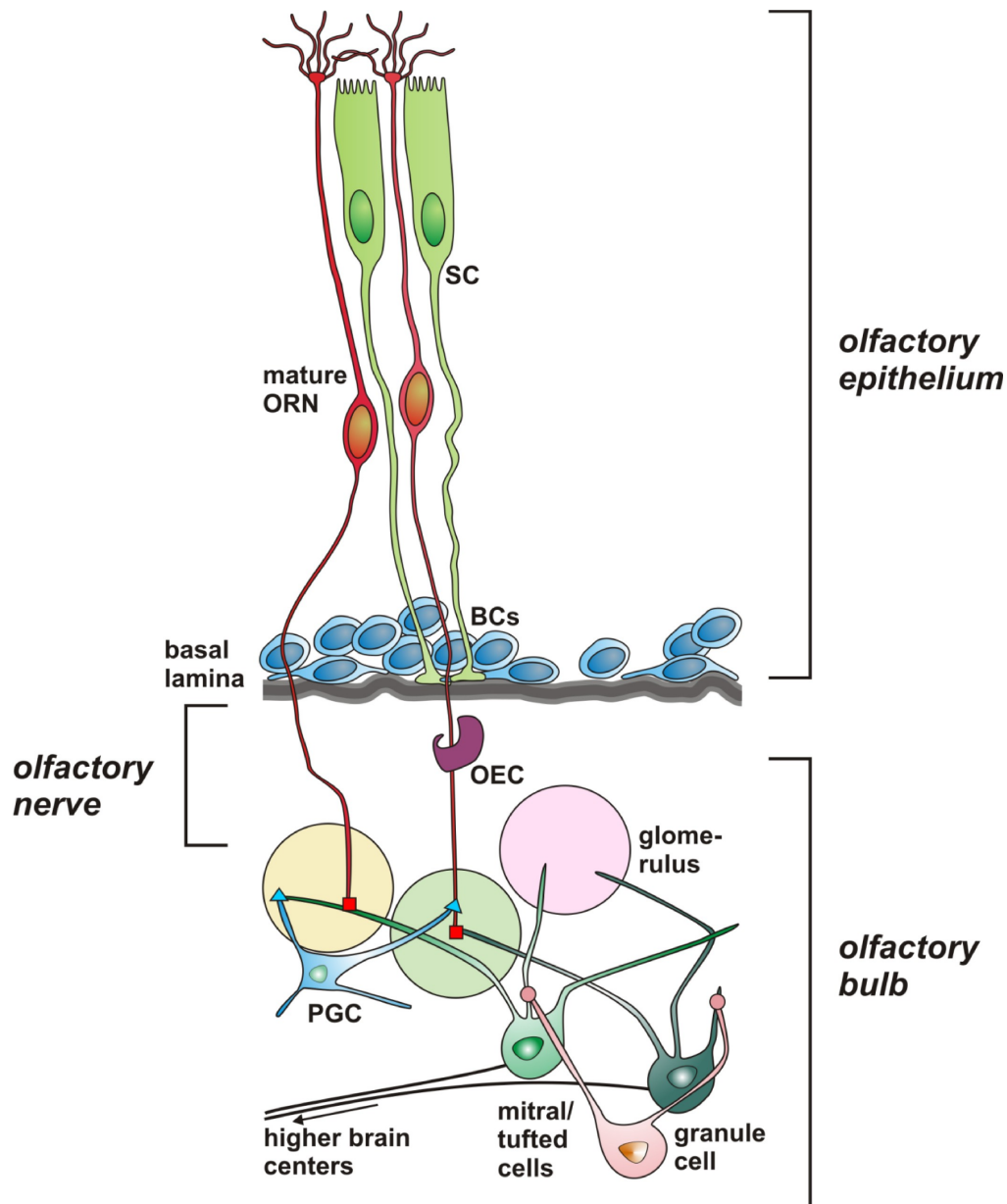
Figure 2. Schematic drawing of cellular components in the vertebrate olfactory system.

The olfactory sensory epithelium consists of three main cell types: basal cells (BCs), non-neuronal supporting cells (SCs) and olfactory receptor neurons (ORNs). Basal cells are the stem cells of the olfactory epithelium and therefore maintain the sense of smell by replacing dying ORNs. Additionally, they can also give rise to supporting cells as well as to olfactory ensheating cells (OEC). Non-neuronal supporting cells have a glia-like function. ORNs are important for the detection of odorants and send their axons to the olfactory bulb where they terminate in olfactory glomeruli. There they form synapses with second order neurons, the mitral/tufted cells and one type of interneurons, the periglomerular cells (PGC). The olfactory information is transmitted to higher brain centers via axonal projections of mitral/tufted cells. Granule cells, another type of interneurons form synapses with mitral/tufted cells.

Figure 2 was taken from Manzini, 2015

The main olfactory epithelium of mammals contain mostly ciliated ORNs that expressing olfactory receptors which transmit olfactory information with the canonical cAMP-mediated transduction pathway (Liberles *et al.,* 2014; Sansone *et al.,* 2014a). After an interaction of an odorant molecule with its matching receptor, the sensory information is transmitted along the axons of ORNs to the olfactory bulb where they terminate in roundish structures, the so-called olfactory glomeruli. Within the glomeruli the ORN axons form synapses with dendrites of second order neurons, the mitral/tufted cells (Komiyama and Luo, 2006, see Figure 2).

Olfactory receptors, the proteins that bind odorant molecules, are expressed in the membrane of cilia or microvilli (Schild and Restrepo, 1998).

	OR	V1R	V2R	TAAR	FPR	GC-D
Human	387(415)	5(115)	0(20)	6(3)	?	?
Chimpanzee	399(414)	0(116)	0(17)	3(6)	?	?
Mouse	1035(356)	191(117)	121(158)	3(6)	5(2)	✓
Chicken	82(476)	0(0)	0(0)	3(0)	?	?
Frog	410(478)	21(2)	249(448)	2(1)	?	?
Fish	102(35)	6(0)	44(8)	109(10)	?	?
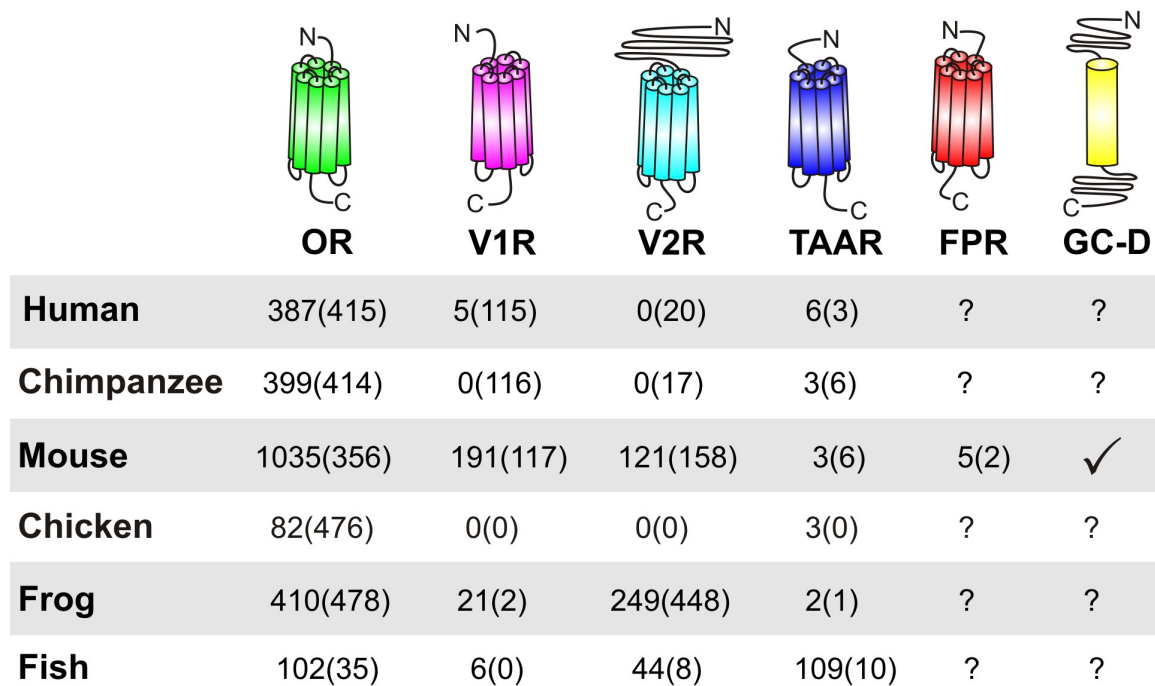
Figure 3. Nasal chemosensory receptor gene repertoires in different vertebrates.

Number of olfactory receptors: OR-type olfactory receptors (ORs), vomeronasal type-1 receptors (V1Rs), vomeronasal type-2 receptors (V2Rs), Trace amine associated receptors (TAARs), formyl peptide receptor (FPR) and membrane guanylyl cyclase receptors (GCD).

Numbers from Tirindelli et al. 2009; Rivière et al. Nature 2009; Shi and Zhang 2009

Mammalian olfactory receptors belong to a large family of seven-transmembrane G protein-coupled receptors (see Figure 3). Specific amino acid residues in the receptor binding pockets mediates recognition of odorants (Buck and Axel, 1991). After an interaction of the olfactory receptor with an appropriate odor molecule, the cAMP-dependent signal pathway is initiated

(Mombaerts, 1999). Typically, each ORN only expresses a single olfactory receptor gene (Malnic *et al.,* 1999; Mombaerts, 2004a) out of a large number of olfactory receptor genes. The axons of ORNs form the olfactory nerve and connect to second order neurons in the olfactory bulb. These synaptic contacts are organized in a dense network of neuropil called glomeruli (Firestein, 2001). In the main olfactory system of rodents, all ORNs expressing one particular olfactory receptor project their axon into a few glomeruli. A single glomerulus is considered as a functional unit. It is activated by a particular odor as it receives input from one type of olfactory receptors, exclusively (Adrian, 1950; Mombaerts *et al.,* 1996; Ressler *et al.,* 1994; Vassar *et al.,* 1994). The olfactory information processed in the glomeruli is transmitted along the axons of mitral/tufted cells, which project via the olfactory tract to the periform and entorhinal cortex (Haberly and Price, 1977; Scalia and Winans, 1975). Additionally, processing of odors is dependent on the input of two distinct populations of inhibitory interneurons named periglomerular and granule cells (Toida *et al.,* 2000).

The second olfactory subsystem, the accessory or vomeronasal olfactory system has been shown to play a role in the detection of pheromones (Munger *et al.,* 2009; Liberles *et al.,* 2014). These chemicals have a defined physiological or behavioral effect on individuals of the same species, including social, aggressive or reproductive behavior (Karlson and Luscher, 1959). The vomeronasal epithelium contains microvillar vomeronasal receptor neurons, non-neuronal supporting cells and basal stem cells. Microvillar vomeronasal receptor neurons express vomeronasal type receptors and project their axons to the accessory olfactory bulb (AOB), where they synapse with second order neurons within the glomeruli (Eisthen, 1992; Mombaerts *et al.,* 1996). The VNO has two subpopulations of microvillar ORNs. One population of microvillar ORNs express vomeronasal type-I receptors (V1Rs) and Gi alpha subunit ($G\alpha_i$), whereas the second subpopulation, vomeronasal type-2 receptors V2Rs and G0 alpha subunit ($G\alpha_0$). Both V1R- and V2R expressing sensory neurons have a phospholipase C- and diacylglycerol-mediated pathway that activated a cation channel crucial for signal transduction in the VNO of rodents (Liberles, 2014; Sansone *et al.,* 2014b).

In conclusion, an attribute of the mammalian olfaction is the organization of the sensory epithelia in several distinct olfactory organs. Each olfactory organ has a own characteristic pattern of olfactory receptor gene expression and function (Munger *et al.,* 2009).

1.2.2 Organization of the olfactory system in teleost fish

In contrast to the rodent olfactory system, the olfactory organ of fish contains only a single olfactory epithelium which has both cilliated and microvillar ORNs. Furthermore, fishes have a third type of ORNs, the so-called crypt cells. All three types of ORNs project to the olfactory bulb (Hamdani and Døving, 2007). ORNs express members of the main olfactory receptor gene families (olfactory type receptors (ORs); trace amine-associated receptors (TAARs) and vomeronasal type receptors(VRs)). All olfactory receptor families are expressed within a common olfactory sensory surface (Hamdani and Døving, 2007). TAARs are expressed by cilliated ORNs (Weth *et al.,* 1996; Hussain *et al.,* 2009) which signal via the canonical cAMP pathway (Hamdani and Døving, 2007; Sansone *et al.,* 2014a). Microvillar ORNs express members of vomeronasal receptors as well as transient receptor potential channels, subfamily 2, member 2 (TRPC2; Hansen *et al.,* 1998a; Sato *et al.,* 2005). In conclusion, in contrast to *Xenopus* and most other tetrapods, teleosts possess a single olfactory epithelium and a common olfactory bulb.
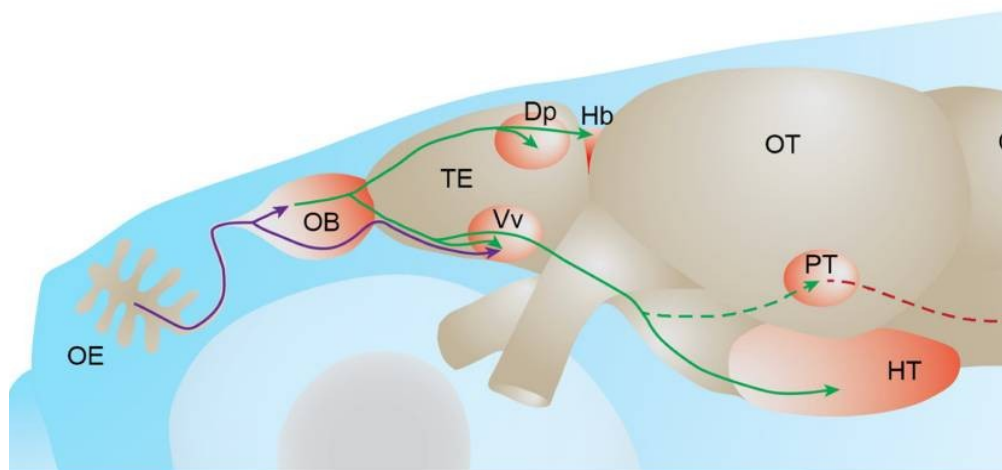
Figure 4. The olfactory system of fish.

Schematic drawing of the olfactory system of fish. The olfactory organ of fish consists of the single olfactory epithelium (OE) and one olfactory bulb (OB). Projections, in purple, indicated primary projections from the olfactory receptor neurons to the olfactory bulb or to the ventral nucleus of the ventral telencephalon (Vv). Secondary olfactory projections (green) project from the olfactory bulb to the telencephalon and diencephalon. (Kermen *et al.,* 2013). Dp: dorsal-posterior part of the telencephalon, Hb: habenula, HT: hypothalamus, TE: telencephalon

Figure 4. was adapted from Kermen et al., 2013

1.2.3 Organization of the olfactory system in the African clawed frog *Xenopus laevis*

Amphibians have a dual life style, with aquatic larvae and secondarily aquatic or terrestrial adults. The African clawed frog, *Xenopus laevis*, is a secondarily aquatic frog, that spends most of his adult life in the water. Larval *Xenopus laevis*, like many other amphibians possesses two distinct olfactory epithelia: a main olfactory epithelium lining the principal cavity (PC) and a VNO (Figure 5), which first appears in amphibians (Eisthen, 1992; Taniguchi *et al.,* 2011; Gonzalez *et al.,* 2010).
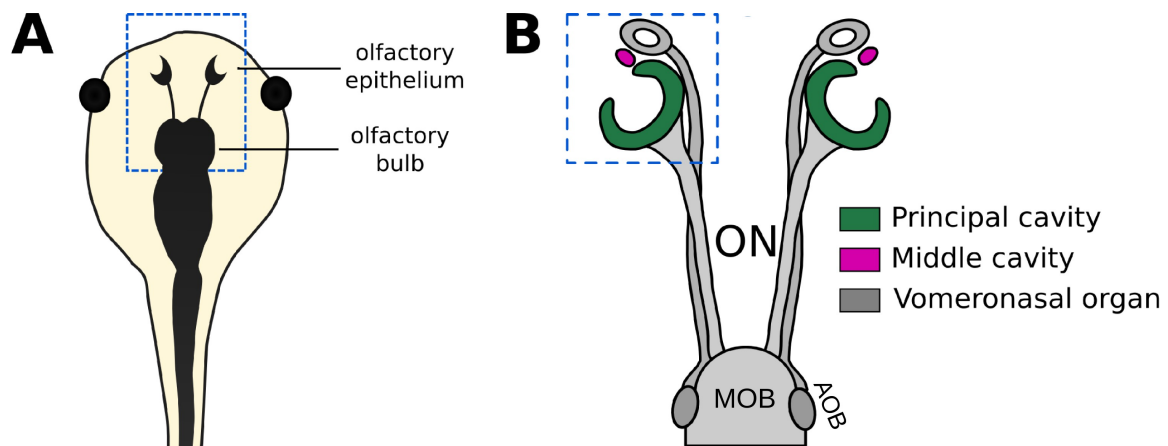
Figure 5. The olfactory organ of *Xenopus laevis.*

A. Scheme of larval *Xenopus laevis* at stage 51.The olfactory organ is located in the anterior part of the head. **B.** Close-up of olfactory sensory epithelia. A sensory olfactory epithelium is lined the principal cavity PC (green), anterior to the sensory epithelium of the vomeronasal organ (VNO, gray). The middle cavity (MC) begins to emerge at stage 51. The olfactory receptor neurons of the PC projects in the main olfactory bulb (MOB, light gray), whereas the vomeronasal receptor neurons projects to the accessory olfactory bulb (AOB, dark gray).

In both olfactory surfaces of *Xenopus laevis,* supporting cells has been described by the molecular marker cytokeratin type II (see Figure 2; Hassenklöver *et al.,* 2009, Dittrich *et al.,* 2014). Cytokeratin type II positive supporting cells are located in a tightly arranged columnar layer in the apical part of the sensory epithelium (Figure 6 C) and extend long prolongations through the entire epithelium. ORNs are bipolar neurons located in the intermediate layer (Figure 6 B) and project their axons to the main olfactory bulb. Individual ORNs project their axons into more than one glomerulus in larval *Xenopus laevis*. (Nezlin and Schild, 2005).

Characteristic markers that exclusively label stem cells or neuronal precursors located in the basal part of the main olfactory epithelium have not been identified in *Xenopus laevis* so far (Figure 6). It has been shown that neurogenesis takes place in the basal part of the olfactory epithelia and that supporting cells located in the apical portion might communicate with basal cells via a purinergic signaling pathway (Dittrich *et al.,* 2014; Hassenklöver *et al.,* 2009; Hassenklöver *et al.,* 2008).
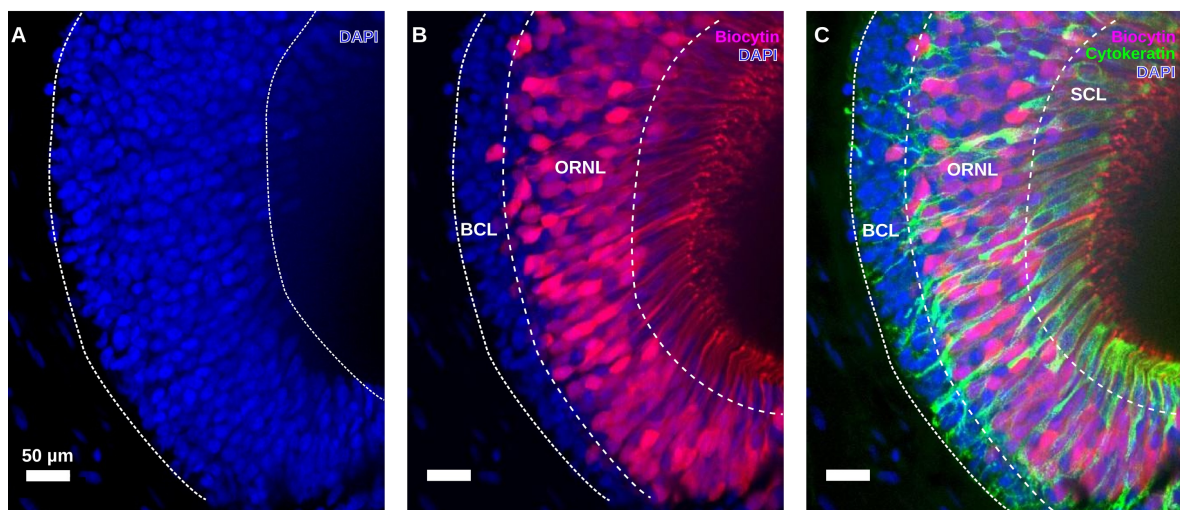
Figure 6. Cellular organization of the main olfactory epithelium of *Xenopus laevis.*

A. Slice of the main olfactory epithelium. Cell nuclei are stained with DAPI. **B**. Same slice with biocytin-streptavidin backfilled olfactory receptor neurons (ORNs) located in the intermediate olfactory receptor neuronal layer (ORNL). **C.** Immunoreactivity to cytokeratin type II antibody of the same slice. The cytokeratin-positive cells form a tightly packed columnar monolayer in the supporting cell layer (SCL) on the apical surface of the olfactory epithelium (OE) and send prolongations across the MOE to the basal cell layer (BCL).

Figure 6. was modified from Hassenklöver et al., 2009).

1.2.4 Reorganization of the olfactory organ of *Xenopus laevis* during metamorphosis

Most amphibians undergo metamorphosis. Their whole body changes to adapt from a fully aquatic lifestyle in larvae to a mainly terrestrial lifestyle in adults (for an overview, see Figure 7). The extensive changes of the habitat requires major adaptations of the body and also of the sensory systems. Anuran larvae possess gills and a tail. During metamorphosis, these structures degenerate via programmed cell death (apoptosis). Adult features, e.g. front and hind limbs, are formed *de novo* during metamorphosis. In addition, a reorganization and transformation of already existing structures and organ systems, like the skin, skeletal

muscles, the digestive tract or the central nervous system takes place. These changes make the animals suitable for their adult lifestyle All these processes are mainly regulated by one single key player, the thyroid hormone (reviewed by Furlow and Neff, 2006).
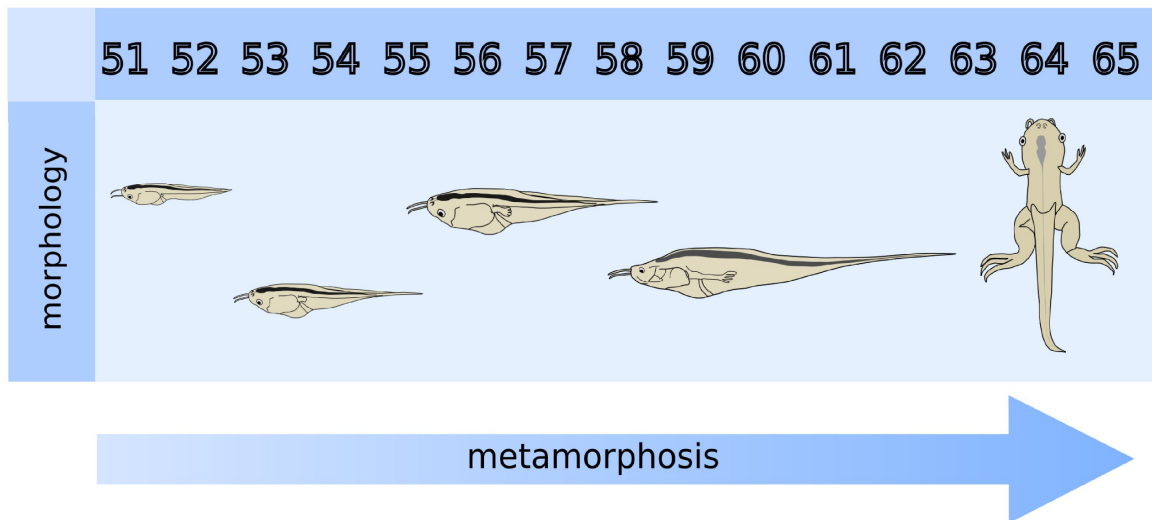
Figure 7. Stage dependent organ remodeling during *Xenopus laevis* metamorphosis.

Three types of organ transformations occur during metamorphosis: *de novo* development (e.g. limbs); total resorption (e.g. tail) and remodeling of existing tissues (e.g. intestine), see review Su *et al.,* 1999).

Pictures of tadpoles adapted from Nieuwkoop and Faber (1994).

In addition to the clearly visible changes (for an overview see Figure 7) more specific adaptations of all major sensory systems take place, including the olfactory system. In contrast to the larval animal, the adult frog needs to be able to smell both air-and waterborne odorants (Reiss and Eisthen, 2008). The ORNs residing in the larval PC epithelium exclusively detect water soluble odorants. The larval VNO is also filled with water but its function is still unclear. During premetamorphosis (at stage 51) a third cavity arises, the so called middle cavity (MC; Figure 5 B), lined by a third sensory epithelium (Hansen *et al.*, 1998b, Higgs and Burd, 2001). After metamorphosis (> stage 66) the frog has a subdivided olfactory organ consisting of three sensory cavities (PC, MC and VNO). The MC functions as an adult water nose and takes over the role of the larval PC. Meanwhile, the larval PC is reorganized and changes its function to an air nose. Pre–and postmetamorphotic stages of *Xenopus laevis* also differ in the composition of ORNs and supporting cell types in the

distinct epithelia. The larval PC is composed of both microvillar and ciliated receptor cells and ciliated and secretory supporting cells. In contrast, the postmetamorphotic PC only contains ciliated receptor neurons and secretory supporting cells. The VNO seems to have a stable set of cells throughout life it has solely microvillous sensory neurons and one type of supporting cells (ciliated supporting cells, Hansen *et al.,* 1998b; Hassenklöver *et al.,* 2009). The newly formed MC is composed of the same cell types as the larval PC (Hansen *et al.,* 1998b).

The repertoire of olfactory receptor genes in *Xenopus laevis* mirrors the amphibian transition from an aquatic to a terrestrial life style, containing olfactory receptor types as described for fish as well as mammals (Niimura and Nei, 2006). This state seen in amphibians is strengthened by studies showing that vomeronasal type-2 receptors are expressed in the single olfactory epithelium of fish, whereas it is restricted to the VNO in mammals. *Xenopus laevis* shows a mixed expression pattern with vomeronasal type-2 receptors present in both the sensory epithelium of the VNO and in the main olfactory epithelium of the larval PC (Syed *et al.,* 2013). In the olfactory system of aquatic vertebrates, in contrast to mammals, cAMP-independent signal transduction is far more common (Czesnik *et al.,* 2006; Ma and Michel, 1998; Manzini *et al.,* 2002a; Manzini *et al.,* 2002b). ORNs of larval *Xenopus laevis* have been shown to detect water-borne odorants i.e. amino acids (Vogler and Schild, 1999). The majority of ORNs seem to initiate a lateral odor transduction in a cAMP-independent way (Manzini and Schild, 2003; Manzini *et al.,* 2002a; Sansone *et al.,* 2014). Another subpopulation of ORNs, reacts to bile acids or amines and transduces odors via a cAMP pathway (Manzini and Schild, 2010). These subsets of neurons are equally distributed throughout the main olfactory epithelium and project to the main olfactory bulb as a medial processing stream (Gliem *et al.,* 2013). During metamorphosis the expression of some main olfactory receptor families is shifted from the larval PC to the emerging MC. It is already known that ciliated as well as microvillar ORNs express olfactory receptors in the larval PC and the MC (Hansen *et al.,* 1998b; Hagino-Yamagishi *et al.,* 2004; Date-Ito *et al.,* 2008; Gliem *et al.,* 2013; Syed *et al.,* 2013). Whereas the olfactory receptor genes of the adult PC are only expressed by ciliated ORNs. Later diverging V2Rs are solely expressed by microvillar vomeronasal receptor neurons in the epithelium of the larval and adult VNO (Hagino-Yamagishi *et al.,* 2004; Syed *et al.,* 2013).

In summary, the sensory epithelia lining larval PC and adult MC of *Xenopus laevis* are still highly similar to the single olfactory epithelium of fish. In contrast, the VNO of *Xenopus laevis* is highly comparable to the VNO of rodents. Taken together, the amphibian olfactory system shows many characteristics of both aquatic and terrestrial olfactory systems.

1.3 Neurogenesis and regenerative capacity of vertebrate olfactory epithelia

Adult neurogenesis, the generation of new neurons in the postembryonic nervous system is limited in mammals. Tissue regeneration is more common in lower vertebrates as fish and amphibia, where it provides distinct survival advantages. Two well characterized neurogenic regions in the postembryonic brain are the subventricular zone of the lateral ventricle and the subgranular zone of the hippocampal formation (Altman and Das, 1965; Doetsch *et al.*, 1999; Gage, 2000; Garcia *et al.*, 2004).

1.3.1 Neurogenesis in the mammalian main olfactory epithelium

An exception to the generally limited capacity of the post-embryonic nervous system to regenerate occurs in the olfactory epithelium, which retains a lifelong ability to regenerate neurons (Murdoch and Roskams, 2007). Mammalian ORNs have a limited life span of 30-90 days and are continuously replaced by the division of neuronal stem cells located in the olfactory epithelium. This makes the olfactory system an interesting anatomical area to study lifelong turnover of neuronal structures (Graziadei and Graziadei, 1979; Mackay-Sim and Kittel, 1991). Neurogenesis includes the generation and the differentiation of novel neurons. These processes are coordinated by inter-and intracellular pathways that initiate the proliferation of neuronal precursor cells and the replacement of ORNs. Adult neurogenesis of cells in the olfactory epithelium is coordinated within the basal layer. This layer contains subpopulations of stem cells as well as diverse progenitors of ORNs, which generate new ORNs throughout the lifetime of the animal (Murdoch and Roskams, 2007). In the mammalian olfactory epithelium two different types of neuronal stem cells have been described, the horizonal and the globose basal cells (Calof *et al.,* 2002). These two cell populations differ in their cell shape as well as in their biological function. Horizontal basal cells have a flattened shape (Holbrook *et al.,* 1995), whereas globose basal cells have a

roundish cell structure. Horizontal basal cells are multipotent stem cells and have the ability to regenerate neuronal as well as non-neuronal cells (Leung *et al.,* 2007). They are in direct contact with the basal lamina (Holbrook *et al.,* 1995) and interact with the globose basal cells, which are the major proliferating stem cell population in the olfactory epithelium (Caggiano *et al.,* 1994; Chen *et al.,* 2004). Globose basal cells generate both neuronal and supporting cells (Huard *et al.,* 1998) during the whole life of an animal. Horizontal basal cells stay quiescent during normal tissue maintenance and get activated only after an extensive injury of the epithelium (Leung *et al.,* 2007). It has been shown that horizontal basal cells are also able give rise to globose basal cells. Through a basal to apical migration of differentiating cells, mature ORNs are finally located in a medial layer of the epithelium (Iwai *et al.,* 2008).

Despite the considerable progress that has been made over the last years, the knowledge about how the lifelong turnover of ORNs is regulated there are still unresolved questions. On the one hand, Hassenklöver *et al.,* 2009 showed that nucleotides and their receptors are involved in the regulation of olfactory epithelium progenitors. It was shown that nucleotide application to the main olfactory epithelium triggers wave-like $[Ca^{2+}]$ increases in supporting cells in the apical part of the main olfactory epithelium in mouse and *Xenopus laevis*. This signal is conducted towards the basal zone of the main olfactory epithelium, the part where proliferative and basal stem cells are located (Hassenklöver *et al.,* 2008; Hegg *et al.,* 2009). The described signal transduction pathway could enable an information transfer from the apical side of the olfactory epithelium to the basal zone.

On the other hand proliferation and differentiation of olfactory epithelium progenitors is regulated by the balance of positive and negative regulatory factors. These are released from different cell types and act in a feedback regulation with each other (Gokoffski *et al.,* 2010). Some of these identified regulatory factors are the brain-derived neurotrophic factor (BDNF), the glial cell-derived neurotrophic factor (GDNF) and the ciliary neurtrophic factor (CNTF, Buckland *et al.,* 1998). Additional factors are the bone morphogenetic proteins (BMP), fibroblast growth factors (FGF) and the transforming growth factor (FGFα, Murdoch and Roskams, 2007).These factors most probably represent only a small fraction of all involved regulatory factors.

It is still unknown whether both pathways interact and how the progenitor cells in the basal zone are instructed to produce new neurons. Additionally, it remains unclear how stem cells stop cell renewal to prevent an overproduction of new cells.

1.3.2 Regenerative capacity of mammalian olfactory epithelia

In addition to its lifelong turnover, the olfactory epithelium has a high regenerative capacity after injury. Lost cells can be continuously replaced from the stem cell pool within the olfactory epithelium in days to weeks (Schwob 2002, Mackay-Sim, 2010). The olfactory epithelium is constantly in direct contact with the environment. It can be exposed to pathogens as well as toxic substances which can cause major harm or even death. Additionally, also an over-stimulation with odorants could lead to the death of ORNs due to hyperexcitation.

It is possible to mimic these conditions by introduced epithelial damage. Lesioning of the olfactory nerve (axotomy) specifically leads to a loss of ORNs (Schwob, 2002). Alternatively, a treatment with harmful chemicals causes degeneration of all epithelial cell types. For instance, methyl bromide gas (MeBr; Schwob and Youngentob, 1992; Schwob *et al.*, 1999) is often used for intranasal irrigation in rodents. Methimazole, normally used as a drug in the therapy against hyperthyroidism, is known to induce hyposmia in humans (Bergström *et al.*, 2003; Bergman and Brittebo, 1999). In zebrafish Triton X-100 or zinc sulfate ($ZnSO_4$) irrigation lead to tissue-wide degeneration (Iqbal and Byrd-Jacobs, 2010). Previous studies show that early diverging vertebrates like fish and amphibia possess the ability to regenerate entire brain parts, which makes them especially interesting for research concerning regeneration (see review Endo *et al.*, 2007).

Rodriguez *et al.*, 2015 reported that odorants induced a fast and reversible decrease in the transcription of genes to activated olfactory receptors in healthy mice

1.3.3 Regenerative capacity of olfactory epithelia of *Xenopus laevis*

Most tissues of *Xenopus laevis* especially in larvae, show a high regenerative capacity (Dent, 1962; Endo *et al.,* 2007; Zardoya and Meyer, 2001). For instance larval *Xenopus laevis* showed a fast tissue recovery after transection of the spinal cord. Postmetamorphotic animals are no longer able to regenerate after treatment (Gibbs *et al.*, 2011).

The olfactory system of *Xenopus leavis* is well suited to study neurogenesis, cellular reorganization during metamorphosis and regeneration after injury. Besides the normal turnover of ORNs during life (see 1.3.1), evidences shown in Hansen *et al.,* 1998b suggest that most of the sensory neurons and supporting cells of the developing PC die during metamorphosis. No quantitative analysis of these cells has been conducted so far.

One already existing model to study the loss of the neuronal populations and therefore regenerative processes happening after lesion is bilateral transection of the olfactory nerves (Cervino *et al.,* 2017; Hawkins *et al.,* 2017). Besides mechanical lesions it is also possible to induce apoptosis within the olfactory epithelium by using diverse chemicals or an odorant overexposure, as described in 1.3.1 Frontera *et al.,* 2015 and Frontera *et al.,* 2016 found that $ZnSO_4$ treatment introduces a severe injury (see 1.3.2) to the main olfactory epithelium of larval *Xenopus laevis.*

It is already known that ATP and other nucleotides play a role in neurogenesis in the olfactory epithelium. As described before there is evidence that nucleotides and their associated receptors are thought to be essential for the regulation of stem cell proliferation in the main olfactory epithelium of larval *Xenopus laevis* (see 1.3.1; Hassenklöver *et al.,* 2009). Additionally, a study of Frontera *et al.,* 2015 showed that the growth factor BDNF is upregulated in basal cells after $ZnSO_4$ treatment. Under healthy conditions only a few supporting and basal cells express BDNF, suggesting that BDNF plays a role in maintaining the function of the olfactory epithelium and in its regeneration after damage (Frontera *et al.,* 2015). However, knowledge about the signal cascades which are activated after an injury of the olfactory epithelium is still very restricted. Also not much is known about the accuracy of olfactory receptor gene expression patterns as well the total recovery of the functionality of cells of *Xenopus laevis* sensory olfactory epithelia after the described injury.

1.4 Aim of the thesis

Little is known about the exact remodeling of the sensory epithelia of the olfactory organ during metamorphosis and after an injury in *Xenopus laevis*. The present thesis shows for the first time a stage by stage survey of anatomical changes of the olfactory organ in premetamorphotic, prometamorphotic, *metamorphotic* and postmetamorphotic developmental stages. In the second part of my thesis I investigated how the olfactory sensory system is able to regenerate after the loss of specific populations of cells as well as after a tissue – wide degeneration. For this I induced degeneration of the olfactory epithelia by with Triton X-100 or $ZnSO_4$ and compared it to samples of healthy control tissue. Furthermore, I introduced a mechanical lesion of the olfactory epithelia by transecting the olfactory nerve and compared it to the degenerated tissue after chemical lesions as well as to healthy control tissue.

My thesis is aimed to answering the following questions:

1. Which morphological changes occur in the olfactory organ during metamorphosis?

2. Does the adult water nose (MC) develop *de novo* or is the adult water nose a split-off of the larval water nose (PC)?

3. Are there differences in the quantity of apoptotic and proliferative cells in the sensory olfactory epithelia lining the sensory cavities (PC, MC, VNO)? Are there specific peaks of apoptosis and proliferation of cells during metamorphotic remodeling of the sensory olfactory epithelia?

4. Which morphological changes occur after an induced mechanical or chemical lesion of the olfactory organ?

5. Which molecular changes occur during metamorphosis or after a mechanical lesion?

2. Materials and Methods

2.1 *Xenopus laevis* as a model animal

The African clawed frog *Xenopus laevis* belongs to the amphibian order "Anura". This species is common in sub-Saharan Africa and lives in the muddy ground of warm and stagnant lakes and ponds. *Xenopus laevis* is mostly nocturnal. The adult frogs (see Figure 8 A) are scavengers, whereas the larvae (see Figure 8 B) feed almost exclusively on algae. To locate food sources this species relies mostly on its sense of smell (Avila and Frye, 1978; Nieuwkoop and Faber, 1994). *Xenopus laevis* is an established animal model in developmental biology and animal physiology. All larvae, metamorphotic and postmetamorphotic *Xenopus laevis* used to this work were bred in the animal facility of the Institute of Neurophysiology and Cellular biophysics, Göttingen. Breeding pairs were housed together overnight in 50 liter water tanks at a temperature of 19°C–22°C. On the following day fertilized eggs were collected and kept in separate aquaria at a temperature of 20°C. Adult frogs were fed with Ponstick food (Tetra Pond, Melle, Germany) while tadpoles were fed with algae (Dose Aquaristik, Bonn, Germany). metamorphotic animals of stage 59-65 were fed with both algae and Ponstick food. Experiments were performed on selected premetamorphotic (stage 49-54), prometamorphotic (stage 55-58), metamorphotic (stage 59-65) and postmetamorphotic animals (stage $\geq$ 66). The stage of the animals was determined according to Nieuwkoop and Faber (Nieuwkoop and Faber, 1994; see Figure 7). All procedures for animal handling were carried out according to the guidelines of the Göttingen University Committee for Ethics in Animal Experimentation.
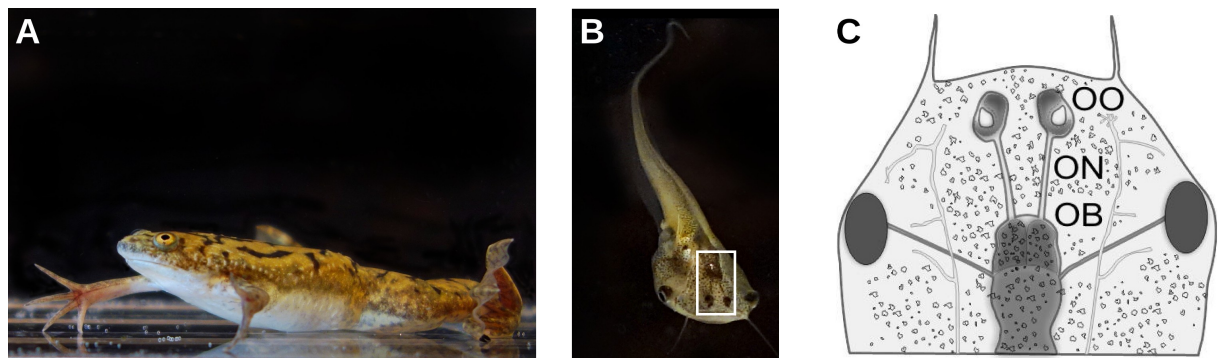
Figure 8. The experimental animal *Xenopus laevis.*

A. Adult *Xenopus laevis.* **B.** Larval *Xenopus laevis* (olfactory system marked by a white rectangle). **C.** Scheme of the larval head. The olfactory organ (OO) is located in the anterior part of the head. The axons of olfactory receptor neurons travel along the olfactory nerve (ON) and terminate in the olfactory bulb (OB), located in the anterior part of the brain.

Pictures and the scheme were kindly provided by I. Manzini and T. Hassenklöver.

2.2 Tissue preparation

For tissue preparation individual *Xenopus laevis* of the appropriate stages (stage 49-66) were anesthetized in 0.02% MS-222 (ethyl 3-aminobenzoate methanesulfonate; Sigma, Steinheim, Germany) until complete immobility. The animals were killed by a transection of the spinal cord and tissue blocks containing the olfactory epithelia, olfactory nerves and the olfactory bulb were excised (for orientation, see Figure 8 B). The prepared blocks were used in the following described experiments.

2.2.1. Biocytin labeling of olfactory receptor neurons

To perform a stage by stage investigation of anatomical changes of the olfactory organ from premetamorphotic stages until adult frogs, axons of olfactory receptor neurons (ORNs) were backtraced with biocytin. *Xenopus laevis* at different developmental stages (49-65) were anesthetized in 0.02% MS-222. To backfill ORNs, olfactory nerves of *Xenopus laevis* were transected and biocytin (ε-biotinoyl-L-lysine, Molecular Probes) crystals were inserted in the lesion. The lesion was closed with tissue adhesive (Hystoacryl L, Braun, Tuttlingen, Germany). After one hour the animals were killed and a tissue block (see above) was excised. The tissue block was fixed in 4% formaldehyde, washed in PBS, embedded in 5% low

melting point agarose (Sigma) and sectioned on a vibratome (VT 1200S; Leica, Bensheim, Germany) at 75-85 µm Sections were washed in PBS containing 0.2% Triton X-100 (PBST) and non-specific binding was blocked with 2% normal goat serum (NGS; ICN, Aurora, Ohio, USA) in PBST for one hour. Alexa 488 conjugated streptavidin was applied at a concentration of 5 µg/ml in PBST overnight at 4°C to visualize the backfilled ORNs. Sections were washed in PBS and then transferred to slides and mounted in mounting medium (Dako, Hamburg, Germany). Images of the olfactory organ were acquired using a laser-scanning confocal microscope (LSM 510/Axiovert 100M; Zeiss, Jena, Germany). For the 3D models of the olfactory organ, animals of stage 50-61 were anesthetized as described above and a microRuby crystals were put into the previously lesioned olfactory nerve. The wound was closed with tissue adhesive. After one hour the animals were killed as described above and a tissue block (see above) was removed. The tissue block was fixed in an imaging chamber, which was placed on the stage of a multiphoton microscope (A1R-MP; Nikon, Düsseldorf, Germany) and images were acquired as described in 2.6.2.

2.2.2 Survey of the amount of cell proliferation and cell death

A phospho-histone H3 staining was used to identify mitotic cells. Tissue blocks (see above) were cut out, fixed, sectioned and processed as described for sections in the biocytin preparation (see 2.2.1). The sections were incubated overnight with the primary antibody at a concentration of 1:400 in 2% NGS/PBST (p-H3; Ser10; polyclonal derived from rabbit; Upstate, Lake Placid, USA). The primary antibody was washed off with PBS and afterwards Alexa 488 or Alexa 546 conjugated goat anti rabbit secondary antibody was added at a final concentration of 1:250 in 1% NGS/PBS. Sections were then washed in PBS and transferred to slides and mounted in mounting medium (Dako, Hamburg, Germany). Images were acquired as described in 2.2.1.

To visualize axons and somata of apoptotic cells in the olfactory nerves and the sensory olfactory epithelia of *Xenopus* olfactory organ an immunostaining using an anti-active caspase 3 antibody was performed. Animals were killed and a tissue block was excised. Tissue blocks were then fixed, sectioned and processed as described for biocytin preparations (2.2.1). The primary antibody against the active form of caspase 3 was applied at a concentration of 1:400 in 2% NGS/PBST overnight (ab13847, derived from rabbit using a synthetic peptide

corresponding to human active + procaspase 3 amino acid 150-250 conjugated to keyhole limpet hemocyanin (KLH), RRID: AB-443014). The primary antibody was washed off with PBS and afterwards Alexa 488 or Alexa 546 conjugated goat anti rabbit secondary antibody was applied at a final concentration of 1:250 in 1% NGS/PBS. Sections were washed in PBS and then transferred to slides and mounted in mounting medium (Dako, Hamburg, Germany). Images were acquired as described in 2.2.1.

2.2.3 Cytokeratin type II labeling of supporting cells

For the examination of supporting cell organization in *Xenopus laevis*, a cytokeratin type II staining was carried out. Staining of Cytokeratin type II was found to specifically label supporting cells of *Xenopus laevis* (Hassenklöver *et al.* 2008). Animals were anesthetized and a tissue block was cut out as described above. Anti-cytokeratin type II antibody (1h5, monoclonal, derived from mouse, Developmental Studies Hybridoma Bank, University of Iowa, Department of Biological Sciences, Iowa City, USA) was applied at a final concentration of 1:1000 in 2% NGS/PBST overnight. The primary antibody was washed off with PBS and Alexa 488 or Alexa 546 conjugated goat anti mouse secondary antibody was applied at a final concentration of 1:250 in 1% NGS/PBS. Sections were washed in PBS and then transferred to slides and mounted in mounting medium (Dako, Hamburg, Germany). Images were acquired as described in 2.2.1.

2.2.4 Monitoring the formation of a new sensory olfactory epithelium

Xenopus laevis tadpoles of stage 51 (Nieuwkoop and Faber, 1994) were anesthetized with 0.02% MS-222 until complete immobility. Afterwards the nasal cavities were dried with tissue paper and small crystals of fluophore coupled dextran (Alexa 594 dextran 10 kDa, 3 mM, Molecular probes) were placed in both nasal cavities. Dye loading of ORNs and supporting cells was performed on electroporation. Two thin platinum electrodes were carefully introduced into the nasal cavities. The electrodes were connected to a voltage pulse generator (ELP–01D, npi electronics) and twelve pulses (20–25 V, 25 ms duration at 2 Hz) were applied. The electroporation procedure did not exceed five minutes. Animals were transferred into a beaker with fresh tap water for recovery. For the period of the whole experiment (several weeks) animals were individually kept in beakers. One or two days following the electroporation, tadpoles were anesthetized and the PC was investigated *in vivo*

via two-photon microscopy (A1R-MP; Nikon, Düsseldorf; Germany) to validate successful electroporation. The anesthetized tadpole was placed in an imaging chamber, and an image stack of the whole intact olfactory organ was acquired from the dorsal side (also see Hassenklöver and Manzini, 2014). Only larvae that showed dextran staining in the entire PC were used for the survey of cellular relocations. Animals that showed incomplete dextran staining were excluded from the experiments. Electroporated animals were kept under normal conditions until they reached appropriate prometamorphotic and young postmetamorphotic stages. Subsequently, these animals were anesthetized in 0.02% MS-222, and the sensory neurons of their olfactory organs were back-filled with biocytin and processed (see 2.2.1). The brightness and contrast of image stacks were adjusted with the image processing software ImageJ (Schindelin *et al.,* 2012).

2.3 Acute section preparation for calcium imaging

A section containing the olfactory epithelia and the olfactory bulb was obtained as described by Manzini *et al.,* 2002b. The tissue block was glued onto the stage of a vibratome (VT 1200S, Leica, Bensheim, Germany) and the PC and the vomeronasal epithelium was cut horizontally into 140 µm thick sections. The sections were then transferred to a recording chamber containing frog Ringer solution (see 2.8.1). The tissue sections were incubated in a Fluo-4/AM mix for 35 minutes in separate recording chambers at room temperature. For calcium imaging one of the tissue sections was placed under a grid to prevent it from moving. The recording chamber was placed on the stage of an inverted microscope, with an attached confocal laser scanning unit (LSM 510/Axiovert 100 M; Zeiss, Jena, Germany). A 488 nm wavelength Argon laser was used for the excitation. A series of 60 images was acquired by recording at a frequency of 1 Hz.

The recording chamber was perfused with frog Ringer solution by gravity feed from a storage syringe through a funnel drug applicator (Figure 9). The tip of the applicator was placed directly in front of the lateral part of the olfactory epithelium. A constant flow of bath solution was created between the outlet funnel and a suction syringe in proximity to the epithelium. This application system ensured an almost complete lack of mechanical stimulation of cells and allowed repetitive stimulation of the exposed tissue.
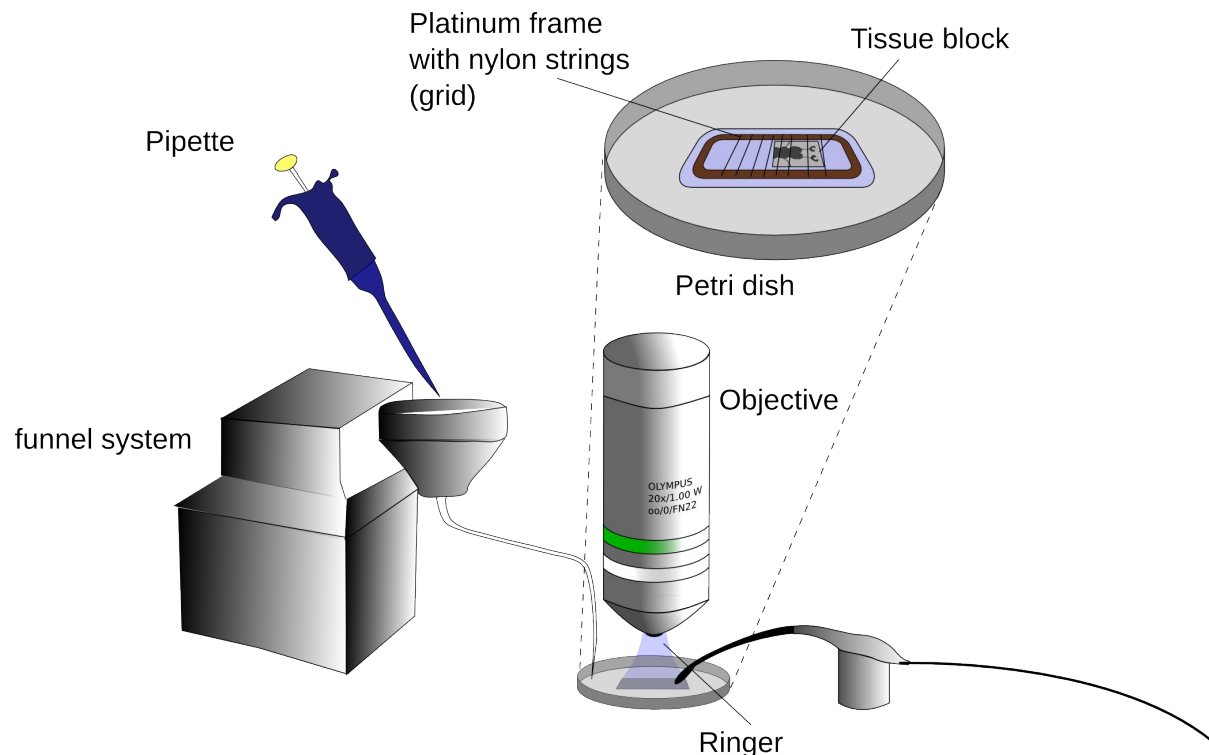
Figure 9. Schematic depiction of the funnel application system used for calcium imaging.

The gravity feed funnel application system was used for the application of frog ringer solution, nucleotides, amino acids and high potassium solution. Stimuli are applied by a pipette and directed to the tissue block via a syringe. A constant flow is ensured by a syringe that constantly removes the frog Ringer solution.

The schematic drawing was kindly provided by Lukas Weiss

2.4 Stimulation of the sensory olfactory epithelium

Nucleotides and amino acids were dissolved in frog ringer solution and used at a final concentration of 100 µM in all conducted experiments. Solutions were prepared immediately before the experiment and pipetted into the gravity feed funnel system (see Figure 9) without stopping the flow of frog ringer solution (Manzini and Schild 2004; Sansone *et al.*, 2014a). In each recording, a stimulus was applied 10 seconds after the begining of the recording (Stimulus applications consisted of 900 µl of either amino acid mixture, high potassium solution or nucleotide mixtures). The olfactory epithelium of *Xenopus laevis* tadpoles contains different cells (basal cells, ORNs and supporting cells (see Hassenklöver *et al.*, 2008)). Basal and supporting cells show a response to diverse purines, whereas basal cells react specifically to 2-MeSATP and 2-MeSADP (Hassenklöver *et al.*, 2009). The lateral part of the olfactory

epithelium contains a group of olfactory receptor neurons that react to amino acids (Manzini and Schild, 2004). To test the viability of ORNs, a high potassium solution was applied.

2.5 Techniques to introduce nasal injury

2.5.1 Olfactory Nerve transection

The olfactory nerves of *Xenopus laevis* (stage 49-51) were transected to specifically damage especially the neuronal population of the olfactory organ. Larval *Xenopus laevis* were anesthetized in 0.02% MS-222 and the olfactory nerves were transected with a fine scissor without damaging surrounding tissue. The wound was closed with tissue adhesive (Histoacryl L; Braun). After transection, tadpoles were transferred to a beaker filled with tap water and kept there for 24, 48, 72 and 168 hours and for 49 days. For subsequent experiments the animals were paralyzed in ice water and killed by cutting the spinal cord. A tissue block containing the whole olfactory organ was excised and several immunostainings (2.2.2 and 2.2.3) were performed. Tissue containing the whole larval nose 48 hours, 168 hours and 49 days after transection was removed and processed for RNA sequencing (see 2.7).

2.5.2 Triton X-100 treatment

Xenopus laevis larvae were anesthetized with 0.02% MS-222 and placed on a dissection plate. A droplet of Triton X-100 (0.7% dissolved in water; Sigma, Steinheim, Germany) was placed into the nasal cavity and the nose was immediately dried with tissue paper. The whole process was repeated three times. Afterwards, the animals were returned to water tanks and killed after 24, 48, 72 and 168 hours to observe changes in the epithelia by performing immunostaining protocols (2.2.2 and 2.2.3).

2.5.3 $ZnSO_4$ irrigation

Larval *Xenopus leavis* were kept in tap water containing $ZnSO_4$ (Sigma, Steinheim, Germany) at a concentration of 25 mg/l for 24 hours. After that, animals were returned back to tanks filled with tap water for recovery. A control group was exposed to tap water without $ZnSO_4$. After 24, 48 and 96 hours of recovery the animals were anesthetized in 0.02 % MS-222 until total immobility. They were then killed by transection of the spinal cord.

A tissue block containing the whole olfactory organ was excised and several immunostainings (2.2.1, 2.2.2 and 2.2.3) were performed.

2.5.4 Exposure to amino acid mixtures

Groups of *Xenopus* larvae were kept in beakers filled with tap water containing two different concentrations of amino acid mixtures (AA-Mix, see 2.8.1) for five hours. One beaker was filled with a 200 µM amino acid mixture, the other beaker contained amino acids of a concentration of 1000 µM.

Afterwards, the animals were anesthetized in 0.02 % MS-222 and killed by a transection of the spinal cord. Tissue containing the whole larval nose was removed and prepared for RNA sequencing (see 2.7).

2.6 Image processing

2.6.1 Image acquisition and processing

Image stacks of immunostainings were recorded with a laser scanning confocal microscope (LSM/Axiovert 100M; Zeiss, Jena, Germany). Samples of regenerated tissue of the olfactory epithelia and the olfactory bulb were recorded with an upright multiphoton microscope (A1R-MP; Nikon, Düsseldorf; Germany) and three-dimensional z-stacks of whole mount preparations of the olfactory bulb and regenerating axons of the olfactory nerves were acquired. All further processing was done with the image processing software ImageJ (Schindelin *et al.,* 2012). Brightness and contrast were adjusted in some images and maximal intensity projections were calculated and used for some pictures as indicated.

2.6.2 3D reconstruction of the olfactory organ at different developmental stages

Processing of the conducted image stacks of the micro–Ruby backfilled *Xenopus laevis* tissues (see above) allowed the creation of 3D reconstructions of the olfactory organ. Tissue blocks were fixed in an imaging chamber, mounted on the stage of a multiphoton microscope (A1R-MP; Nikon, Düsseldorf; Germany) and three dimensional stacks of images of the olfactory organ were obtained. The acquired image stacks were processed using the image processing software ImageJ (Schindelin *et al.,* 2012).

2.6.3 Cell counting

Active caspase 3 positive axons in the ON were manually counted in ImageJ (Schindelin *et al.*, 2012). Maximum stacks of sections that included the whole diameter of an intact ON were used for quantitative counting of the total number of stained axons. Active caspase-3-positive and phospho-histone H3 positive cell somata were manually counted in neuromantic software (V1.6.3; http://www.reading.ac.uk/neuromantic). It was developed developed by Darren Myatt (Myatt *et al.,* 2012). Image stacks of the olfactory cavities (75-85 µm thickness) were acquired at 1 µm intervals between the different planes. Multiple sections of each cavity (PC, MC and VNO) were used for the quantitative analysis. The average diameter of counted cell profiles was 9 µm. Labeled structures smaller than 4 µm in diameter were excluded from the quantification. Data of active caspase 3 is shown as mean ± SEM. Statistical significance for active caspase 3 and phospho-histone H3 stainings was analyzed using unpaired *t*-tests.

2.7 RNA sequencing

2.7.1 Sample preparation for RNA purification

Premetamorphotic (stage 51) and postmetamorhic *Xenopus laevis* (stage 66) were anesthetized using 0.02% MS222. The whole nose of larval *Xenopus* was isolated under normal healthy conditions at the beginning (stage 51) and the end of metamorphosis (stage > 66) to study gene expression within the entire nose. Moreover, the entire nasal tissue of premetamorphotic animals (stage 51) was isolated 2 days, 7 days and 49 days after transection of the olfactory nerves and after amino acid exposure (see, 2.5.4). These samples allowed investigation of gene expression after an injury and after an overstimulation with odorants. Additionally, in samples of premetamorphotic animals (stage 51), the anterior part of the VNO and the lateral part of the PC of larval *Xenopus laevis* were separated in order to analyze gene expression in both sensory epithelia individually. Only these parts of the sensory cavities were used, as they are neither connected nor close to each other, thus preventing a mixture of epithelial tissue of the PC and the VNO. Also, the olfactory bulb of larval and adult animals (Figure 10) was isolated. The total RNA was extracted using 400 µl TRIzol reagent as described by the manufacturer (Invitrogen Canada Inc. Burlington, ON, Canada). The homogenization of each tissue sample in TRIzol was accomplished by using prefilled 2 ml tubes with ceramic beads and homogenized with the Minilys Personal Homogenizer (Bertin instruments, Bretonneux, France). Afterwards, the samples were stored at -80°C. Isolated total *Xenopus laevis* RNA was subsequently resuspended in 50 µl DEPC treated water and stored at - 80°C. For all 39 samples (three replicates of 13 prepared samples) total RNA concentration was measured using Nanodrop ND-1000 (ThermoFisher Scientific Inc., Nepean, ON, Canada).
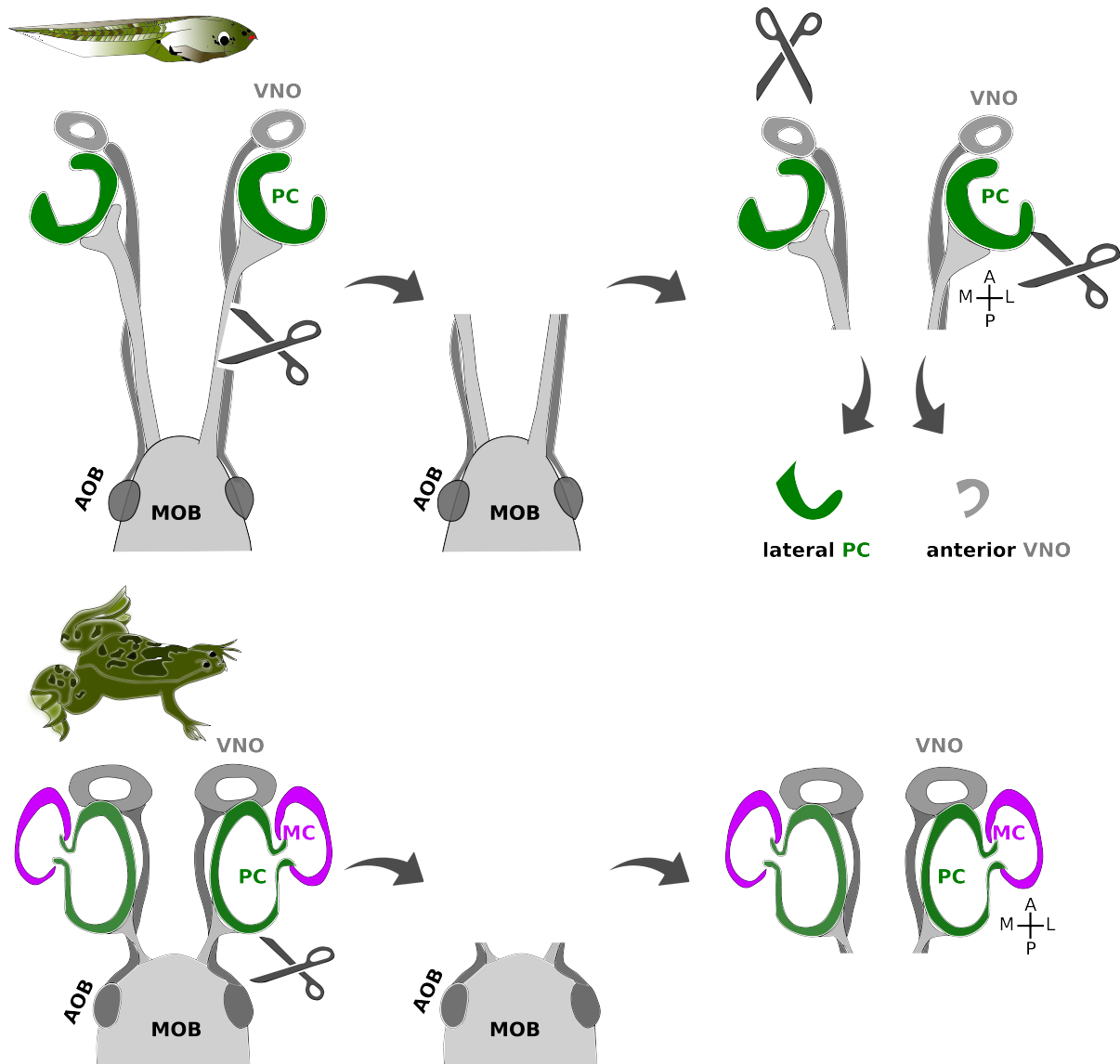
Figure 10. Schematic drawing of the olfactory organ and its sensory cavities

Samples for RNA sequencing were separately taken from the Principal cavity (PC), middle cavity (MC), vomeronasal organ (VNO), the main olfactory bulb (MOB) and accessory olfactory bulb (AOB).

A, anterior, P; posterior; M, medial; L, lateral

2.7.2 RNA sequencing protocol

For sequencing, the RNA samples described in (Table 1) were prepared with the TruSeq RNA Sample Prep Kit v2 according to the recommended protocol of the company Illumina. Paired end (2x150bp) sequencing was conducted using HiSeq 4000 (Illumina). Subsequently, the

quality was checked with the FastQC software (www.bioinformatics.babraham.ac.uk/projects/fastqc/). The reads of the conducted sequencing were aligned to the reference sequence of *Xenopus laevis* (genome 9.1., Xenbase, www.xenbase.org/). The alignment of the reads was performed using STAR alignment software (PUBMED ID 223104886. version 2.5) allowing for 10 mismatches within 300 bases. Additionally, counting of uniquely mapping hits was performed with featureCounts (PUBMED ID 24227677, version 1.5). Resulting data was preprocessed and analyzed in the R/Bioconductor (www.bioconductor.org) using the DEseq2 package (PUBMED ID 25516281). For further processing the data was normalized and tested for differentially expressed genes based on a generalized linear model likelihood ratio test assuming negative binomial data distribution. Candidate genes were filtered to a minimum of 2-fold change and FDR-corrected p-value < 0.05. Gene annotation was conducted using the *Xenopus laevis* GFF annotation file from Xenbase (version 1.8.3). Annotations for the expected genes were derived by querying the Ensemble database (www.ensembl.org) using biomaRt package (PUBMED ID 19617889).

Table 1. Samples of the olfactory organ used for RNA isolation.

For each condition three biological replicates were used. MC, middle cavity; PC, principal cavity; VNO, vomeronasal organ; OO, olfactory organ

Stage	Metamorphotic period	Part of the OO	Treatment	Time until RNA extraction
66	postmetamorphosis	whole nose (MC; PC and VNO)	/	0
51	premetamorphosis	whole nose (PC and VNO)	/	0
51	premetamorphosis	PC	/	0
51	premetamorphosis	VNO	/	0
51	premetamorphosis	olfactory bulb	/	0
51	premetamorphosis	whole nose (PC, VNO)	nerve transection	2 days
51	premetamorphosis	whole nose (PC, VNO)	nerve transection	7 days
54	premetamorphosis	whole nose (MC; PC and VNO)	nerve transection	49 days
51	premetamorphosis	olfactory bulb	nerve transection	2 days
51	premetamorphosis	olfactory bulb	nerve transection	7 days
54	premetamorphosis	olfactory bulb	nerve transection	49 days
51	premetamorphosis	whole nose (PC and VNO)	amino acid exposure with a concentration of 200 µM	5 hours
51	premetamorphosis	whole nose (PC and VNO)	amino acid exposure with a concentration of 1000 µM	5 hours

2.8 Materials

2.8.1 Solutions

Frog ringer solution contained 98 mM NaCl, 2 mM KCl, 1 mM $CaCl_2$, 2 mM $MgCl_2$, 5 mM Glucose, 5 mM sodium-pyruvate, 10 mM HEPES dissolved in Milli–Q purified water. The solution was adjusted to pH 7.8 and an osmolarity of 230 mOsmol l^{-1}.

Frogs ringer solution with a high potassium level contained 17 mM NaCl, 80 mM KCl, 2 mM $MgCl_2$, 1 mM $CaCl_2$, 5 mM glucose, 5 mM sodium-pyruvate, 10 mM HEPES, 230 mOsmol/l, pH 7.8.

A mixture of 19 amino acids dissolved in frog's ringer solution was used at a concentration of 100 µM as an odorant stimulant. The amino acid mixture contained L – alanine, L – arginine, L – asparagine, L–aspartat, L–cysteine, L-glutamt, L–glutamine, L–glycine, L–histidine, L–isoleucine, L–leucine, L –lysine, L–methionine, L–phenylalanine, L–proline, L–serine, L–threonine, L–tryptophan and L– valine.

As stimuli for basal and supporting cells Adenosine-5'-triphosphate (ATP), 2-methylthio-ATP (2-MeSATP) and 2-methylthio-ADP (2-MeSADP) were applied. Both purines were dissolved in standard frog ringer solution at a concentration of 100 µM.

3. Results

The results of my thesis are divided into two main parts. In the first part I analyze the morphological changes in the sensory epithelia of the olfactory organ of *Xenopus laevis* during metamorphosis. The main focus was to identify critical developmental stages for the remodeling of the olfactory organ (cell proliferation vs. cell death) and how a third sensory cavity is formed. In the second part I studied morphological and functional changes during degenerative and regenerative processes after injury of the olfactory organ. Finally, a RNA sequencing of of premetamorphotic and postmetamorphotic olfactory organs as well as regenerative tissue of transected animals was performed to investigate changes in gene expression during metamorphosis and under degenerative and regenerative conditions.

To get a first overview about the olfactory subsystems in the olfactory organ Figure 11 shows a maximum intensity projection of the olfactory epithelia lining the principal cavity (PC) and the vomeronasal organ (VNO) of an animal of the prometamorphotic stage 57. Olfactory receptor neurons (ORNs) were labeled using a biocytin backfill (2.2.1) and visualized with fluophore-coupled streptavidin. Stained axons of ORNs and VRNs converge into the olfactory nerve.
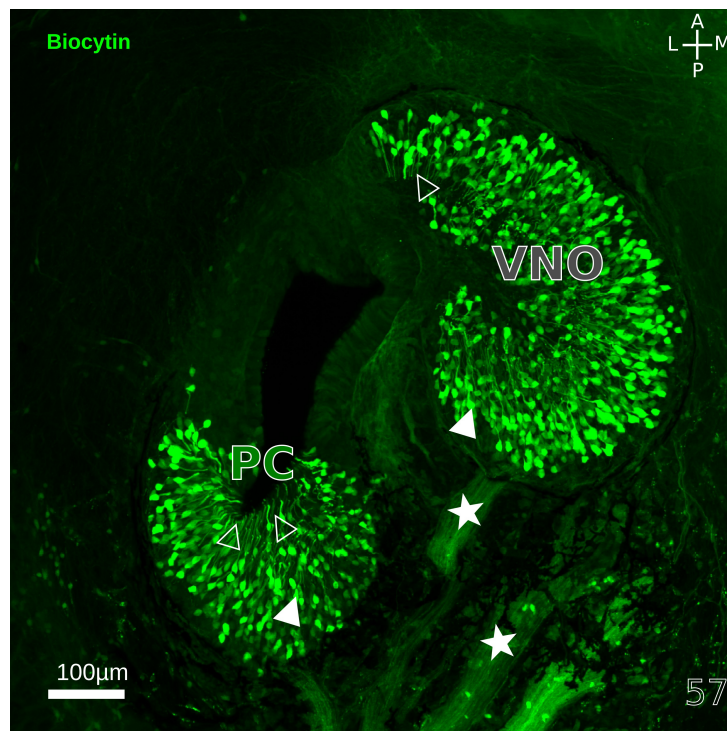
Figure 11. Visualization of the sensory epithelia of the principal cavity (PC) and vomeronasal organ (VNO) of larval *Xenopus laevis*.

A maximum intensity projection of the olfactory organ of stage 57 larval *Xenopus laevis* showing biocytin backfilled olfactory receptor neurons (green). Stars indicate stained axons of the olfactory nerve. Filled triangles show stained cell somata of olfactory receptor neurons whereas non-filled triangles highlight dendrites of biocytin backfilled ORNs. A, anterior; P, posterior; M, medial; L, lateral. The Number indicates the developmental stage.

3.1 Anatomical study of the olfactory organ over the time course of metamorphosis

For a thorough study of the metamorphotic changes I performed a Biocytin backtrace of ORNs of the PC, the middle cavity (MC) and of the VNO. This labeling method allowed a stage by stage investigation of the anatomical changes of the sensory chambers of the olfactory organ from premetamorphotic larval *Xenopus laevis* to juvenile adult (postmetamorphotic) frogs. To assess how the olfactory epithelia change during metamorphosis I compared the morphology and localization of ORNs of animals from stage 49 to 66. Figure 12 shows maximum intensity projections of the olfactory epithelia from developmental stage 49 to stage 65. The somata of ORNs are located in an intermediate layer of the epithelium with dendrites extending towards the cavity and axonal projections converging into the olfactory nerve. Up to stage 50 (early premetamorphosis) only the sensory epithelia of the PC and VNO were discernible. The VNO is located in an anteroventral

postion to the PC. At premetamorphotic stage 51 the first labeled sensory neurons were visible in the newly formed epithelium of the developing MC, located anteriorly to the PC. In later premetamorphotic stages (stage 52-54) the epithelium of the MC enlarges and the number of stained sensory neurons increased. In these stages the MC and the PC are in close contact with each other, so the affiliation of neurons located at the boundaries between both cavities was unclear. In prometamorphotic stages (stage 55-58) the number of sensory neurons of the MC constantly increased. The space between the MC and PC steadily increased but unsorted neurons were still observable (see Figure 12). The VNO constantly grew in size while retaining its roundish structure. During metamorphotic stages (stage 59 – 65) the sensory epithelium lining the PC flattens, but there was a progressive increase in surface size of the whole structure that now has a tunnel like appearance. The epithelia of the MC and the VNO displayed a further increase in size and were rarely found in the same horizontal plane due to their position on the dorsolateral axis. The VNO was located ventrolaterally to the epithelium of the MC (see Figure 12). At the end of metamorphosis, it was visible that the sensory epithelia of the PC and MC were connected via a narrow duct (asterisks, Figure 12). The final complex structure of the whole olfactory organ was complete around the metamorphotic stage 64, where the VNO was still located anteroventrally to the cavities of MC and PC. In this final state the MC was now located anterolaterally to the PC (Dittrich *et al.,* 2016).
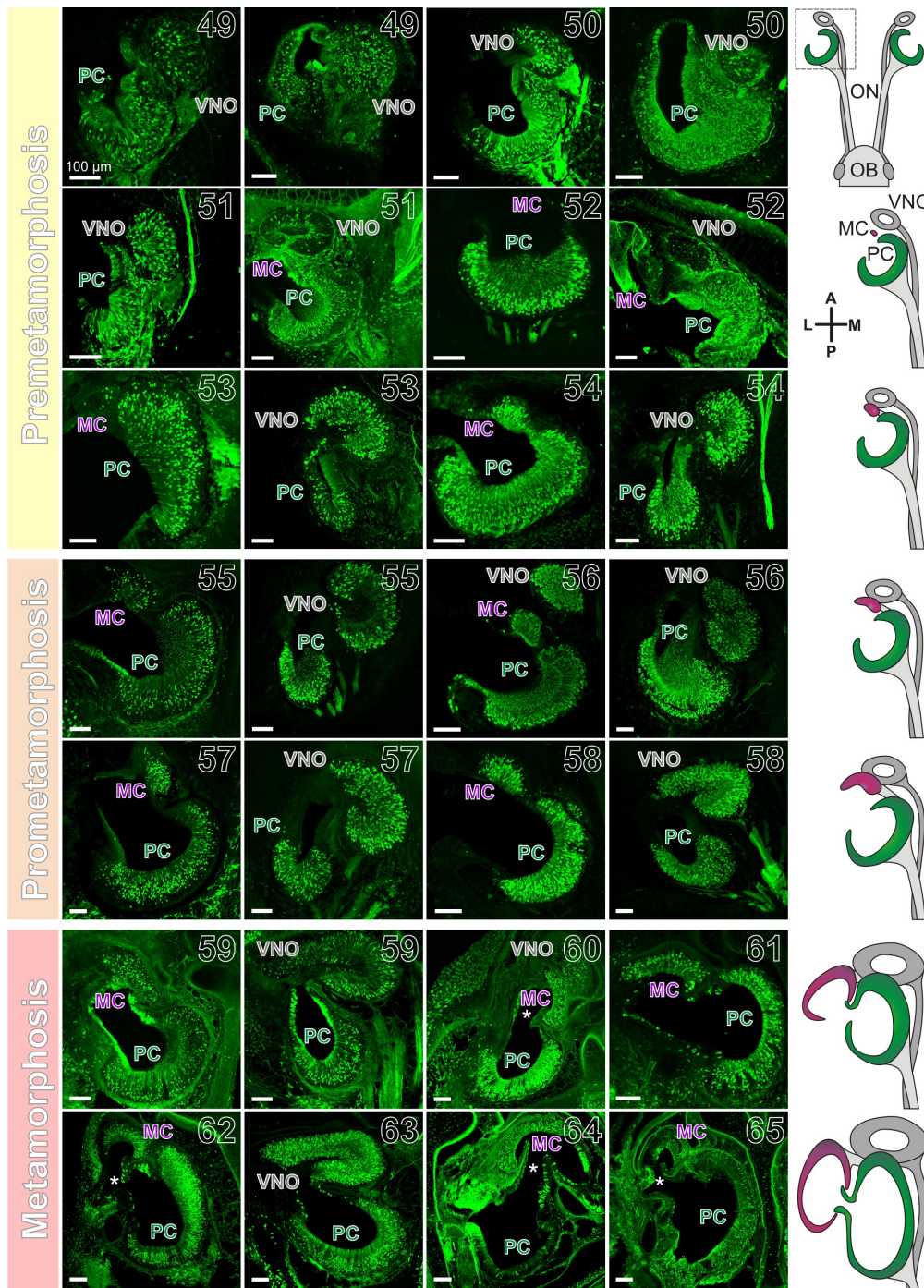
Figure 12. Development of the principal cavity (PC) and the vomeronasal organ (VNO) and formation of the newly arising middle cavity (MC).

Images show slices of olfactory organs with the whole population of olfactory receptor neurons labeled with biocytin-streptavidin via olfactory nerve tracing. Depicted are maximum intensity projections of image stacks.

Schematic representations of the depicted stages illustrate the size and localization of the three epithelia during larval development (right panels). A dashed square indicates the approximate location of the field of view shown in the microscopic images. The arrangement in three different sensory epithelia (PC, VNO, MC) is depicted over larval development. During premetamorphosis, the MC emerges and grows in size until metamorphosis. Metamorphosis reshapes the larval PC into a thinner, more extensive sensory surface thought to be specialized for airborne odorant detection. Also, the VNO undergoes spatial expansion during development. A narrow duct (asterisk) connects PC and MC at higher stages. Numbers indicate the developmental stage.
A, anterior; P, posterior; M, medial; L, lateral.

Figure 12 was taken from Dittrich et al., 2016

3.2 3D models of the spatial organization of the sensory olfactory epithelia at different key stages of metamorphosis

After studying the precise location of ORNs within the sensory epithelia it was important to get a better understanding of the spatial organization of the sensory epithelia. For this purpose three-dimensional reconstructions of the olfactory organ at different developmental stages were prepared (see 2.6.2), allowing the visualization of the complex system of sensory cavities.

I performed a microRuby backfill (see 2.2.1) of all sensory neurons of the whole intact olfactory organ via olfactory nerve tracing. Subsequently the acquired image stacks were used for three-dimensional reconstructions (Figure 13). The first 3D reconstruction shows a premetamorphotic olfactory organ at stage 50/51. It is subdivided into the PC (green) and the VNO (magenta). The dorsal part of the principal cavity (PC, green) was found to be open to the external environment allowing olfactory stimuli to reach the sensory epithelia through an internal system of interconnected canals. The VNO (gray) is located ventrolaterally to the PC and has a roundish structure. At a late premetamorphotic stage the MC (purple) begins to form anterodorsally from the PC. During prometamorphotic stages (56/57) and metamorphotic stages (60/61) all three cavities grow and form a more complex structured olfactory organ. During this process the VNO is repositioned to a more ventral position and the PC volume enlarged considerably and transformed from a half moon-shaped olfactory organ to a funnel-like structure (Dittrich *et al.*, 2016).
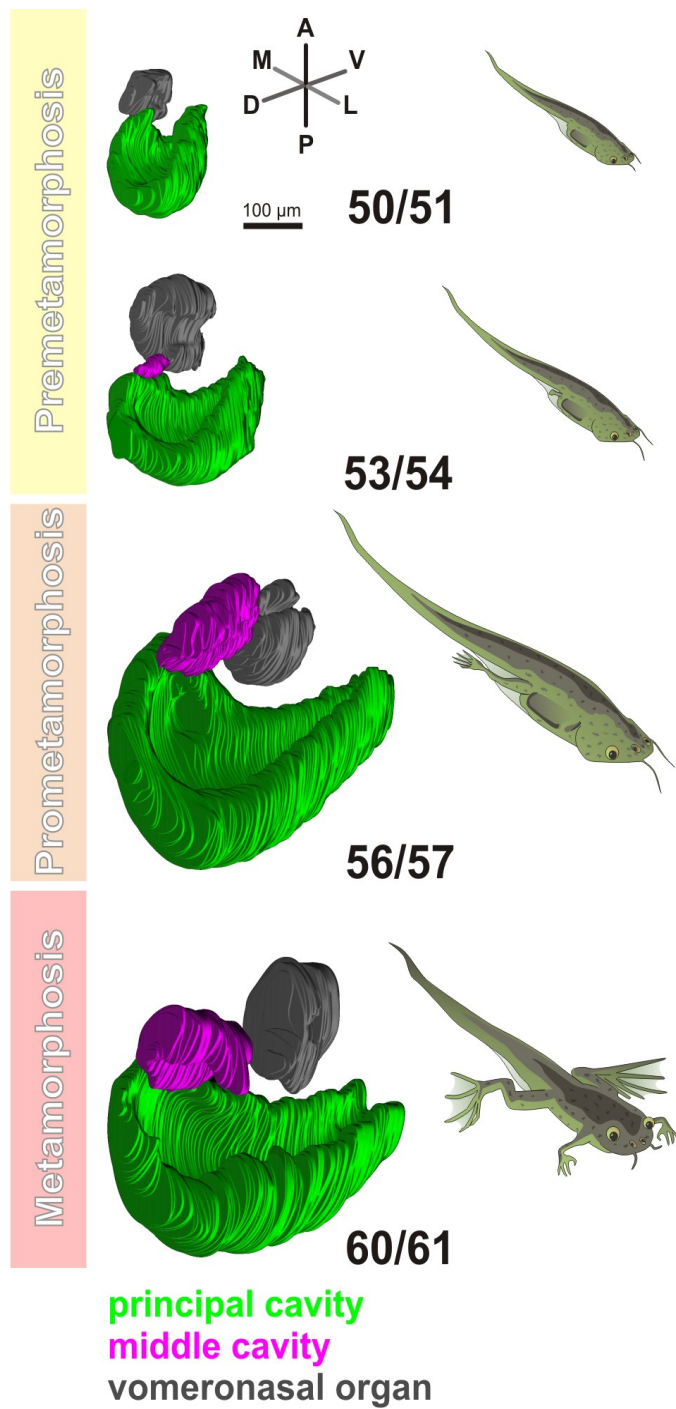
Figure 13. Three-dimensional visualization of the spatial organization of sensory epithelia in the whole olfactory organ.

The images represent dorsolateral views of the olfactory organ at selected developmental stages. Initially, tadpoles possess sensory epithelia in the principal cavity (PC, green) and vomeronasal organ (VNO, gray).

During premetamorphosis, the middle cavity (MC, magenta) is newly formed at the anterodorsal boundaries of the PC. During prometamorphosis, the MC grows in size and is located dorsally to the VNO. Planes in the volumetric reconstructions represent 5 mm thickness. A, anterior; P, posterior; M, medial; L, lateral; D, dorsal; V, ventral. Numbers indicate the developmental stage.

Figure 13 was taken from Dittrich et al., 2016

3.3 Determination of the origin of the sensory epithelium formed in the emerging middle cavity

From the results of the first part of my thesis, it is unclear whether the sensory epithelium of the MC is built up from migrating cells of the PC epithelium or if it emerges from a *de novo* epitheliogenesis. To investigate the origin of the cells of the MC, I acquired higher magnification images of biocytin backfilled sensory neurons of the tissue boundaries between the PC and the newly formed MC. The first developing backfilled ORNs that are clearly attributable to the epithelium of the emerging MC were always located close to the boundary of the PC epithelium (Figure 14).
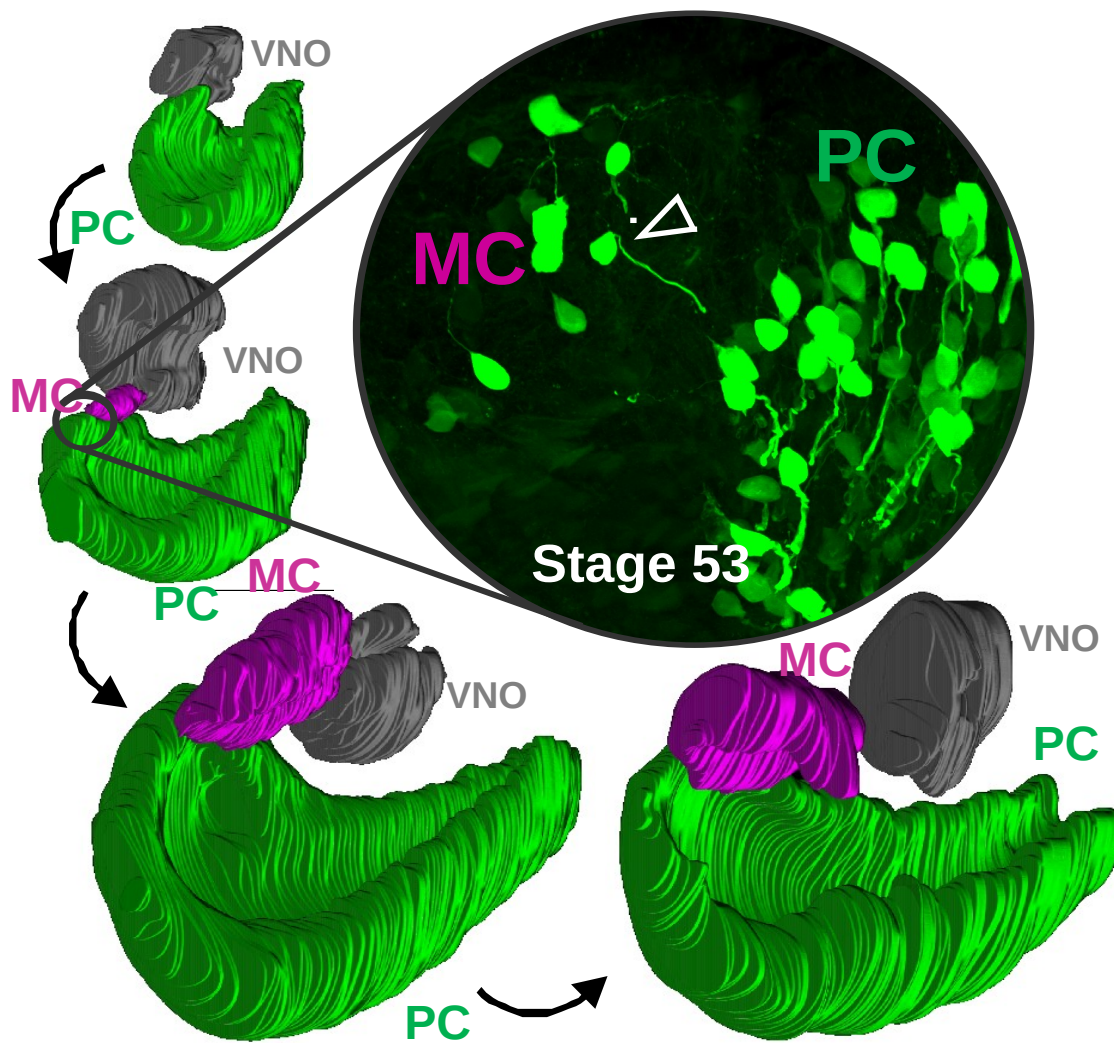
Figure 14. Localization of olfactory receptor neurons (ORNs) at the boundary between the principal cavity (PC) and the middle cavity (MC).

The first developing backfilled olfactory receptor neurons (green) of the MC can be seen in the epithelium of the emerging MC. An olfactory receptor neuron located in the newly forming MC, with a dendrite projecting towards of the PC (indicated with an open arrowhead). Number indicate the developmental stage.

Figure 14 was taken from Dittrich et al., 2016 (abstract figure; https://onlinelibrary.wiley.com/toc/10969861/524/5)

The boundaries between the epithelia of the MC and the PC often contain unsorted backfilled sensory receptor neurons of an uncertain origin (see Figure 15). No conclusive answer about the origin of ORNs of the MC could be made by analysis of biocytin backfilled olfactory epithelia. Additionally, the described experiments include no information about the origin of

supporting cells within the sensory neuroepithelium of the MC as only sensory neurons were labeled.
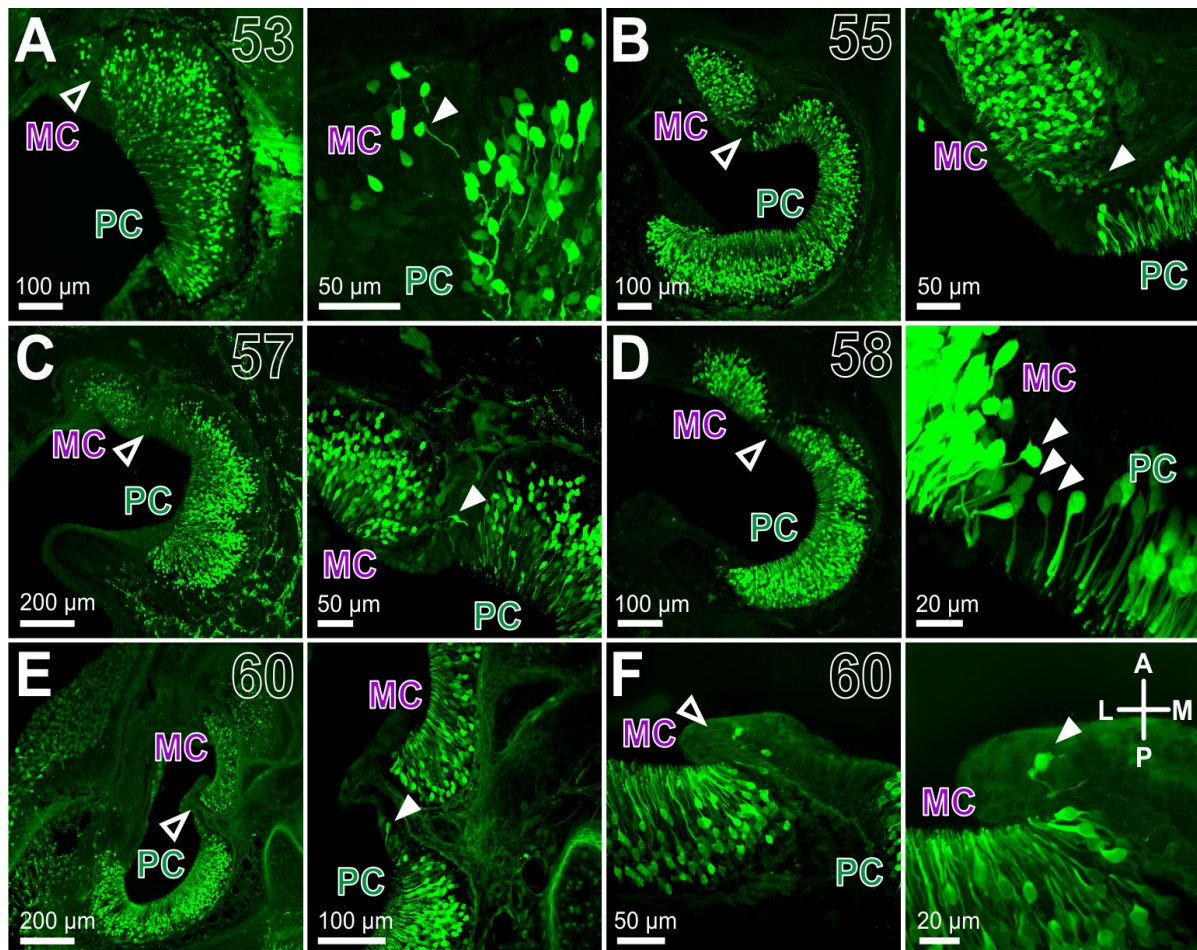
Figure 15. Formation of the middle cavity (MC) and indistinct localization of olfactory receptor neurons at the boundaries of MC and principal cavity (PC).

A–F: Maximum projections of sliced olfactory organs depicting representative examples of the early stages of MC formation. Images highlight the unclear position of sensory neurons at the boundaries of PC and MC (open arrowheads), labeled via olfactory nerve tracing. The right panel shows the PC/MC border at higher magnification. Some individual sensory neurons cannot be clearly attributed to an individual sensory epithelium (solid arrowheads). It is possible that these PC neurons are incorporated into the emerging MC. Numbers indicate the developmental stage. A, anterior; P, posterior; M, medial; L, lateral. Numbers indicate the developmental stage.

Figure 15 was taken from Dittrich et al., 2016

Taking these results into account, a new experimental protocol was designed to obtain more detailed information about the origin of sensory neurons and supporting cells in the olfactory

organ during its metamorphotic remodeling. At early premetamorphotic stages (stages 47-50) with no MC yet present, most of the cells of the PC and the VNO were labeled via bulk electroporation with a fluorophore coupled dextran (Alexa 594 dextran 10kDa; see 2.2.4) in the olfactory organ. Approximately 21 days later, after the beginning of MC formation (stages 54-57), I investigated the cells. Animals were then killed and sensory neurons of the olfactory organ were labeled via olfactory nerve backfill (streptavidin coupled dextran 488, described in 2.2.1). Dextran labeled cells (magenta, see Figure16) represent cells that were already present at the time of electroporation, belonging to the population of sensory neurons and supporting cells that persisted throughout the observed time span of around 21 days (Figure16). Cells labeled only via biocytin-streptavidin nerve backfill represent populations of neurons newly generated during the progress of the experiment. In the conducted stainings I also observed dextran particles not localized in cell bodies. These were most probably cellular debris from cells that degenerated during the course of the experiment. Higher magnification images showed that in the MC a few cells were also dextran labeled (Figure16, shown in magenta). I can therefore conclude that these cells were originally part of the larval PC. None of the investigated tadpoles (n=15, 30 slices of MC), displayed a single, dextran labeled cell with a neuronal morphology (dendrites or axonal prolongations) in the MC. In contrast, almost all 30 slices of the MC showed sparsely distributed, dextran labeled supporting cells in the MC (Figure 16, filled arrowheads). Electroporated animals that were allowed to complete metamorphosis showed no visible cellular dextran staining in any of the three olfactory surfaces (n=11; 8 slices of the MC, 11 slices of the PC, 3 slices of the VNO). In summary, I found that supporting cells of the premetamorphotic PC are included in the formation of the emerging MC, but apparently no supporting- or neuronal cell populations are retained in the long term. Distributed particles of dextran dye remaining in the sensory epithelia of the olfactory organ are most likely remaining parts of those lost cells (Dittrich *et al.*, 2016).
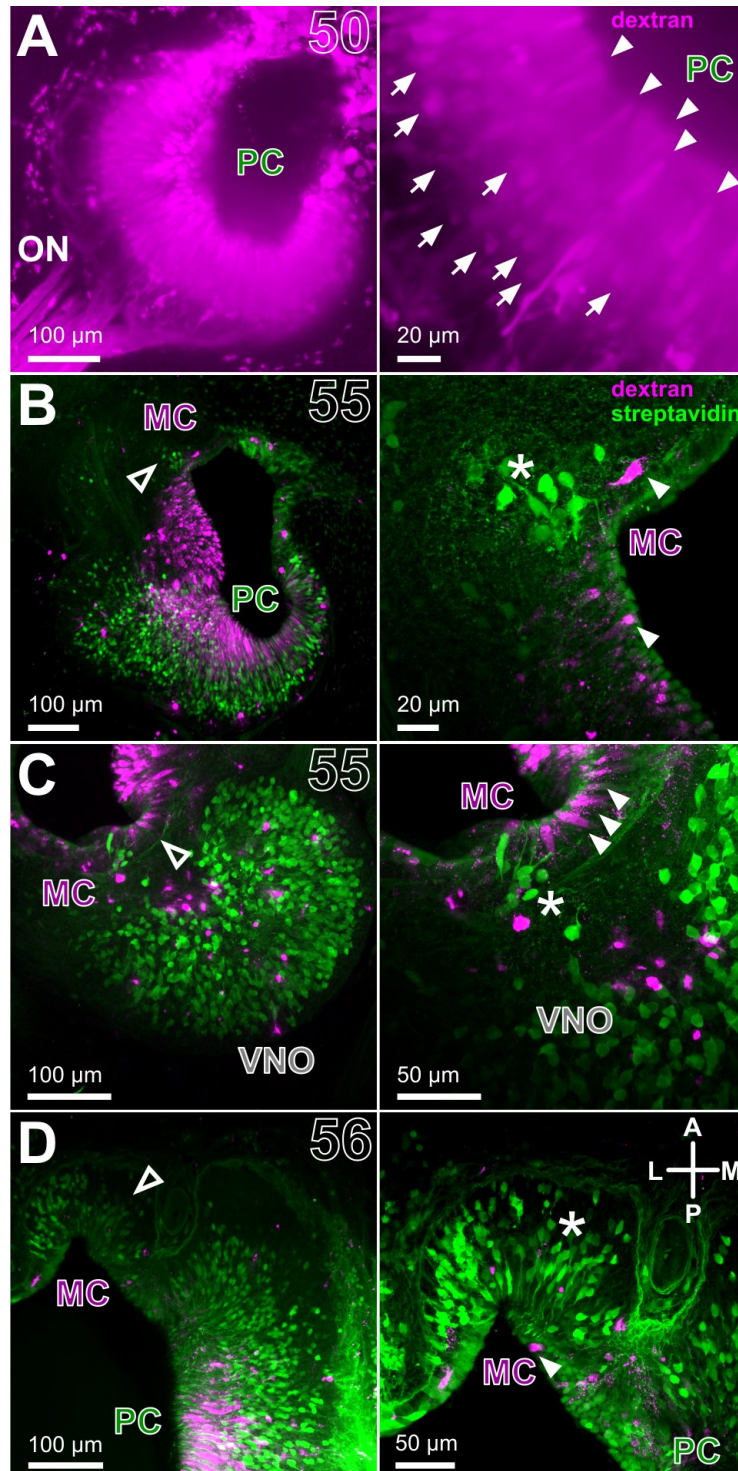
Figure 16. Incorporation of supporting cells, but not olfactory receptor neurons (ORNs), into the forming middle cavity (MC).

A: Larval olfactory organs were electroporated with dextran (magenta) before the MC was apparent (at stages 47–/50). Successful electroporation was verified by in vivo two-photon microscopy. Images depict maximum

projections of an image stack. The whole epithelium of the principal cavity (PC) and the olfactory nerve (ON) showed widespread and uniform dextran labeling in supporting and sensory neuron layers. The higher magnification view in the right panel highlights that both supporting cells (solid arrowheads) and sensory neurons (arrows) were labeled. **B–D**: After formation of the MC (at stages 54–/57), all sensory neurons were traced via the olfactory nerve with biocytin-streptavidin (green). Images depict maximum intensity projections of slices of olfactory organs. Dextran labeled cells represent cells that were already present before MC formation and persisted until the olfactory organ was investigated. The right panel shows the MC at higher magnification. Punctate, dextran labeled cell debris and supporting cells (solid arrowheads) can be visualized in the MC (open arrowheads). In the emerging MC, mature sensory neurons (marked by an asterisk), already extending their axon into the olfactory nerve, can be identified via biocytin-streptavidin tracing (green). Dextran labeling never revealed a cell with neuronal morphology and/or colabeling with biocytin-streptavidin in any of the investigated MCs (n=5, 15, 30 slices of the MC). The slices depicted in A and B originate from the same animal. Numbers indicate the developmental stage. PC, principal cavity; A, anterior; P, posterior; M, medial; L, lateral. Numbers indicate the developmental stage.

Figure 16 was taken from Dittrich et al., 2016

3.4 Quantification of cell death and proliferation in the sensory epithelia over the time course of metamorphosis

Quantification of apoptotic and proliferative cells within the PC, VNO and the MC (table 2) yields information about cell turnover during metamorphosis and might to determine critical metamorphotic stages during the remodeling process of the sensory epithelia. Since metamorphosis of the olfactory organ is associated with extensive reorganization and presumably programmed cell death, the performed immunostainings allowed me to assess the number of apoptotic cells in the olfactory organ over the course of metamorphosis. I stained olfactory organ sections for active caspase 3 (2.2.2), a key enzyme that is activated during apoptotic cell death in ORNs (Cowan and Roskams, 2002). Active caspase 3-like labeling can clearly be detected in apoptotic cells (Figure 17). A major interest was to study the contribution of apoptotic events in the individual olfactory epithelia in relation to the total number of dying cells during metamorphosis (Dittrich *et al.*, 2016).
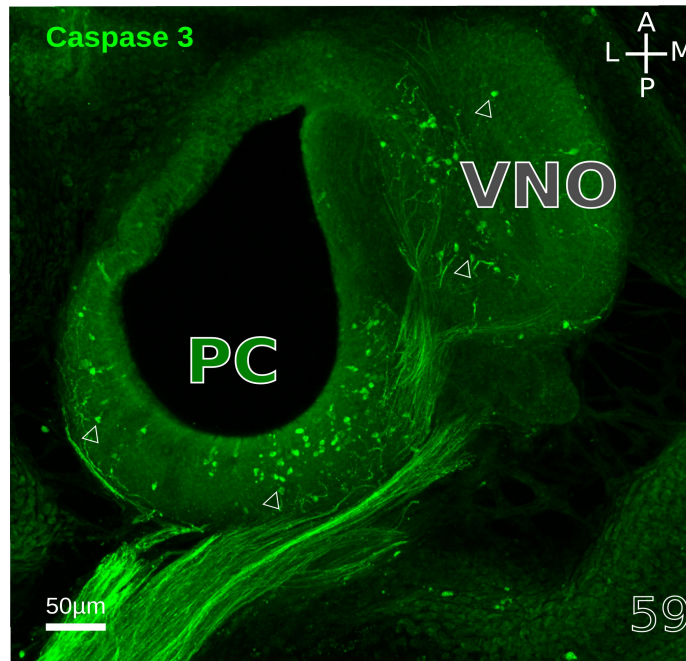
Figure 17. Apoptotic cell death within the sensory epithelia of the principal cavity (PC) and vomeronasal organ (VNO).

A maximum intensity projection of the olfactory organ of an animal of stage 59 of *Xenopus laevis*. An antibody against active caspase 3 labeled apoptotic cells (green) of the sensory epithelium of the PC and the VNO was used. Unfilled triangles indicate examples of apoptotic cells in the PC and the VNO. A, anterior; P, posterior; M, medial; L, lateral. Numbers indicate the developmental stage.

To get a better idea about the apoptotic cell rate in the individual olfactory epithelia, the number of active caspase 3 positive cell bodies of the PC, VNO and the emerging MC were quantified (Table 2). Bright, green spots in Figure 17 and Figure 18 can be considered as active caspase 3 positive (i.e. apoptotic) cells. Some cells can be defined as ORNs, judging by the location of the soma in the intermediate layer of the olfactory epithelium (Figure 17 and Figure 18), from the visible thin dendritic projections towards the apical part of the cavity and axonal projections towards the basal layer. Other cells lack features that give information about the cell morphology and are instead most probably blebs of dead cell material. Across all developmental stages of metamorphosis, the average number of active caspase 3 positive cells varied in the PC, VNO and MC (see 2.6.3) with 26 ± 2, 21 ± 2, and 8 ± 1, (Table 2; number of slices: MC = 61, PC = 104, VNO = 76; Dittrich *et al.*, 2016) respectively.
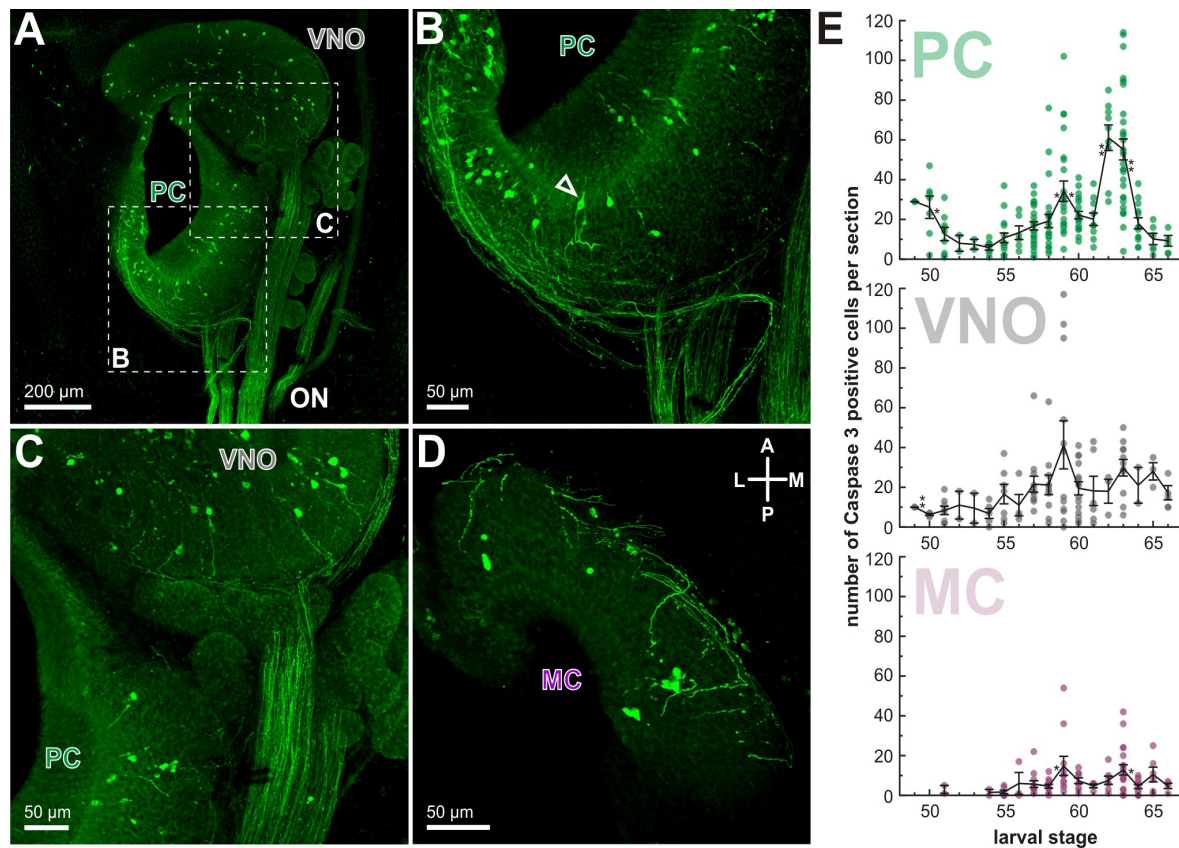
Figure 18. Active caspase 3 positive cells in the sensory epithelia of the principal cavity (PC), vomeronasal organ (VNO) and middle cavity (MC).

A. Maximum intensity projection of a sectioned larval olfactory organ and connecting olfactory nerve (ON) labeled for active caspase 3 (green) at stage 58. Note that the MC is not visible in the presented horizontal plane. **B.** Higher magnification of the PC (boxed area in A). Among labeled apoptotic cells, sensory neurons with an apical dendrite and/ or a basal axon can be identified (open arrowhead). **C.** Higher magnification of the VNO and PC (boxed area in A). **D.** Maximum intensity projection of a sectioned olfactory organ illustrating active caspase 3 like immunofluorescence in the MC at stage 58/59. The number of apoptotic cells is much lower than in the PC and VNO. **E.** Average number of active caspase-3-positive cells per section in the PC (green), VNO (gray) and MC (magenta) over the course of larval development. Statistical significance was determined using an unpaired t-test (*p<0.05, **p<0.01). Numbers indicate the developmental stage.

Figure 18 was taken from Dittrich et al., 2016

The scatter diagrams in Figure 18 E. show the average number of stained apoptotic cells (Table 2) in the PC (green), VNO (gray) and MC (magenta) during metamorphotic development. In the PC, the mean number of caspase 3 positive cells was significantly decreasing from stage 50 to 51, reaching a stable level around stage 54 and is then continuously increasing until stage 58. A significant peak in apoptotic events was detectable at stage 59 followed by another significant increase at stage 61/62. At developmental stage 62, apoptosis reached its peak and was decreased at stages higher than postmetamorphotic stage

63, returning to numbers comparable to premetamorphotic stages. The VNO showed a moderate number of apoptotic cells in premetamorphotic stages. During the onset of metamorphosis the level of active caspase 3 positive cells slightly increased and reached a significant peak at the transition of stage 58/59 ($p<0.05$). After stage 63, the number of apoptotic events was significantly decreasing ($p<0.05$). In general, the occurrence of apoptotic cells in the MC was consistently lower than in the sensory epithelia of the PC and the VNO (Dittrich *et al.,* 2016).
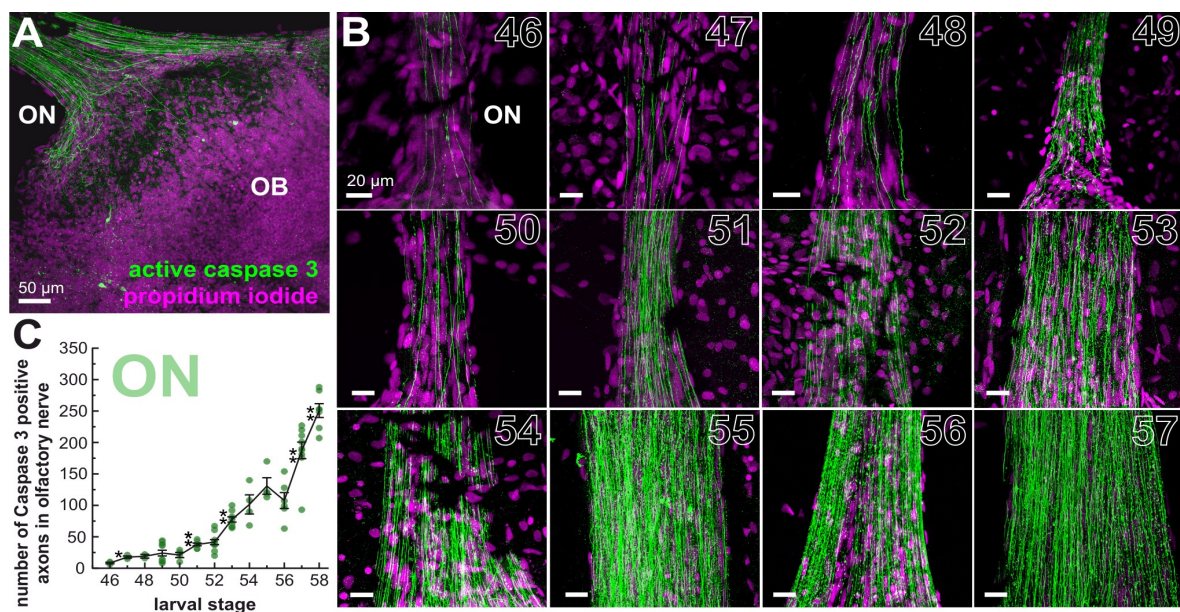
Figure 19. Active caspase 3 positive axons in the olfactory nerve (ON).

A. A maximum intensity projection of a section of the anterior telencephalon showing active caspase 3 like immunofluorescence in olfactory receptor neurons (green) and propidium iodide stained cell nuclei (magenta). Apoptotic axons of olfactory receptor neurons prolong into the olfactory nerve and terminate in the olfactory bulb (OB). **B.** Representative immunostainings of intact olfactory nerves of different developmental stages (46-58) are shown as maximum projections. **C.** A scatter diagram points out the average number of active caspase 3 positive axons in the unlesioned olfactory nerve of developmental stages 46-58 (number of olfactory nerve samples per stage: 46/3, 47/3, 48/2, 49/11, 50/4, 51/7, 52/11, 53/9, 54/4, 55/4, 56/6, 57/9, 58/7). Statistical significance was determined using an unpaired t-test (*$p<0.05$, **$p<0.01$). Numbers indicate the developmental stage.

Figure 19 was taken from Ditttrich et al., 2016; results produced by Josua Kuttler

Active caspase 3 positive immunofluorescence was not only observed in the olfactory epithelia, but also in stained axons of apoptotic receptor neurons. These stained axons could be followed through the olfactory nerve and terminated within the olfactory bulb, where they showed degenerate morphology of axonal terminals (Figure 19 A).The average number of

active caspase 3 positive axons in the intact olfactory nerve of the developmental stages 46-58 was quantified (Figure 19 B, Table 2). The conducted quantification shows the total number of apoptotic neurons in all three olfactory epithelia (MC, PC and VNO). The transition from stage 46-47 led to a significant increase of (8±1 to 18±2) active caspase 3 positive axons in the OE (p<0-05). The number of axons and therefore the total number of apoptotic cells in the olfactory organ did not increase significantly between stage 47-50 (from 18±2 to 21±4 active caspase 3 positive axons). After the developmental stage 51, the gradual increase in total apoptotic olfactory neurons was more distinct, with a highly significant increase between stages 50/51, 52/53, 56/57 and 57/58 (p<0,01; Dittrich *et al.*, 2016).

Table 2. Quantification of active caspase 3 positive axons and cell somata over the time course of metamorphosis.

Stage by stage quantification of active caspase 3 positive axons of sections of the olfactory nerve and cells of sections of the middle cavity (MC), principal cavity (PC) and the vomeronasal organ (VNO). Data of active caspase 3 postive cell somata and axons are shown as mean ± SEM.

Table 2 was taken from Dittrich et al., 2016

Stage	Average number of caspase3-positive axons in olfactory nerve	Average number of caspase3-positive cell somata in		
		MC	PC	VNO
46	8 ± 1	N/A	N/A	N/A
47	18 ± 2	N/A	N/A	N/A
48	19 ± 3	N/A	N/A	N/A
49	24 ± 5	N/A	29 ± 0	10 ± 0
50	21 ± 4	N/A	26 ± 6	6 ± 0
51	38 ± 2	3 ± 2	13 ± 3	8 ± 2
52	42 ± 4	N/A	8 ± 4	11 ± 7
53	78 ± 4	N/A	8 ± 3	10 ± 8
54	102 ± 15	2 ± 1	8 ± 3	7 ± 2
55	131 ± 13	2 ± 1	11 ± 2	17 ± 5
56	108 ± 13	6 ± 6	13 ± 3	11 ± 5
57	187 ± 13	6 ± 2	17 ± 2	22 ± 4
58	251 ± 11	5 ± 1	19 ± 3	21 ± 5
59	N/A	15 ± 5	34 ± 5	41 ± 12
60	N/A	7 ± 1	22 ± 2	19 ± 3
61	N/A	5 ± 1	20 ± 3	18 ± 7
62	N/A	8 ± 2	61 ± 6	18 ± 6
63	N/A	13 ± 3	55 ± 5	30 ± 4
64	N/A	4 ± 1	18 ± 3	21 ± 9
65	N/A	11 ± 4	10 ± 3	28 ± 4
66	N/A	5 ± 1	9 ± 3	17 ± 4

The degree of cell proliferation in the sensory epithelia has not been conclusively investigated yet. To visualize proliferative cells an anti phospho-histone H3 antibody was used (see 2.2.2, Figure 21). The quantification of phospho-histone H3 labeled cells in the different sensory epithelia of the olfactory organ provides information about the critical stages of proliferation during metamorphosis. Figure 20 shows a maximum intensity projection of the sensory epithelia of the PC and the MC with phospho-histone H3 positive labeled cells in the intermediate layer and the basal cell layer of the PC. The phospho-histone H3 labeled cells of the newly formed MC are distributed over all layers.
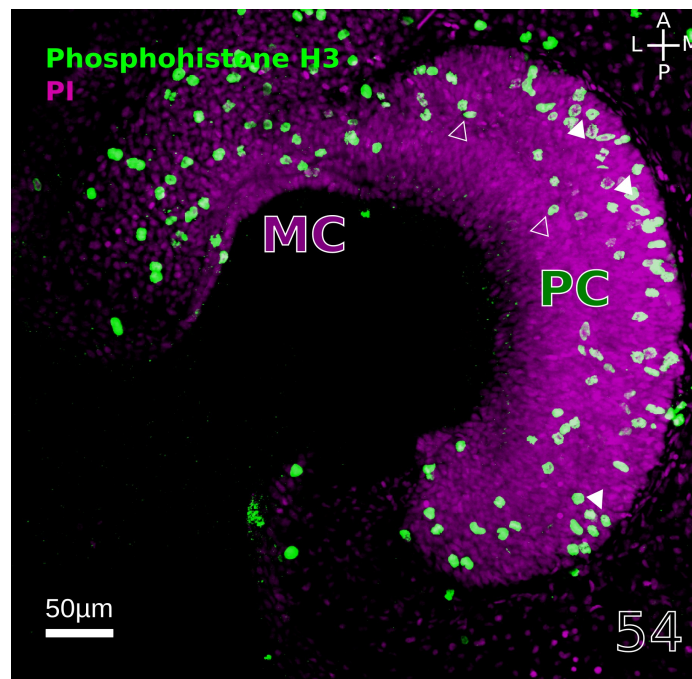
Figure 20. Phospho-histone H3 positive cells in the sensory epithelia of principal cavity (PC) and middle cavity (MC).

Maximum intensity projection of sectioned sensory epithelia of the PC and middle MC at stage 54 larval *Xenopus* with propidium iodide stained cell nuclei (PI, magenta) and phospho-histone H3 positive cells (green). Unfilled triangles indicate stained proliferating cells in the intermediate layer of the PC. Filled triangles indicate proliferating cells in the basal cell layer of the sensory epithelia of the PC. A, anterior; P, posterior; M, medial; L, lateral. Number indicate the developmental stage.

Section was taken from Figure 21
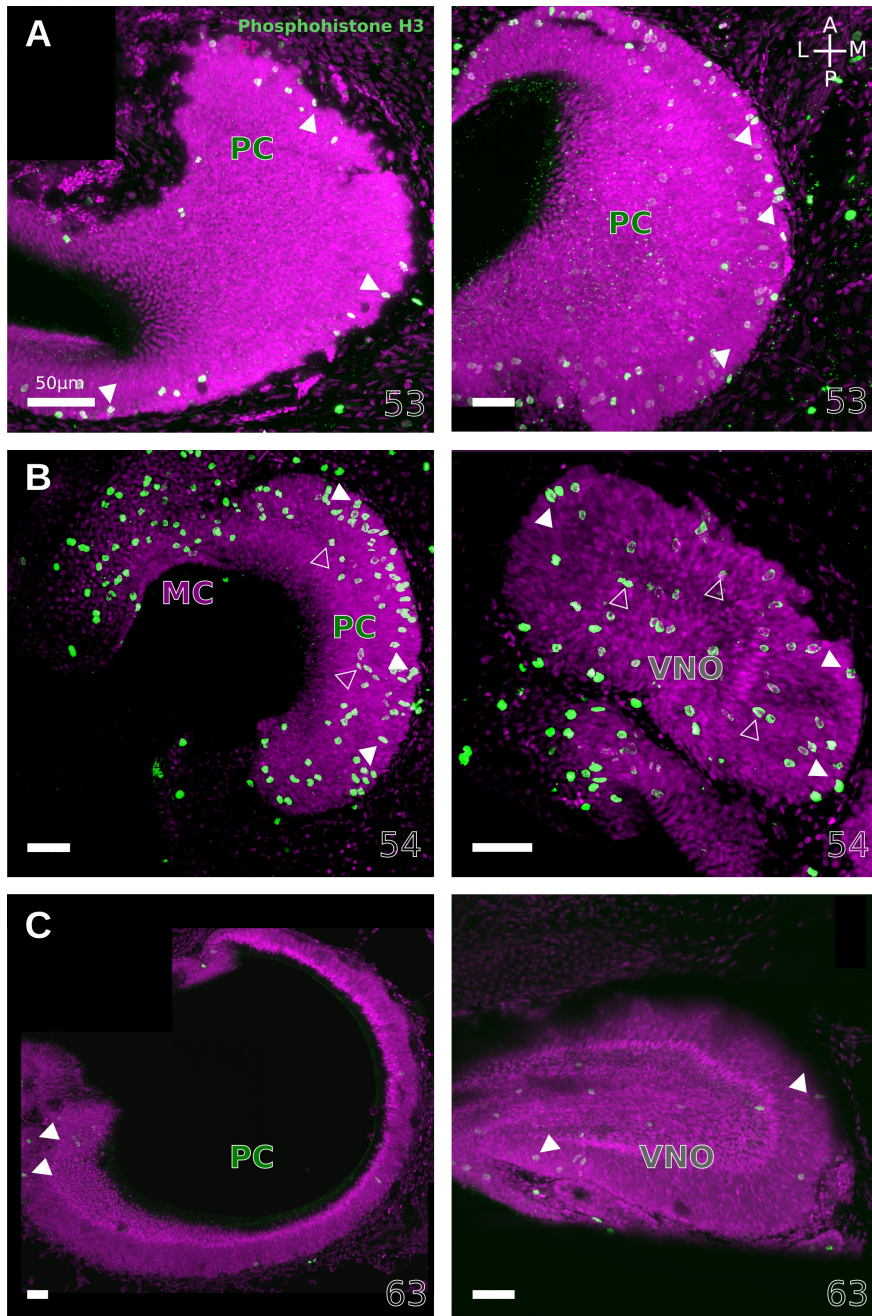
Figure 21. Phospho-histone H3 positive cells in the sensory epithelia of the principal cavity (PC), the vomeronasal organ (VNO) and the middle cavity (MC)

Maximum intensity projections of sectioned olfactory organs illustrating phospho-histone H3 positive cells (green) over the time course of metamorphosis. Cell nuclei were labeled with propidium iodide (PI, magenta) **A.** Phospho-histone H3 positive cells (green) of the PC, MC and VNO in premetamorphotic *Xenopus laevis*. **B.** A high number of proliferating cells was observable at stage 54. **C.** The lowest number of proliferation was observed at postmetamorphotic stages. A, anterior; P, posterior; M, medial; L, lateral. Numbers indicate the developmental stage.
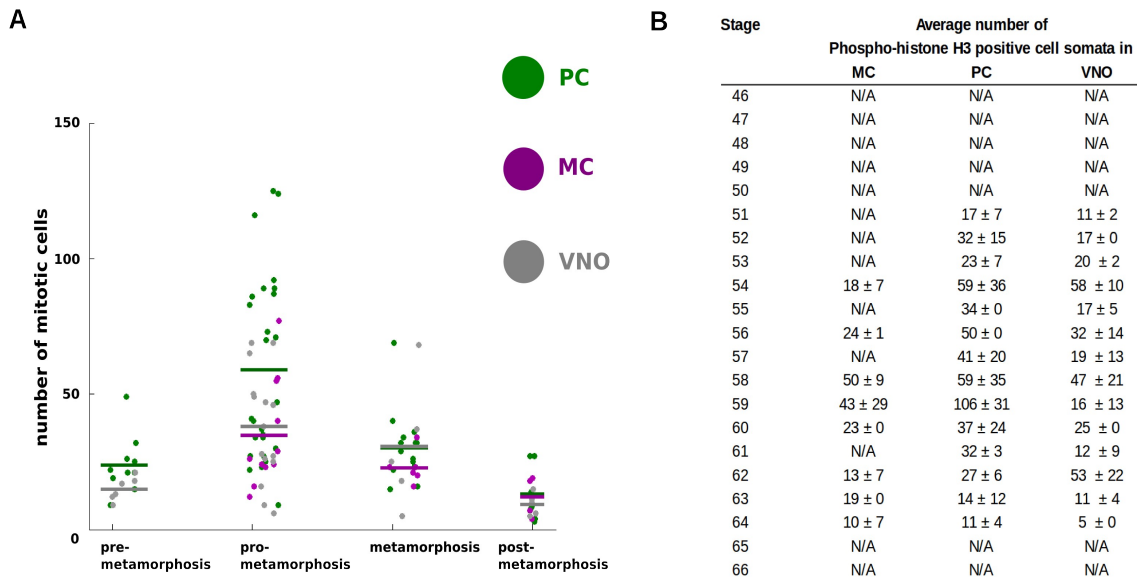
Figure 22. Stage by stage quantification of phospho-histone H3 postive cell somata

A. and **B.** Stage by stage quantification of phospho-histone H3 postive cell somata of sections of olfactory sensory epithelia of the principal cavity (PC), the middle cavity (MC) and the vomeronsasal organ (VNO). **B.** Data of phospho-histone H3 postive cell somata are shown as mean ± SEM.

The massive remodeling of the olfactory organ is not only associated with programmed cell death, but also with newly generated cells which ensure functional stability of the olfactory epithelia. To gain more information about cell proliferation I quantified the number phospho-histone H3 positive cells. The scatter diagrams in Figure 22 A show the number of phospho-histone H3 positive cells per section of the PC (green), VNO (gray) and MC (magenta) during metamorphotic development (see 2.6.3). Slices of the PC, VNO and MC were grouped in premetamorphosis (stage 49-54), prometamorphosis (stage 55-58), metamorphosis (stage 59-65) and postmetamorphosis (stage 66) and proliferative cells were counted (Figure 22). At stage 51 the PC and VNO exhibited 17 ± 7 and 11 ± 2 phospho-histone H3 positive cells (3 slices each), respectively. At stage 54 the number of mitotic cells increased in the PC and VNO and proliferative cells are become visible in the newly formed MC. In the sensory epithelium of the PC, the mean number of proliferating cells significantly increased in prometamorphotic stages where proliferating events reached peak levels. At stage 59 the number of phospho-histone H3 is the highest with 106 ± 31 and 43 ± 29 phospho-histone H3

positive cells in the PC (3 slices) and MC (3 slices) respectively. In the VNO the number of mitotic cells showed a first peak at stage 54 (58 ± 10; 4 slices) and a second one at stage 62 (53 ± 22; 2 slices).

Together the results of the first part of my thesis indicate that during metamorphosis, the olfactory organ of *Xenopus laevis* undergoes fundamental changes. The precise analysis of biocytin backfilled olfactory receptor neurons combined with 3D-reconstructions of the olfactory organ allowed the visualization of the complex structure of the sensory olfactory cavities in the olfactory organ. *In vivo* monitoring of metamorphotic changes and a terminal biocytin-backfill showed that the MC emerged *de novo*, with only some supporting cells of the PC taking part in the formation of the MC. The quantification of cell death and proliferation showed a high cell turnover especially in prometamorphotic and metamorphotic stages. The initial cell proliferation followed by massive cell death indicate that there are peak apoptotic and proliferative events, which suggests that cell death and proliferation are coordinated events. Some open questions remain about how these metamorphotic changes are regulated on the molecular level and which genes are involved in the reorganization of these changes. Therefore, a transcriptome analysis of the sensory epithelium of the larval PC and separately of the VNO was generated by isolating RNA samples. Furthermore RNA samples of the whole larval and adult nose epithelia were isolated to enable a comparison of the total receptor gene expression between larval and adult stages. Larval and adult bulb samples were extracted to analyze the gene expression in the first relay station of the olfactory system at the beginning and the end of metamorphosis. Additionally tissue samples of degenerating and regenerating olfactory epithelia were collected (see RNA sequencing).

3.5 Recovery of the olfactory epithelium after injury

After a thorough analysis of the morphological changes in the olfactory organ during metamorphosis I aimed to analyze the morphology and the process of regeneration of injured olfactory organs. In order to survey how the olfactory epithelia regenerate after an injury, I introduced lesions and caused the degeneration of the olfactory epithelium. Afterwards the amount of apoptosis was analyzed and the morphology of lesioned epithelia was compared to healthy control tissue. Additionally, several immunostainings were performed to obtained information about which cell populations were affected by the lesion. These experiments were conducted to define crucial time points for the degeneration and regeneration of cells. I used

the chemicals Triton X-100 and ZnSO$_4$ to introduce a tissue-wide degeneration of cells and a bilateral transection to especially lesion the population of ORNs.

3.5.1 Degeneration and recovery after chemical irrigation of the olfactory epithelium

To obtain an understanding of the arrangement of cells in healthy control tissue diverse immunostainings were performed (cytokeratin type II, active caspase 3 and biocytin-streptavidin labeling, see 2.2.1-2.2.3). In control tissues of the PC (see Figure 23) cytokeratin type II labeled cells formed a tightly packed columnar monolayer in the most apical part of the PC. Supporting cells span long prolongations throughout the entire sensory epithelium terminating on the basal lamina (Hassenlöver *et al.,* 2008). Caspase 3 positive cells were sparsely distributed within the whole PC (Figure 23 A). Biocytin-streptavidin labeling showed stained somata and axons of ORNs of the larval PC under control conditions.
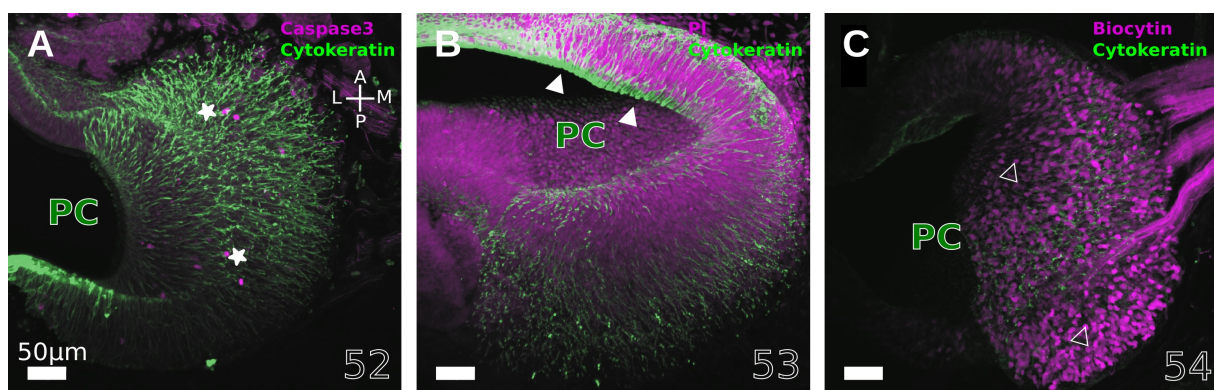
Figure 23. Control tissue sections of premetamorphotic *Xenopus laevis* larvae. Maximum intensity projections of sectioned principal cavities (PCs) of the developmental stages 52-54.

A. A antibody against active caspase 3 labeled apoptotic cells (magenta, indicated by filled stars). **B.** Filled triangles indicate cytokeratin type II positive cells arranged in a tight columnar apical layer of the PC. **C.** Backtraced olfactory receptor neurons stained with biocytin are indicated by unfilled triangles. A, anterior; P, posterior; M, medial; L, lateral. Numbers indicate the developmental stage.

To study how a chemical lesion affects the morphology of the larval main olfactory epithelium, animals were treated with ZnSO$_4$ (see 2.5.3).
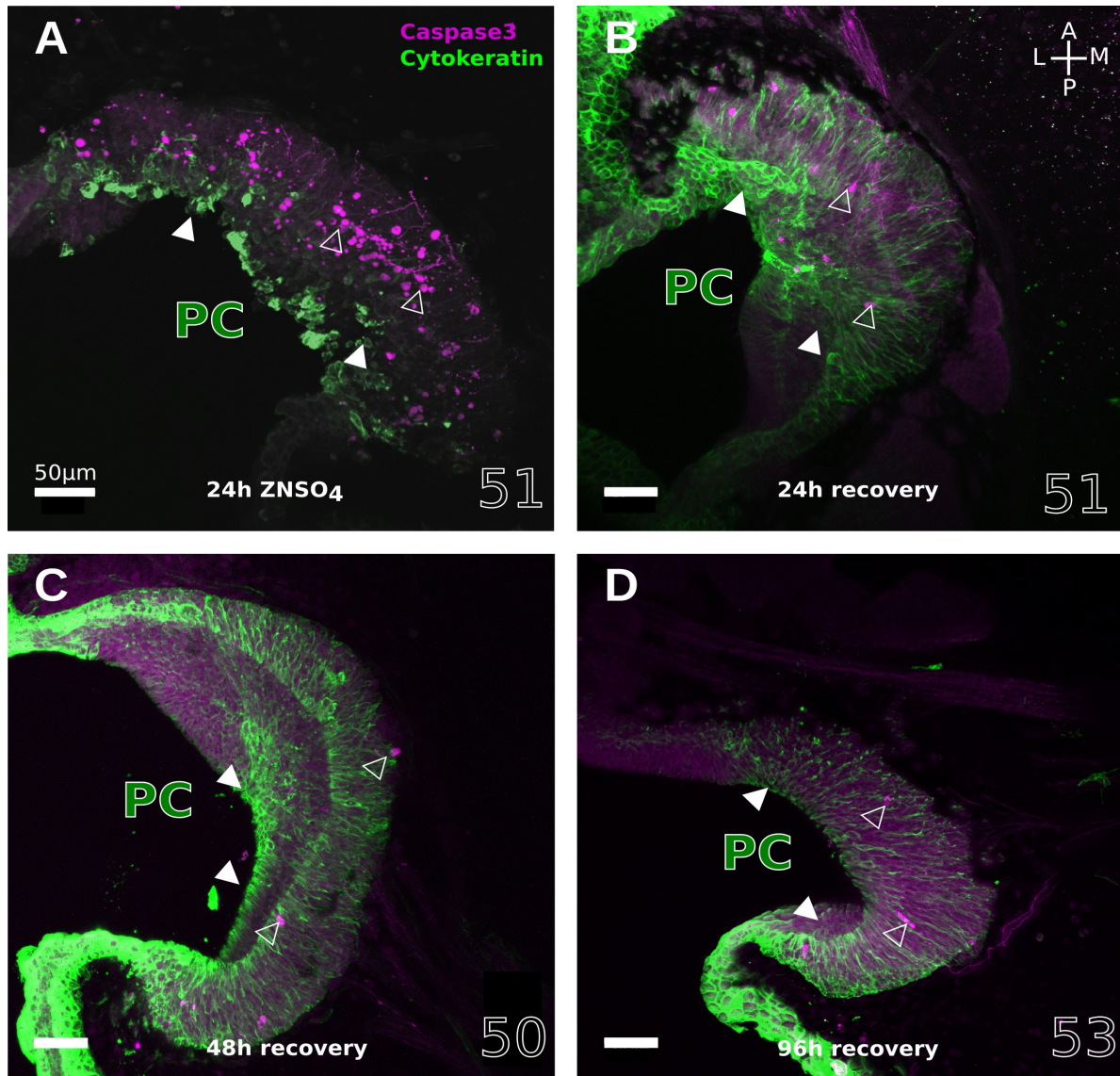
Figure 24. Distribution of active caspase 3 positive cells and cytokeratin type II positve cells after irrigation with ZnSO₄.

Maximum intensity projections of $ZnSO_4$ injured olfactory sensory epithelia sections of the principal cavity (PC) **A.** after 24 hours $ZnSO_4$ treatment, **B.** after 24 hours of recovery, **C.** after 48 hours of recovery and **D**. after 96 hours of recovery. Unfilled triangles indicate apoptotic cells (caspase 3 positive cells, shown in magenta). After 24 hours of $ZnSO_4$ treatment a high number of anti-active caspase 3 labeled cell bodies were located in the apical supporting cell layer and in the intermediate olfactory receptor neuronal layer. Filled triangles indicate cytokeratin type II supporting cells. A, anterior; P, posterior; M, medial; L, lateral. Numbers indicate the developmental stage. Numbers indicate the developmental stage.

I investigated anti-active caspase 3 immunoreactivity to assess the extent of cell death in the PC after $ZnSO_4$ treatment. The level of apoptotic cells was highly increased one day after

$ZnSO_4$ exposure. The apoptotic cells have the same blob-like structure as observed for active caspase 3 labeling during metamorphosis (Figure 23 A). Labeled cell bodies were distributed in all three layers of the pseudostratified sensory epithelium of the PC. A high amount of apoptotic cells was located in the apical supporting cell layer and in the intermediate ORN layer. Five days after $ZnSO_4$ treatment the number of active caspase 3 positive cells decreased back to that level of control tissues (Figure 24). Cytokeratin type II stainings were performed to observe morphological changes of supporting cells. I found that 24 hours of $ZnSO_4$ irrigation caused major changes in the morphology and structure of cells of the supporting cell layer (Figure 25 A). The entire layer looked detached and destroyed. Furthermore, the prolongations of the supporting cells no longer reached the basal lamina 96 hours after $ZnSO_4$ treatment the morphology of the supporting cell layer is comparable to healthy control tissues (Figure 23 B).
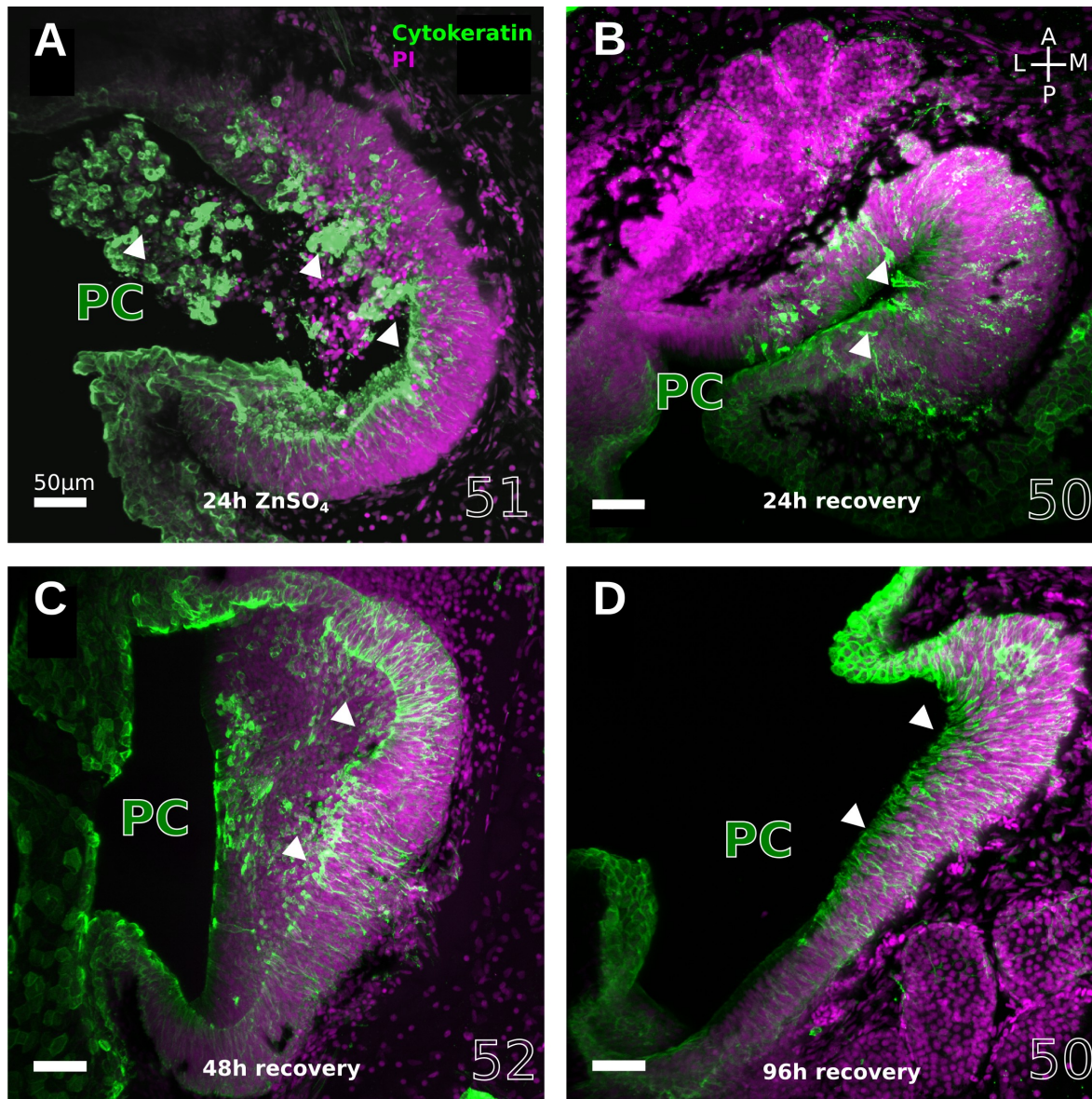
Figure 25. Distribution of cytokeratin type II positive cells after ZnSO₄ treatment.

Maximum intensity projections of ZnSO₄ damaged olfactory sensory epithelia of the sectioned principal cavites (PC).Cell nuclei were stained with propidium iodide. Filled triangles indicate cytokeratin type II positive cells (green) **A.** after 24 hours of ZnSO₄ treatment and **B**. after 24 hours of recovery, **C.** 48 hours of recovery and **D.** 96 hours of recovery. Cytokeratin type II positive cells (green) are indicated by filled triangles. The entire supporting cell layer looked detached and destroyed. Also the prolongations of the supporting cells did not reach the basal lamina of the olfactory epithelium. 96 hours after ZnSO₄ treatment the morphology of the supporting cell layer is comparable to control tissues. A, anterior; P, posterior; M, medial; L, lateral. Numbers indicate the developmental stage.

The population of ORNs was labeled via a biocytin backfill. 24 hours of ZnSO₄ treatment affected the morphology and the arrangement of ORNs (see Figure 26). Biocytin labeled ORNs seemed to be distributed in a unsorted manner when compared to the composition of

the ORN layer in control tissues (see Figure 23 C). 96 hours after $ZnSO_4$ treatment the sensory epithelium seemed to be intact again and ORNs resembled the morphology of control tissues (Figure 23 C).
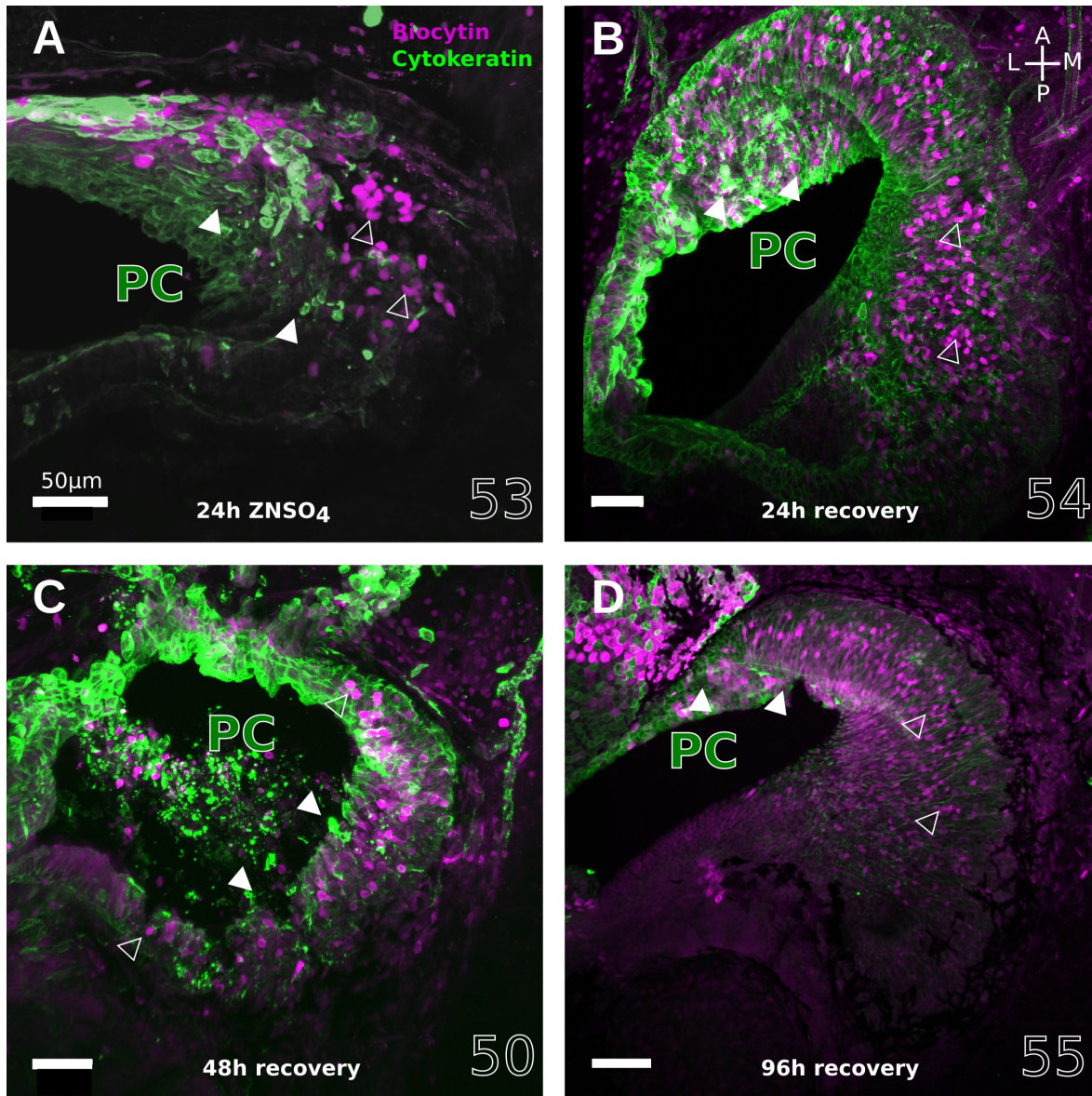
Figure 26. Distribution of biocytin backfilled olfactory receptor neurons and cytokeratin type II positive cells after $ZnSO_4$ treatment.

Maximum intensity projections of $ZnSO_4$ damaged olfactory sensory epithelia in sections of the principal cavity (PC). Biocytin labeled receptor neurons are shown in magenta and indicated with unfilled rectangles A. after 24 hours $ZnSO_4$ treatment and B. after 24 of recovery, C. 48 hours of recovery and D. 96 hours of recovery. The olfactory receptor neuronal layer looked disrupted and unsorted after 24 hours $ZnSO_4$ treatment. A morphology comparable to control tissue was reached 96 hours after $ZnSO_4$ treatment. Filled triangles indicate cytokeratin type II positive supporting cells (green fluorescence). A, anterior; P, posterior; M, medial; L, lateral. Numbers indicate the developmental stage.

Together these results indicate that a single exposure of $ZnSO_4$ caused significant but temporary damage to the olfactory sensory epithelium of the PC followed by a fast regeneration of the injured tissue. To analyze the correlation between the morphologically damaged structure after $ZnSO_4$ treatment and function of the PC, calcium imaging experiments were conducted. As stimulations, I applied a solution containing a purinergic receptor agonist, ATP, 2-MeSADP or 2-MeSATP to induce a specific response in non-neuronal cells (basal cells and supporting cells). These cells exhibit specific response profiles therefore allowing a clear distinction between the non-neuronal cell populations (Hassenklöver *et al.*, 2008, 2009) of basal cells and supporting cells. To observe a response in ORNs I applied a mixture of amino acids as well as a high K^+ bath solution to activate all ORNs. Unfortunately, the OE was disrupted after $ZnSO_4$ treatment. Under these circumstances it was not possible to fix the tissue under the grid in a way to successfully conduct experiments. Out of all analyzed animals it was not possible to get one positive recording of calcium signals. In summary, Ca^{2+} Imaging was not a successful method to study the functional changes after $ZnSO_4$ treatment.

To introduce a widespread cell degeneration in the main olfactory epithelium of larval *Xenopus laevis* Triton X-100 was applied to the nostrils (2.5.2). To observe morphological changes in the sensory epithelium of the PC after Triton X-100 treatment, I labeled apoptotic cells with an anti active caspase 3 antibody and supporting cells with a cytokeratin type II antibody (Figure 27). No changes in the structure of cytokeratin type II positive supporting cells were detected (Fig 27 A-D). The cell bodies of supporting cells are tightly arranged in an apical monolayer 24 hours, 48 hours, 72 hours and 168 hours after Triton X-100 treatment, comparable to control tissues. (Figure 27; for control tissue see, Figure 23 B). The number of active caspase 3 positive cells peaked two days after Triton X-100 treatment. Apoptotic cells have the same blob-like structure as observed for anti-active caspase 3 labeling during metamorphosis (see Figure 19 A). The majority of apoptotic cells was located in the intermediate ORN layer, indicating that Triton X-100 especially affects olfactory receptor neurons (Figure 27 B). 24 hours, 72 hours and 168 hours after Triton X-100 treatment the amount of anti-active caspase 3 positive cells was comparable again to the situation in control tissues (Figure 23 A). Supporting cells seemed not to be affected and stayed morphologically intact (Figure 23 B; Figure 27).
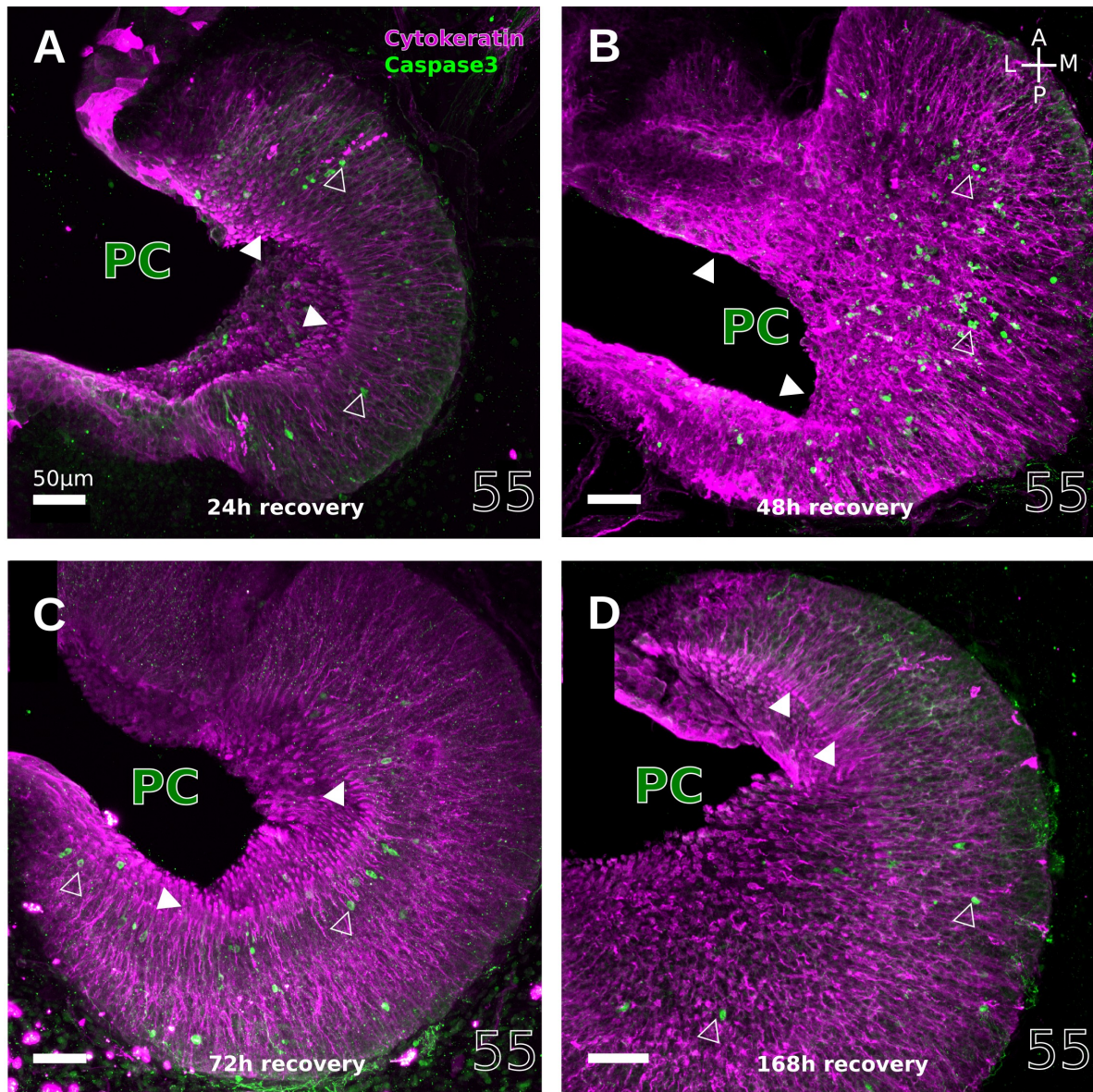
Figure 27. Distribution of active caspase 3 and cytokeratin type II positive cells after Triton X-100 treatment.

Maximum intensity projections of Triton X-100 damaged sectioned olfactory organs. Filled triangles indicate cytokeratin type II positive cells (green fluorescence) **A.** after 24 hours of recovery **B.** after 48 of recovery **C.** after 72 hours of recovery **D.** and 168 hours of recovery. Cytokeratin type II positive cells (green fluorescence) are indicated by filled triangles. The entire supporting cell layer looked unaffected. The number of apoptotic cells was highly increased after 48 hours of recovery. Maximum intensity projections of sections of the PC 24 hours, 72 hours and 168 hours after Triton X-100 treatment indicate a low number of caspase 3 positive cells comparable to sections of control animals. A, anterior; P, posterior; M, medial; L, lateral. Numbers indicate the developmental stage.

3.5.2 Introduction of a mechanical lesion by transection of the olfactory nerve

After the analysis of the morphology of the main olfactory epithelium after a chemical treatment I analyzed anatomical changes after mechanical lesions. I performed bilateral olfactory nerve transection to lesion especially the population of ORNs. To observe anatomical changes in the sensory epithelium of the PC after bilateral olfactory nerve transection, I stained apoptotic cells (see 2.2.2) and supporting cells (2.2.3, see Figure 28).
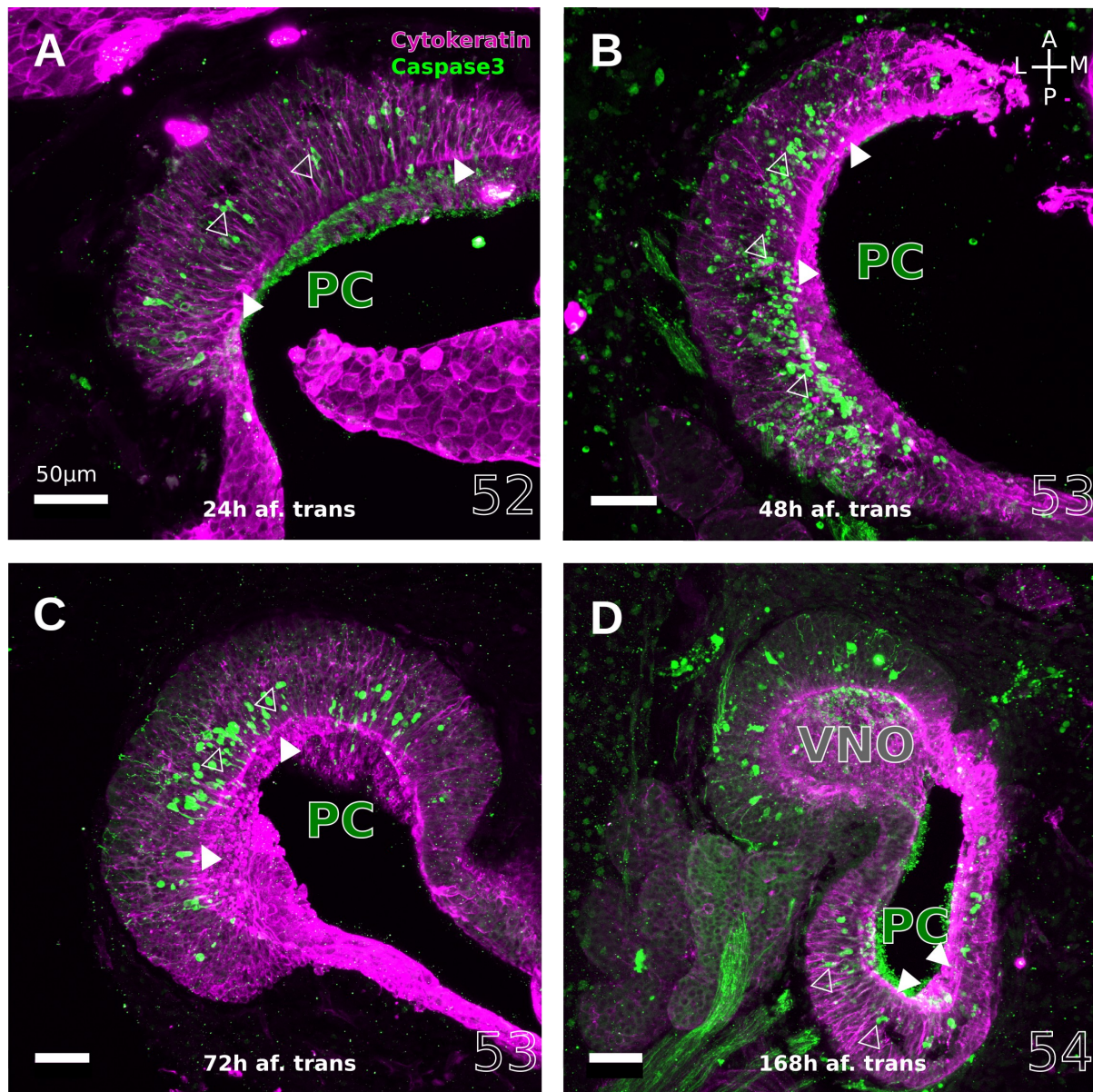

Figure 28. Distribution of active caspase 3 and cytokeratin type II positive cells after olfactory nerve transection.

Supporting cells (magenta, fillied triangles) and apoptotic cells (green, unfilled triangles) were labeled and investigated for anatomical changes post-transection.

A. 24 hours, **B**. 48 after, **C.** 72 hours and **D.** 168 hours after transection. Cytokeratin type II positive cells (green fluorescence) are indicated by filled triangles. The entire supporting cell layer looked unaffected. The number of apoptotic cells was increased the first 72 hours after bilateral transection. 168 hours after transection the amount of caspase 3 positive cells was comparable to healthy control tissues. A, anterior; P, posterior; M, medial; L, lateral. Numbers indicate the developmental stage.

I found no changes in the apical arrangement of labeled cell bodies of supporting cells. The whole supporting cell layer seemed unaffected. The typical cytokeratin type II labeled supporting cells were clearly detectable in control tissue (Figure 23 B) as well as after 24, 48 , 72 and 168 hours recovery. The amount of active caspase 3 positive cells was highly increased 24, 48 and 72 hours after olfactory nerve transection (Figure 28 A, B, C). The apoptotic cells had the same anatomy as observed for anti-active caspase 3 labeling during metamorphosis (see Figure 17). Labeled cell bodies were distributed in all three layers of the pseudostratified sensory epithelium of the PC. The majority of apoptotic cells was located in the intermediate ORN layer (Figure 28 B). 168 hours post transection the number of anti-active caspase 3 positive cells returned back to control levels (Figure 28 D). These results contributed to another study of our group. Calcium imaging experiments within this study conducted by Hawkins *et al.,* 2017 showed that the olfactory epithelium of the PC functionally recovered 168 days post bilateral transection. Additionally, in this set of experiments (Hawkins *et al.,* 2017) they established a timeline of post transectional degenerating events, until the point of recovery of the olfactory system.

Together these preliminary results indicate that in *Xenopus laevis*, a chemical degeneration of the sensory epithelium by $ZnSO_4$ treatment leads to tissue-wide degeneration of the main olfactory epithelium within 24 hours of $ZnSO_4$ treatment. Exposure to Triton X-100 or a bilateral transection of the olfactory nerves leads to severe injury of ORNs within the first three days following treatment, with peaked apoptotic cell death on the second day post injury. The morphology of the sensory epithelium of the PC seems to regenerate quickly and was comparable to the control situation 168 hours after a mechanical or chemical lesion. Experiments done by our group showed that the olfactory epithelium of the PC was functionally recovered 168 days post transection. The information obtained from the above described experiments were essential to isolate the tissue samples for RNA sequencing. Tissue samples of the entire nose and the whole olfactory bulb were isolated 48 hours after transection, to analyze the gene expression pattern at the time point of peaked apoptosis. Additionally, 168 hours after transection, after a recovery of the function and morphology of

the olfactory epithelium additional nose and bulb tissue samples were isolated. Also, tissue samples of both the olfactory bulb and the nose were isolated 49 days post transection to analyze the gene expression after glomerular clusters were reformed again (for detail see Hawkins *et al.*, 2017).

Therefore, degenerative nose and bulb tissue were extracted from bilaterally transected *Xenopus laevis* 48 hours after transection, 168 hours and 49 days after transection for RNA sequencing. Bulb tissue was extracted to compare the gene expression in the first relay station in control and regenerative tissue.

3.6 RNA sequencing

In total, I analyzed 39 samples (3 biological replicates per different conditions, see Table 1). A prepared principal component analysis (PCA) suggests that the samples of the 3 biological replicates of each condition are very similar, with respect to their gene expression (Figure 26). The PCA is a good way to identify patterns in a data set and helps to express this data in such a way as to point out their differences and similarities. One advantage is that once patterns in your data have been identified, you are able to compress the data i.e. by reducing the number of dimensions without losing much information. The PCA (Figure 26) indicates that all 3 biological replicates of one tissue sample group together. Remarkably, all samples of the olfactory bulb show a close similarity to each other as well as all samples of the nasal cavities. This points out that the preparation of all 39 samples was precise enough to allow further analysis. For further analysis of all genes expressed within the nose of *Xenopus laevis* we will perform a *de novo* transcriptome analysis (in cooperation with Prof. Alexander Goessmann, institute of bioinformatics and systems biology, JLU Gießen) because not all of the genes found are currently annotated or named in existing databases.
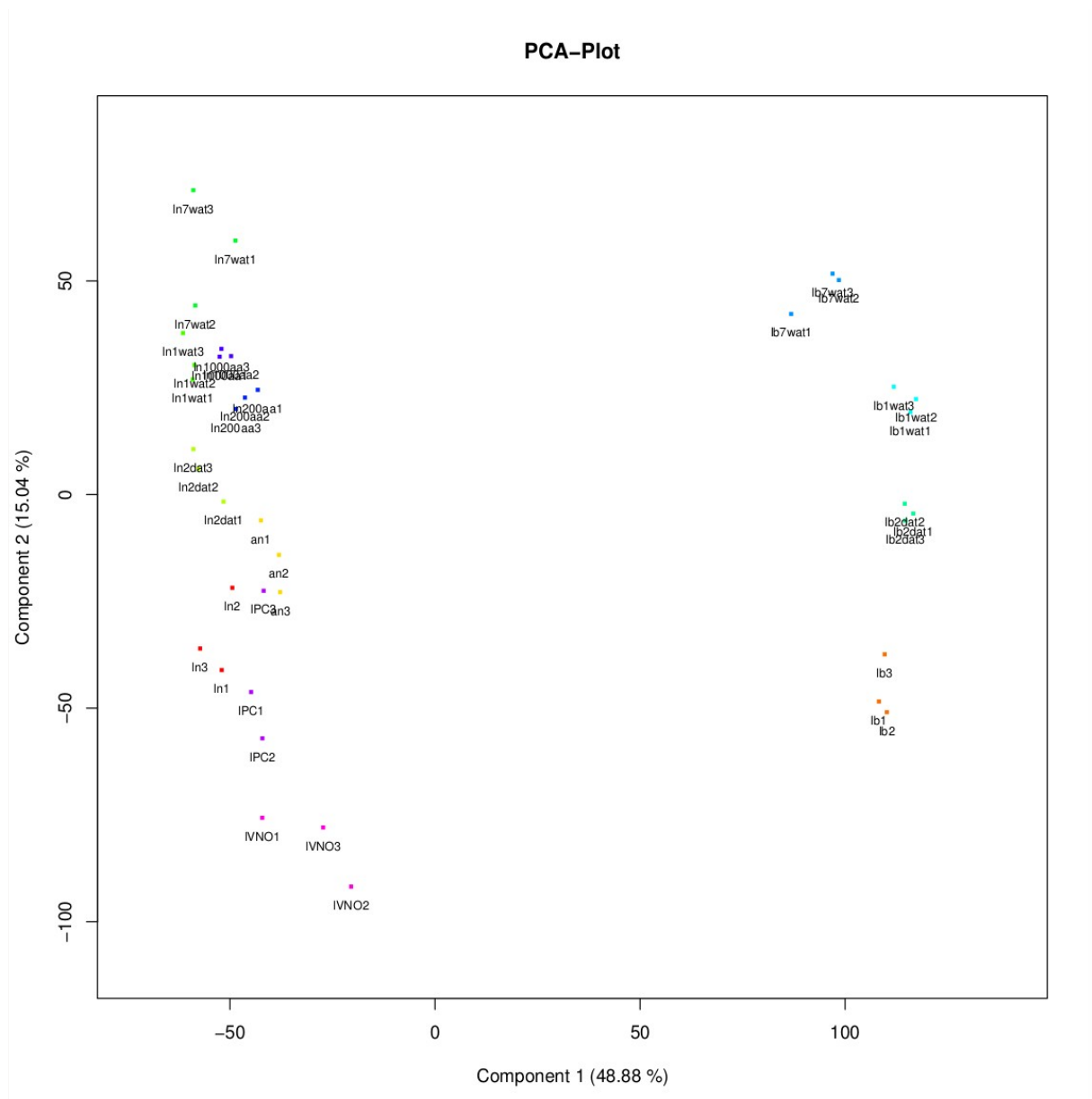
Figure 29. PCA (principal component analysis) of all conducted samples of three biological replicates.

an, adult nose; ln, larval nose; lPC, larval PC; lVNO, larval VNO; ln2dat, larval nose 2 days after transection; ln1wat, larval nose one week after transection; ln7wat, larval nose 7 weeks after transection; ln 200aa, larval nose 200 µM amino acid exposure for 5 hours, ln 1000aa, larval nose amino acid exposure 1000 µM for 5 hours; lb, larvalbulb; lb2dat, larval bulb 2 days after transection; lb1wat, larval bulb one week after transection; lb7wat, larval bulb 7 weeks after transection.

4. Discussion

During metamorphosis, most amphibians undergo fundamental changes from aquatic to a mostly terrestrial lifestyle. This extensive environmental change requires major morphological and physiological adaptations, including changes to sensory systems like the olfactory system (Reiss and Eisthen, 2008).

4.1 Morphological changes of the olfactory organ during metamorphosis

Xenopus laevis is a secondarily aquatic amphibian and is a suitable model to study developmental and functional aspects of the olfactory system. I conducted a detailed analysis of the metamorphotic remodeling of the *Xenopus laevis* olfactory organ. *Xenopus laevis*, like most amphibians has a vomeronasal organ (VNO) (Eisthen, 1992) in addition to the main olfactory epithelium in the principal cavity (PC; larval water nose). The epithelia of the olfactory organ consist of three main cell types: olfactory receptor neurons (ORNs) which transmit the olfactory information to the olfactory bulb, non-neuronal supporting cells that mostly cover glial-like functions and basal stem cells (Hassenklöver *et al.*, 2009). During premetamorphosis, at stage 51/52, a third sensory epithelium in the middle cavity (MC) arises (Hansen *et al.*, 1998b; Higgs and Burd, 2001). During prometamorphotic and metamorphotic stages a drastic reorganization of the epithelium in the PC takes place (Hansen *et al.*, 1998b; Higgs and Burd, 2001). After termination of metamorphosis, the postmetamorphotic frog has a tripartite olfactory organ consisting of the VNO, the reorganized PC (now an air nose) and the newly formed MC (adult water nose). Until now, it was unknown whether the MC is formed *de novo* or as a split-off of the larval epithelium of the PC. It has been suggested that at least a few cells originating in the PC are incorporated into the emerging MC (Higgs and Burd, 2001).

I was able to show that olfactory receptor neurons of the larval PC are not involved in the formation of the MC. Furthermore, I found that during formation of the MC, supporting cells of the larval PC are transitionally incorporated into the olfactory epithelium of the emerging MC. Nevertheless, these cells were eliminated during the growth of the MC. I can now

confirm that some supporting cells of the PC are taking part in the formation of the MC. ORNs of the larval PC are not involved in MC formation. However, it cannot be excluded that some olfactory receptor neurons are transitionally incorporated into the MC where they are quickly replaced (see Dittrich *et al.*, 2016).

Another open question is how the population of basal stem cells takes part in the *de novo* formation of the MC. As described in the results, the transition zone between the olfactory epithelium of the larval PC and the newly formed MC often contains unsorted ORNs, whose origin is unclear. It could be speculated that a stem cell niche is located within the transition zone, contributing to newly generating ORNs that either migrate to the PC or to the emerging MC. I observed that ORNs and supporting cells of the larval PC do not survive until postmetamorphosis. In my experiments I observed dextran particles in the epithelium of the PC. These particles are most likely remnants of those lost cells (Dittrich *et al.*, 2016). Supporting cells and macrophages are known to phagocyte dead cells and accordingly accumulate dextran labels (Suzuki *et al.*, 1996). Supporting cells of the larval PC and the MC can be either ciliated or secretory (Hansen *et al.*, 1998b). During metamorphosis ciliated supporting cells of the PC are sorted out (Oikawa *et al.*, 1998). A major reorganization of supporting cells in the olfactory epithelium is also illustrated by the fact that secretory supporting cells of the PC show morphological differences after metamorphosis (Hansen *et al.*, 1998b).

The extent of cellular reorganization of olfactory epithelia during metamorphosis differs in recent amphibians: anura (frogs and toads), caudata (salamanders and newts), and caecilians (Stuelpnagel and Reiss, 2005). The presence of both ciliated and microvillous sensory neurons in the main olfactory epithelium and only microvillous sensory neurons in the VNO seems to be characteristic for premetamorphotic anuran larvae (Taniguchi *et al.*, 1996; Hansen *et al.*, 1998b). After metamorphosis, the anuran PC has only ciliated sensory neurons, whereas the VNO does not change during metamorphosis (Taniguchi *et al.*, 1996; Hansen *et al.*, 1998). In all aquatic and terrestrial salamanders investigated so far, the main olfactory epithelium consists of both ciliated and microvillous sensory neurons in larval and adult animals (Eisthen *et al.*, 1994; Jones *et al.*, 1994; Reiss and Eisthen, 2008). In the neotenic *Ambystoma mexicanum*, these receptor cell types are distributed in non-overlapping clusters (Eisthen *et al.*, 1994). The adult caecilian *Typhlonectes compressicauda* features an antero-ventral and a

postdorsal compartment in the postmetamorphotic main olfactory epithelium endowed with ciliated/microvillous sensory neurons and solely ciliated sensory neurons, respectively (Saint Girons and Zylberberg, 1992). The life style of postmetamorphotic *Typhlonectes compressicauda* might have led to specialized olfactory epithelia for aquatic and aerial olfaction comparable to the situation in *Xenopus* and pipid frogs in general. Passage was taken from Dittrich *et al.,* 2016.

Previous studies have characterized distinct classes of olfactory and vomeronasal receptor neurons based on their expression of olfactory receptor families and the associated signal transduction cascades and morphology. ORNs of the larval main olfactory epithelium of *Xenopus laevis* express class I and class II olfactory type odorant receptors (ORs; Mezler *et al.,* 1999 and Gliem *et al.,* 2013) and trace amine associated receptors (TAARs; Gliem *et al.,* 2013). This expression pattern is comparable to the situation in mammals (Munger *et al.,* 2009). The distribution of the two vomeronasal receptor families, vomeronasal type-1 receptors (V1R) and vomeronasal type-2 receptors is not restricted to one olfactory epithelium and reflects the intermediate characteristics of the *Xenopus* olfactory system. In mammals, vomeronasal receptor type-2 receptors are expressed exclusively in the VNO. In contrast, in *Xenopus laevis* early diverging members of the V2R family are expressed in the larval main olfactory epithelium (Syed *et al.,* 2013). In *Xenopus* the expression of V1Rs is also restricted to the larval main olfactory epithelium (Date-Ito *et al.,* 2008; Gliem *et al.,* 2013). Vomeronasal receptor neurons of the larval VNO of *Xenopus laevis* express later-diverging V2Rs (Hagino-Yamagishi *et al.,* 2004; Syed *et al.,* 2013). In addition to cell reorganization during metamorphosis the expression pattern of olfactory receptors changes. The expression of class I and class II OR-type receptors shifts from the larval PC to the developed MC (Freitag *et al.,* 1995). Additionally, the V1R expression segregates predominantly to the adult MC and is not present in the adult PC (Date-Ito *et al.,* 2008). It was shown that in adult *Xenopus laevis* early diverging members of the V2R family are expressed in the MC and later-diverging V2Rs in the VNO (Syed *et al.,* 2013; Syed *et al.,* 2017).

The larval PC contains two morphological classes of ORNs (Gliem *et al.,* 2013; Syed *et al.,* 2013). Cilated ORNs expressing OR-type receptors transduce olfactory information via the canonical cAMP-mediated pathway (Liberles, 2014; Sansone *et al.,* 2014b). Olfactory receptor neurons expressing V1R and V2R initiate a phospholipase C/diacylglyerol-mediated

pathway which activates the Transient receptor potential cation channel, subfamily C, member 2 (TRPC2, Liberles *et al.,* 2014; Sansone *et al.,* 2014b). Sansone and colleagues showed that TRPC2 seems to be involved in mediating amino acid odorant responses of V2R-expressing cells. It is known that cells within the larval main olfactory epithelium responds to amino acids. Syed *et al.,* 2017 used calcium imaging experiments to examine whether cells of the adult PC are still responsive to amino acids. They found that the amino acid responses do not persist in the adult PC and that they migrate to the MC. Together these findings indicate that cellular reorganization of ORNs has an impact on the distribution of the amino acid responsive cells. It was also shown that the paired box protein Pax-6 plays a role in the establishment of both water-exposed epithelia, the larval PC and the new MC, but not in the metamorphotic reorganization of the PC (Franco *et al.,* 2001). These findings indicate that the postmetamorphotic MC is a replication of the larval PC and that a dramatic change in neuronal populations occurs in the metamorphotic PC. Interestingly, nearly nothing is known about mechanisms that are involved in the regulation of the onset of the outgrowth of the MC and reorganization of the PC. Passage was adapted from Dittrich *et al.,* 2016.

Analysis of RNA sequencing data from olfactory organ tissues of premetamorphotic and postmetamorphotic animals might offer the opportunity to study the olfactory receptor gene expression and associated pathways at the beginning and at the termination of metamorphosis.

As described above, during metamorphosis amphibians undergo a drastic remodeling of organs and tissues. Therefore, the number of well-coordinated apoptotic events increases in general (Ishizuya-Oka *et al.,* 2010; Exbrayat *et al.,* 2012). Apoptosis occurs in the mature as well as in the developing olfactory epithelium, and caspase 3 is a key enzyme involved in this process (Cowan and Roskams, 2002). The dramatic changes during prometamorphosis and metamorphosis are governed by the endogenous concentration of thyroid hormones (Just and Kraus-Just, 1996; Ishizuya-Oka *et al.,* 2010). The plasma concentration of thyroid hormones in *Xenopus laevis* increases at stages 57–59, reaches a maximum at stages 60–62, and declines toward complete tail loss of the animal (Just and Kraus-Just, 1996). As reported above ORNs and non-neuronal supporting cells of the larval PC cells do not survive metamorphosis. I quantified apoptosis and proliferation of cells in the different olfactory epithelia of the PC, MC and the VNO to obtain information about the degree of cell reorganization during metamorphosis. I observed that the PC shows some major changes in apoptotic activity during

metamorphotic remodeling (passage was adapted from Dittrich *et al.,* 2016).

The amount of caspase 3 positive cells increases at stage 59 and reaches a maximum at stage 62, which corresponds to the reported changes in concentrations of thyroid hormones (Just and Kraus-Just, 1996). This reflects the transformation of this epithelium in order to perform the task of air olfaction. Thus the hypothesis is supported that all former, premetamorphotic sensory neurons of the PC undergo apoptotic cell death and are replaced by sensory neurons with different properties, including different odor sensitivities. I found that the rate of apoptosis in the developing MC is less clearly related to metamorphosis. However, the MC features a significant increase of apoptosis at stage 59 that corresponds to a peak of apoptotic events in the PC. This indicates that, even in the newly formed MC, numerous cells are actively sorted out. Even during normal cell turnover some immature neurons, presumably due to axon misrouting or incorrect synaptic connections, regularly undergo apoptotic cell death in the olfactory epithelium (Holcomb *et al.,* 1995). Metamorphotic changes in other tissues of *Xenopus* show a time course that is roughly similar to the one I found in the PC. Apoptotic events in the anterior brain were detected at stages 55–63, peaking at stage 60 (Coen *et al.,* 2007) and cells of the intestinal epithelium are substituted at stages 60–62 (Ishizuya-Oka and Ueda, 1996). Even though the number of apoptotic cells in the VNO increases during development, I could not find any clear maxima connected to metamorphosis. This supports the view that the VNO is a stable structure throughout larval development and does not undergo major reorganization or rewiring during metamorphosis (Reiss and Burd, 1997; Higgs and Burd, 2001). Sparsely distributed caspase 3 positive cells at postmetamorphotic stages suggested that the turnover of neurons of the olfactory epithelia is not restricted to particular developmental stages. Passage was taken from Dittrich *et al.,* 2016. I conducted phospho-histone H3 stainings for the visualization of mitotic cells. Phospho-histone H3 positive cells were mainly located in the basal part of the olfactory epithelia. I found that the PC, MC and the VNO show the most prominent changes in proliferative activity at prometamorphotic stages (55-58). This suggests that major cell division started before the peak in the apoptotic rate was reached. This might be attributed to the fact that apoptosis and proliferation are well coordinated in order to maintain the sense of smell. Ishizuya-Oka (see review, 2011) described that cellular responses to thyroid hormone differ and depend on the cell-types. They showed that the intestinal epithelium of larval *Xenopus laevis* consists of larval-proper cells and adult progenitor/stem cells. After the onset of

metamorphotic climax (Ishizuya-Oka *et al.,* 2010) thyroid hormone initiates apoptosis in proper cells, whereas it induces cell proliferation of progenitor/stem cells (Ishizuya-Oka, 2011). The herein presented results might indicate a similar effect of thyroid hormone on cell apoptosis and proliferation in the olfactory epithelia of *Xenopus laevis*. At the moment nearly nothing is known about molecular mechanisms that are involved in the fine tuning of cell proliferation and cell death within the olfactory organ during the time course of metamorphosis.

4.2 Morphological and functional changes of the olfactory organ under regenerative conditions

It has been shown that the olfactory epithelium rapidly regenerates after chemical or mechanical lesions (Iqbal and Byrd-Jacobs, 2010) and that axons of ORNs reconnect to the olfactory bulb. It seems that the zonal pattern of olfactory receptor gene expression reemerges after specific (Gogos *et al.,* 2000) or general (Iwema and Schwob, 2003) lesions. However, not much is known about how accurately the expression of olfactory receptors by ORNs reestablishes. It is also not clear how accurately glomerular projections and response patterns to odorants recover. Together with Hawkins *et al.,* 2017 we studied the morphology and the functional recovery of the larval main olfactory epithelium after a bilateral transection of the olfactory nerve. Bilateral transection causes a disruption of the olfactory input to the olfactory bulb and therefore a loss of functional olfactory receptor neurons (Hawkins *et al.,* 2017). Axons of the peripheral nervous system in vertebrates have the capability to regrow after transection. Regenerating axons have their origin in the neuronal stem cells within the olfactory epithelium (Graziadei and Metcalf, 1971). The highest amount of apoptotic cells were visible within the first three days after transection. These were mainly located in the intermediate neuronal olfactory receptor layer, whereas the supporting cells were unaffected. Apoptosis of ORNs and proliferation of stem cells were immediately increased one day after transection. The entire morphology of the olfactory epithelium as well as the functionality of ORNs was recovered one week after treatment. As pointed out before, the morphological organization of the olfactory organ is defined by its precise anatomical and molecular specificity with respect to the expression of members of the main olfactory receptor families. It would certainly be interesting to see how morphological changes induced by injury are also

reflected by changes of the expression of the olfactory receptor families.

Hawkins *et al.,* 2017 showed that axonal projections of ORNs started to re-innervate the olfactory bulb again after the morphological and functional recovery of the olfactory epithelium. Additionally they analyzed whether odorant responses in the OB are restablished and found out that first odorant induced responses in the olfactory bulb were visible three weeks after transection. The whole olfactory network seems to be fully regenerated morphologically and functionally seven weeks post transection (Hawkins *et al.,* 2017). Previous studies showed that the glomerular map in mouse was poorly recovered after ORN transection (Costanzo, 2000; Christensen *et al.,* 2001). A single treatment with methimazole caused the loss of most mature ORNs, but in this case was followed by regeneration and the correct glomerular map was restored (Blanco-Hernández *et al.,* 2012). Preliminary results of my thesis showed that $ZnSO_4$ irrigation affects more than one cell type. A full recovery of the olfactory epithelium was reached seven days after treatment. The same effects of $ZnSO_4$ treatment were investigated and published by Frontera *et al.,* 2015.

At the moment nearly nothing is known about the glomerular re-innervation after a chemical lesion. It seems that larval *Xenopus laevis* has a higher regenerative capacity than mouse, most probably due to the mechanisms that regulate the drastic reorganization of cells within the olfactory epithelia during metamorphosis.

Previous studies of Hassenklöver *et al.,* 2008 and Hassenklöver *et al.,* 2009 indicated that puringergic signaling by supporting cells contributes to the cell turnover in the olfactory epithelium. It was demonstrated that the number of 2-MeSATP responsive basal cells increased after transection of the olfactory nerve. This fact supports the hypothesis that purinergic signaling is involved in the activation of proliferative cells after an injury (Hawkins *et al.,* 2017). We speculated that nucleotides released from damaged or dying ORNs in the apical part of the olfactory epithelium most probably initiate an activation of neighboring supporting cells. The supporting cells in turn transmit that information to the basal cells. However, sources of extracellular ATP and molecular mechanisms involved in communication between supporting cells and basal cells are still unknown. It was found that the expression of growth factor BDNF was increased after $ZnSO_4$ treatment, whereas no change of BDNF expression was observed after transection of the olfactory nerve (Frontera *et al.,* 2015 and Cervino *et al.,* 2017). It seems that transection induced injuries initiate other signaling mechanisms than $ZnSO_4$ irrigation, most probably due to their effect on different cell

populations.

It is still unknown, how signaling mechanisms by the local concentration of stimulating and inhibitory tissue-derived growth factors (Gokoffski *et al.,* 2010) are coordinated. It is also not known if purinergic signaling and mechanisms initiated by stimulatory and inhibitory factors co-exist and how they are regulated.

At last no conclusive answer about the contribution of these pathways during tissue maintenance and repair conditions is available. To identify possible pathways related to apoptosis and proliferation of cells, RNA samples of regenerated tissues were prepared and will be evaluated. High throughput signaling of transcriptomes (RNA sequencing) has the potential to rapidly and economically transform our knowledge on a molecular level. In the absence of a reference genome or when the reference genome is poorly annotated, *de novo* assembly of RNA-seq reads offers the opportunity to study the transcriptome of non annotated genomes. The analysis of *de novo* transcriptome assembly data is a nontrivial endeavor. It is associated with an optimized bioinformatics pipeline and quality controlled work to avoid falsely interpreted results.

This thesis provides a profound understanding of the morphological changes of the olfactory organ during metamorphosis and forms the basis for further studies on the functional and molecular changes over the time course of metamorphosis. Together, the presented results of this study combined with the work of Hawkins *et al.,* 2017 form the basis for further investigations of molecular changes that take place in degenerative and regenerative conditions.

Summary and future perspective

The results obtained within this thesis clearly demonstrate that the olfactory organ of *Xenopus laevis* is a valuable model to study neurogenesis during natural turnover, cell reorganization during metamorphosis and cell degeneration as well as regenerative processes after an injury.

1. When analyzing metamorphotic changes in the *Xenopus* olfactory system various important questions arise: how is this system reorganized and how is neuronal replacement coordinated. Staining of olfactory receptor neurons using Biocytin backfill labelings, as well as generating 3D reconstructions of the olfactory organ allowed me to follow the arrangement of ORNs throughout metamorphotic development of *Xenopus laevis*. A methodical combination of biocytin backfill labeling and bulk electroporation showed that the middle cavity (MC) is formed *de novo*, and does not form by splitting-off from the larval main epithelium (PC). Quantification of apoptotic and proliferating cells in the sensory olfactory epithelia led to the conclusion that major cell proliferation starts before the number of apoptotic cells reaches its peak. The well regulated reorganization of cells within the epithelia ensures structural stability and a functional sense of smell during metamorphosis. All results mentioned above describe morphological and functional changes of the olfactory organ during metamorphosis

In the future I will focus on the evaluation of RNA sequencing data, to study the pattern of olfactory receptor gene expression in premetamorphotic and postmetamorphotic animals to investigate differential olfactory receptor gene expression in the different nasal cavities.

2. Cells populations within the cavities of the olfactory organ are able to recover morphologically and functionally after injury. Our results showed that a bilateral transection of the olfactory nerve causes a degeneration of nearly all ORNs within the first three days following the injury. The entire main olfactory epithelium recovers functionally and morphologically 168 hours post transection. Furthermore, by using the RNA sequencing data I will try to study the changes in gene expression of important candidates of signaling mechanisms that regulate cell regeneration. At last I wish to investigate how accurately the olfactory receptor gene expression was restored within the olfactory epithelia.

5. References

Adrian ED. 1950. The electrical activity of the mammlian olfactory bulb. Electroencephalogr Clin Neurophysiol 2:377-388

Altman J and Das GD. 1965. Post-natal origin of microneurons in the rat brain. Nature 207:953-956

Avila VL and Frye PG. 1978. Feeding behaviour of the African Clawed frog (*Xenopus laevis* Daudin): effect of prey type. J Herpetol 12:391-396

Bergman U, Ostergren A, Gustafson AL and Brittebo B. 2002. Differential effects of olfactory toxicans on olfactory regeneration. Ach Toxicol 76:104-112

Bergström U, Giovanetti A, Piras E and Brittebo B. 2003. Methimazole-induced damage in the olfactory mucosa: effects on ultrastructure and glutathione levels. Toxicol Pathol 31:379-387

Blanco-Hernández E, Valle-Leija P, Zomosa-Signoret V, Drucker-Colín R and Vidaltamayo R. 2012. Odor memory stability after reinnervation of the olfactory bulb. PLoS One 7, e46338

Breipohl W, Laugwitz HJ and Bornfeld N. 1974. Topological relations between the dendrites of olfactory sensory cells and sustentacular cells in different vertebrates. An ultrastructural study. J Anat 117:89-94

Buck L and Axel R. 1991. A novel multigene family may encode odorant receptors: a molecular basis for odor recognition. Cell 65:175-87

Buckland ME and Cunningham AM. 1998. Alterations in the neurotrophic factors BDNF, GDNF and CNTF in the regenerating olfactory system. Ann NY Acad Sci 855:260-265

Caggiano M, Kauer JS and Hunter DD. 1994. Globose basal cells are neuronal progenitors in the olfactory epithelium: a lineage analysis using a replication-incompetent retrovirus. Neuron 13:339-352

Calof AL, Bonnin A, Crocker C, Kawauchi S, Murray RC, Shou J and Wu HH. 2002. Progenitor cells of the olfactory receptor neuron lineage. Microsc Res Tech 58:176-188

Cervino AS, Paz DA and Frontera JL. 2017. Neuronal degeneration and regeneration induced by axotomy in the olfactory epithelium of *Xenopus laevis*. Dev Neurobiol 77:1308-1320

Chen X, Fang H and Schwob JE. 2004. Multipotency of purified, transplanted globose basal cells in olfactory epithelium. J Comp Neurol 469:457-474

Christensen MD, Holbrook EH, Costanzo RM and Schwob JE. 2001. Rhinotopy is disrupted during re-innervation of the olfactory bulb that follows transection of the olfactory nerve. Chem

senses 26:359-369

Coen L, Le Blay K, Rowe I and Demeneix BA. 2007. Caspase-9 regulates apoptosis/proliferation balance during metamorphotic brain remodeling in *Xenopus*. Proc Natl Acad Sci USA 104:8502-8507.

Costanzo RM. 2000. Rewiring the olfactory bulb: changes in odor maps following recovery from nerve transection. Chem Senses 25:199-205

Cowan CM and Roskams AJ. 2002. Apoptosis in the mature and developing olfactory neuroepithelium. Microsc Res Tech 58:204-15

Czesnik D, Schild D, Kuduz J and Manzini I. 2007. Cannabinoid action in the olfactory epithelium. Proc Natl Acad Sci USA 104:2967-2972

Date-Ito A, Ohara H, Ichikawa M, Mori Y and Hagino-Yamagishi K. 2008. *Xenopus* V1R vomeronasal receptor family is expressed in the main olfactory system. Chem Senses 33:339-346

Dent JN. 1962. Limb regeneration in larvae and metamorphosing individuals of the South African clawed toad. J Morphol 110:61-77

Dittrich K, Sansone A, Hassenklöver T and Manzini I. 2014. Purinergic receptor-induced Ca^{2+} signaling in the neuroepithelium of the vomeronasal organ of larval *Xenopus laevis*. Purinergic Signal 10:327-336

Dittrich K, Kuttler J, Hassenklöver T and Manzini I. 2016. metamorphotic remodeling of the olfactory organ of the African clawed frog *Xenopus laevis*. J Comp Neurol 524: 968-998

Doetsch F, Caillé I, Lim DA, García-Verdugo JM and Alvarez-Buylla A. 1999. Subventricular zone astrocytes are neural stem cells in the adult mammalian brain. Cell 97:703-716

Eisthen HL. 1992. Phylogeny of the vomeronasal system and of receptor cell types in the olfactory and vomeronasal epithelia of vertebrates. Micros Res Tech 23:1-21

Eisthen HL, Sengelaub DR, Schroeder DM and Alberts JR. 1994. Anatomy and forebrain projections of the olfactory and vomeronasal organs in axolotls (*Ambystoma mexicanum*). Brain Behav Evol 44:108-124.

Endo T, Yoshino J, Kado K and Tochinai S. 2007. Brain regeneration in anuran amphibians. Dev Growth Differ 49:121-129

Exbrayat J-M, Moudilou EN, Abrouk L and Brun C. 2012. Apoptosis in amphibian development. Adv Biosci Biotechnol 3:669-678

Firestein S. 2001. How the olfactory systems makes sense of scents. Nature 413:211-218

Franco MD, Pape MP, Swiergiel JJ and Burd GD. 2001. Differential and overlapping expression patterns of X-dll3 and Pax-6 genes suggest distinct roles in olfactory system development of the African clawed frog *Xenopus laevis*. J Exp Biol 204:2049–2061.

Freitag J, Krieger J, Strotmann J and Breer H. 1995. Two classes of olfactory receptors in *Xenopus laevis*. Neuron 15:1383–1392.

Frontera JL, Cervino AS, Jungblut LD and Paz DA. 2015. Brain-derived neurotrophic factor (BDNF) expression in normal and regenerating olfactory epithelium of *Xenopus laevis*. Ann Anat 198:41-8

Frontera JL, Raices M, Cervino AS, Pozzi AG and Paz DA. 2016. Neural regeneration dynamics of *Xenopus laevis* olfactory epithelium after zinc sulfate-induced damage. J Chem Neuroanat 77:1–9

Furlow JD and Neff ESA. 2006. Developmental switch induced by thyroid hormone: *Xenopus laevis* metamorphosis. Trends in endocrinology and metabolism: TEM 17:40-47

Gage FH. 2000. Mammalian neural stem cells. Science 287:1433-1438

Garcia ADR, Doan NB, Imura T, Bush TG, Sofroniew MV. 2004. GFAP-expressing progenitors are the principal source of constitutive neurogenesis in adult mouse forebrain. Nat Neurosci 7:1233-1241

Getchell ML and Getchell TV. 1992. Fine structural aspects of secretion and extrinsic innervation in the olfactory mucosa. Microsc Res Tech 23:111-127

Gibbs KM, Chittur SV and Szaro BG. 2010. Metamorphosis and the regenerative capacity of spinal cord axons in *Xenopus laevis*. Eur J Neurosci 33:9-25

Gliem S, Syed AS, Sansone A, Kludt E, Tantalaki E, Hassenklöver T, Korsching SI and Manzini I. 2013. Bimodal processing of olfactory information in an amphibian nose: Odor responses segregate into a medial and a lateral stream. Cell Mol Life Sci 70:1965-1984

Gogos JA, Osborne J, Nemes A, Mendelsohn M and Axel R. 2000. Genetic ablation and restoration of the olfactory topographic map. Cell 103:609-20

Gokoffski KK, Kawauchi S, Wu HH, Santos R, Hollenbeck PLW, Lander AD and Calof AL. 2010. Feedback Regulation of neurogenesis in the mammalian olfactory epithelium: new insights from genetics and systems biology. In: Menini A, editor. The Neurobiology of Olfaction., Boca Raton (FL): CRC Press; Chapter 10

Gonzalez A, Morona R, López JM, Moreno N and Northcutt RG. 2010. Lungfishes, like tetrapods, posses a vomeronasal system. Front Neuroanat 4. pii: 130. doi:10.3389/fnana.2010.00130

Graziadei PP and Metcalf J. 1971. Autoradiographic and ultrastructural observations on the frog's olfactory mucosa. Z Zellforsch Mikrosk Anat 116, 305-318

Graziadei GA and Graziadei PP. 1979. Neurogenesis and neuron regeneration in the olfactory system of mammals. II. Degeneration and reconstitution of the olfactory sensory neurons after axotomy. J Neurocytol 8:197-213

Haberly LB and Price JL. 1977. The axonal projection patterns of the mitral and tufted cells of the olfactory bulb in the rat. Brain Res 129:152-157

Hamdani el H and Døving KB. 2007. The functional organization of the fish olfactory system. Prog Neurobiol 82:80-6

Hagino-Yamagishi K, Moriya K, Kubo H, Wakabayashi Y, Isobe N, Saito S, Ichikawa M and Yazaki K. 2004. Expression of vomeronasal receptor genes in *Xenopus laevis*. J Comp Neurol 472:246-256

Hansen A, Zeiske E. 1998a. The peripheral olfactory organ of the zebrafish, *Danio rerio*: an ultrastructural study. Chem Senses 23:39-48

Hansen A, Reiss JO, Gentry CL and Burd GD. 1998b. Ultrastructure of the olfactory organ in the clawed frog, *Xenopus laevis*, during larval development and metamorphosis. J Comp Neurol 398:273-288

Hassenklöver T, Kurtanska S, Bartoszek I, Junek S, Schild D and Manzini I. 2008. Nucleotide-induced Ca^{2+} signaling in sustentacular supporting cells of the olfactory epithelium. Glia 56:1614-1624

Hassenklöver T, Schwartz P, Schild D and Manzini I. 2009. Purinergic signaling regulates cell proliferation of olfactory epithelium progenitors. Stem Cells 27:2022-31

Hassenklöver T and Manzini I. 2014. The olfactory system as a model to study axonal growth patterns and morphology *in vivo*. J Vis Exp 92:e52143

Hawkins SJ, Weiss L, Offner T, Dittrich K, Hassenklöver T and Manzini I. 2017. Functional reintegration of sensory neurons and transitional dendritic reduction of mitral/tufted cells during injury-induced receovery of the larval *Xenopus* olfactory circuit. Front Cell Neurosci. 11:380

Hegg CC and Lucero MT. 2006. Purinergic receptor antagonists inhibit odourant-induced heat schock protein 25 induction in mouse olfactory epithelium. Glia 53:182-190

Hegg CC, Irwin M and Lucero MT. 2009. Calcium store-mediated signaling in sustentacular cells of the mouse olfactory epithelium. Glia 57:634-644

Higgs DM and Burd GD. 2001. Neuronal turnover in the *Xenopus laevis* olfactory epithelium during metamorphosis. J Comp Neurol 433:124-130

Holbrook EH, Szumowski KE and Schwob JE. (1995). An immunochemical, ultrastructural, and developmental characterization of the horizontal basal cells of rat olfactory epithelium. J Comp Neurol 363:129-146

Holcomb JD, Mumm JS and Calof AL. 1995. Apoptosis in the neuronal lineage of the mouse olfactory epithelium: regulation in vivo and in vitro. Dev Biol 172:307-323

Huard JM, Youngentob SL, Goldstein BJ, Luskin MB and Schwob JE. 1998. Adult olfactory epithelium contains multipotent progenitors that give rise to neurons and non- neural cells. J Comp Neurol 400, 469-486

Hussain A, Saraiva LR, Korsching SI. 2009. Positive Darwinian selection and the birth of an olfactory receptor clade in teleosts. Proc Natl Acad Sci USA 106:4313-8

Iqbal T and Byrd-Jacobs C. 2010. Rapid degeneration and regeneration of the zebrafish olfactory epithelium after triton X-100 application. Chem Senses 35:351-61

Ishizuya-Oka A and Ueda S. 1996. Apoptosis and cell proliferation in the *Xenopus* small intestine during metamorphosis. Cell Tissue Res 286:467-476

Ishizuya-Oka A, Hasebe T and Shi YB. 2010. Apoptosis in amphibian organs during metamorphosis. Apoptosis 15:350-364

Ishizuya-Oka A. 2011. Amphibian organ remodeling during metamorphosis: Insight into thyroid hormone-induced apoptosis. Develop Growth Differ 53:202-212

Iwai N, Zhou Z, Roop DR and Behringer RR. 2008. Horizontal basal cells are multipotent progenitors in normal and injured adult olfactory epithelium. Stem Cells 26:1298-306

Iwema CL and Schwob JE. 2003. Odorant receptor expression as a function of neuronal maturity in the adult rodent olfactory system. J Comp Neurol 459:209-22

Jones FM, Pfeiffer CJ and Asashima M. 1994. Ultrastructure of the olfactory organ of the newt, *Cynops pyrrhogaster*. Ann Anat 176:269-275

Just JJ and Kraus-Just J. 1996. Control of thyroid hormones and their involvement in haemoglobin transition during *Xenopus* and Rana metamorphosis. In: Tinsley RC, Kobel HR, editors. The biology of *Xenopus*. New York: Oxford University Press. P 213-229

Karlson P and Luscher M. 1959. Pheromones: a new term for a class of biologically active substances. Nature 183:55-6

Kermen F, Franco LM, Wyatt C and Yaksi E. 2013. Neural circuits mediating olfactory-driven behavior in fish. Front Neural Circuits 7:62

Komiyama T and Luo L. 2006. Development of wiring in the olfactory system. Curr Opin Neurobiol 16:67-73

Lazard D, Zupko K, Poria Y, Nef P, Lazarovits J, Horn S, Khen M and Lancet D. 1991. odourant signal termination by olfactory UDP glucuronosyl transferase. Nature 349:790-793

Leung CT, Coulombe PA and Reed RR. 2007. Contribution of olfactory neural stem cells to tissue maintenance and regeneration. Nat Neurosci 10:720-726

Liberles SD. 2014. Mammalian pheromones. Annu Rev Physiol 76:151-175

Ma L and Michel WC. 1998. Drugs affecting phospholipase C-mediated signal transduction block the olfactory cyclic nucleotide-gated current of adult zebrafish. J Neurophysiol 79:1183-1192

Ma M. 2010. Multiple olfactory subsystems convey various sensory signals. In: Menini A, editor. The Neurobiology of Olfaction. Boca Raton (FL): CRC Press; Chapter 9

Mackay-Sim A. 2010. Stem cells and their niche in the adult olfactory mucosa. Arch Ital Biol 148:47-58

Mackay-Sim A and Kittel PW. 1991. On the Life Span of Olfactory Receptor Neurons. Eur J Neurosci 3:209-215

Malnic B, Hirono J, Sato T, Buck LB. 1999. Combinatorial receptor codes for odors. Cell 96:713-23

Manzini I, Rössler W and Schild D. 2002a. cAMP-independent responses of olfactory neurons in *Xenopus laevis* tadpoles and their projection onto olfactory bulb neurons. J Physiol, 545:475-484.

Manzini I, Peters F and Schild D. 2002b. Odorant responses of *Xenopus laevis* tadpole olfactory neurons: a comparison between preparations. J Neurosci Methods 121:159-67

Manzini I and Schild D. 2003. Multidrug resistance transporters in the olfactory receptor neurons of *Xenopus laevis* tadpoles. J Physiol 546:375-385

Manzini I and Schild D. 2004. Classes and narrowing selectivity of olfactory receptor neurons of *Xenopus laevis* tadpoles. J Gen Physiol 123:99-107

Manzini I and Schild D. 2010. Olfactory coding in larvae of the african clawed frog *Xenopus laevis*. In: Menini A, editor. The Neurobiology of Olfaction. Boca Raton (FL): CRC Press; Chapter 4

Manzini I and Korsching SI. 2011. The peripheral olfactory system of vertebrates: molecular, structural and functional basics of the sense of smell. E-Neuroforum 2:68

Manzini I. 2015. From neurogenesis to neuronal regeneration: the amphibian olfactory system as a model to visualize neuronal development *in vivo*. Neural Regen Res 10:872-874

Mezler M, Konzelmann S, Freitag J, Rössler P, Breer H. 1999. Expression of olfactory receptors during development in *Xenopus laevis*. J Exp Biol 202:365-376

Mombaerts P, Wang F, Dulac C, Chao SK, Nemes A, Mendelsohn M, Edmondson J and Axel R. 1996. Visualizing an olfactory sensory map. Cell 87:675-86

Mombaerts P. 1999. Seven-transmembrane proteins as odorant and chemosensory receptors. Science 286:707-711

Mombaerts P. 2004a. Odorant receptor gene choice in olfactory sensory neurons: the one receptor-one neuron hypothesis revisited. Curr Opin Neurobiol 14:31-6

Mombaerts P. 2004b. Genes and ligands for odourant, vomeronasal and taste receptors. Nat Rev Neurosci 5:263-78

Munger SD, Leinders-Zufall T and Zufall F. 2009. Subsystem organization of the mammalian sense of smell. Annu Rev Physiol 71:115-140

Murdoch B and Roskams AJ. 2007. Olfactory epithelium progenitors: insights from transgenic mice and in vitro biology. J Mol Histol 38:581-599

Myatt DR, Hadlington T, Ascoli GA and Nasuto SJ. 2012. Neuromantic - from semi-manual to semi automatic reconstruction of neuron morphology. Front Neuroinform 6:4.

Nezlin LP and Schild D. 2005. Individual olfactory sensory neurons project into more than one glomerulus in *Xenopus laevis* tadpole olfactory bulb. J Comp Neurol 481:233-9

Nimmermark S. 2004. Odour influence on well-being and health with specific focus on animal production emissions. Ann Agric Environ Med 11:163-173

Nieuwkoop PD and Faber J. 1994. Normal table of *Xenopus laevis* (Daudin). New York: Garland Publishing Inc.

Niimura Y and Nei M. 2005. Evolutionary dynamics of olfactory receptor genes in fishes and tetrapods. Proc Natl Acad Sci USA 102:6039-44

Oikawa T, Suzuki K, Saito TR, Takahashi KW and Taniguchi K. 1998. Fine structure of three types of olfactory organs in *Xenopus laevis*. Anat Rec 252:301-310

Reiss JO and Burd GD. 1997. Metamorphotic remodeling of the primary olfactory projection in *Xenopus*: developmental independence of projections from olfactory neuron subclasses. J Neurobiol 32:213-222

Reiss JO and Eisthen HL. 2008. Comparative anatomy and physiology of chemical senses in amphibians. Sensory Evolution on the Threshold: Adaptations in Secondarily Aquatic Vertebrates, pages 43-63

Ressler KJ, Suillivan SL and Buck LB. 1994. Information coding in the olfactory system: evidence for a stereotyped and highly organized epitope map in the olfactory bulb. Cell 79: 1245-1255

Rivière S, Challet L, Fluegge D, Spehr M and Rodriguez I. 2009. Formyl peptide receptor-like proteins are a novel family of vomeronasal chemosensors. Nature 459: 574-7

Rolls ET. 2005. Taste, olfactory, and food texture processing in the brain, and the control of food intake. Physiol Behav 85:45-56

Ronnett GV and Moon C. 2002. G proteins and olfactory signal transduction. Annu Rev Physiol 64:189-222

Saint Girons H, Zylberberg L. 1992. Histologie comparée des glandes céphaliques exocrines et des fosses nasales des Lissamphibia. II. Épitheliums des fosses nasales. Ann Sci Nat Zool Biol Anim 13:121-145

Sansone A, Hassenklöver T, Syed AS, Korsching SI and Manzini I. 2014a. Phospholipase C and diacylglycerol mediate olfactory responses to amino acids in the main olfactory epithelium of an amphibian. PLoS One 9:e87721

Sansone A, Syed AS, Tantalaki E, Korsching SI and Manzini I. 2014b. Trpc2 is expressed in two olfactory subsystems, the main and the vomeronasal system of larval *Xenopus laevis*. J Exp Biol 217:2235-2238

Sato Y, Miyasaka N and Yoshihara Y. 2005. Mutually exclusive glomerular innervation by two distinct types of olfactory sensory neurons revealed in transgenic zebrafish. J Neurosci 25:4889-97

Scalia F and Winans SS. 1975. The differential projections of the olfactory bulb and accessory olfactory bulb in mammals. J Comp Neurol. 161:31-55

Schild D and Restrepo D. 1998. Transduction mechanisms in vertebrate olfactory receptor cells. Physiol Rev 78:429-466

Schindelin J, Arganda-Carreras I, Frise E, Kaynig V, Longair M, Pietzsch T, Preibisch S, Rueden C, Saalfeld S, Schmid B, Tinevez JY, White DJ, hartenstein V, Eliceiri K, Tomancak P and Cardona A. 2012. Fiji: an open-source platform for biological-image analysis. Nat Methods 28:676-82

Schwob JE and Youngentob SL. 1992. Reconstitution of the olfactory epithelium and reinnervation of the olfactory bulb after methyl bromide lesions. Chem Senses 17:696

Schwob JE, Youngentob SL, Ring G, Iwema CL and Mezza RC. 1999. Reinnervation of the rat olfactory bulb after methyl bromide-induced lesion: timing and extent of reinnervation. J Comp Neurol 412(3):439-57

Schwob JE. 2002. Neural regeneration and the peripheral olfactory system. Anat Rec 269:33-49

Schultz EF and Tapp JT. 1973. Olfactory control of behaviour in rodents. Psychol Bull 79:21-44

Shi P and Zhang J. 2009. Extraordinary diversity of chemosensory receptor gene repertoires among vertebrates. Results Probl Cell Differ 47:1-23

Stuelpnagel JT and Reiss JO. 2005. Olfactory metamorphosis in the coastal giant salamander (*Dicamptodon tenebrosus*). J Morphol 266:22-45

Su Y, Damjanovski S, Shi Y and Shi YB. 1999. Molecular and cellular basis of tissue remodeling during amphibian metamorphosis. Histol Histopathol 14:175-83

Suzuki Y, Takeda M and Farbman AI. 1996. Supporting cells as phagocytes in the olfactory epithelium after bulbectomy. J Comp Neurol 376:509-517

Syed AS, Sansone A, Nadler W, Manzini I and Korsching SI. 2013. Ancestral amphibian v2rs are expressed in the main olfactory epithelium. Proc Natl Acad Sci USA 110:7714-7719

Syed AS, Sansone A, Hassenklöver T, Manzini I, and Korsching SI. 2017. Coordinated shift of olfactory amino acid responses and V2R expression to an amphibian water nose during metamorphosis. Cell Mol Life Sci 74:1711–1719

Takahashi LK, Nakashima BR, Hong H and Watanabe K. 2005. The smell of danger: a behavioural and neural analysis of predator odour-induced fear. Neurosci Biobehav Rev 29:1157-1167

Taniguchi K, Saito S and Taniguchi K. 2011. Phylogenic outline of the olfactory system in vertebrates. J Vet Med Sci 72:139-47

Toida K, Kosaka K, Aika Y and Kosaka T. 2000. Chemically defined neuron groups and their subpopulations in the glomerular layer of the rat main olfactory bulb-IV. Intraglomerular synapses of tyrosine hydroxylase-immunoreactive neurons. Neuroscience 101:11-17

Tirindelli R, Dibattista M, Pifferi S and Menini A. 2009. From pheromones to behavior. Physiol Rev 89:921-56

Vassar R, Chao SK, Sitcheran R, Nuñez JM, Vosshall LB and Axel R. 1994. Topographic organization of sensory projections to the olfactory bulb. Cell 19:981-991

Vogler C and Schild D. 1999. Inhibitory and excitatory responses of olfactory receptor neurons of *Xenopus laevis* tadpoles to stimulation with amino acids. J Exp Biol 202:997-1003

Weth F, Nadler W and Korsching SI. 1996. Nested expression domains for odorant receptors in zebrafish olfactory epithelium. Proc Natl Acad Sci USA 93:13321-6

Yeomans MR. 2006. Olfactory influences on appetite and satiety in humans. Physiol Behav 87:800-804

Zardoya R and Meyer A. 2001. On the origin of and phylogenetic relationships among living amphibians. Proc Natl Acad Sci USA 98:7980-7383

Acknowledgements

First of all, I would like to thank my supervisor Prof. Ivan Manzini and Dr. Thomas Hassenklöver, for the scientific topic and the continuous support and help during my thesis.

Many thanks go to the whole group, especially to Lukas Weiss, Sara Joy Hawkins, Thomas Offner and Lukas Wichmann for their suggestions, advices, fruitful discussions and the friendly and lovely atmosphere in the lab. I would like to thank my thesis committee members Prof. Dr. Thomas Dresbach and Dr. Kristine Henningfeld for the helpful comments during the thesis committee meetings and also whenever I had questions. Special thanks go to Dr. Kristine Henningfeld who provided me the chance to isolate RNA of *Xenopus laevis* olfactory epithelium and the help with the analysis of sequencing data. My warmest thanks go to my family, who made this way possible and continuously encouraged and strengthened me.

Curriculum Vitae

Personal data

Name:	Katarina Dittrich
Date of Birth:	26.05.1989
Place of Birth:	Altdöbern
Phone:	+496419935261
E-mail:	Katarina.Dittrich@physzool.bio.uni-giessen.de
Nationality:	german

Education

since 04/2017	PhD thesis
	Department of Animal Physiology and Molecular Biomedicine
	Justus Liebig University Gießen
	Supervisor: Prof. I. Manzini
since 04/2014	PhD thesis
	Department of Neurophysiology and Cellular Biophysics
	Georg August University Göttingen
	member of the GGNB PhD program „Molecular Physiology of the Brain"
	Supervisor: Prof. I. Manzini
10/2012-09/2013	MSc thesis
	Department of neurophysiology and Cellular Biophysics
	Georg August University Göttingen
10/2011-09/2013	MSc Molecular Life Sciences
	Friedrich Schiller University Jena
10/2008-09/2011	BSc Biochemistry
	Friedrich Schiller University Jena

Publications

Hawkins Sara Joy, Weiss Lukas, Offner Thomas, Dittrich Katarina, Hassenklöver Thomas and Manzini Ivan. 2017. Functional reintegration of sensory neurons and transitional dendritic reduction of mitral/tufted cells during injury-induced recovery of the larval *Xenopus* olfactory circuit. Front Cell Neurosci 11:380. doi: 10.3389/fncel.2017.00380

Dittrich Katarina, Kuttler Joshua, Hassenklöver Thomas and Manzini Ivan.
metamorphotic remodeling of the olfactory organ of the African clawed frog, *Xenopus laevis*.
J Comp Neurol 524:986-98, 2016

Dittrich Katarina, Sansone Alfredo, Hassenklöver Thomas and Manzini Ivan. 2014. Purinergic receptor-induced Ca^{2+} signaling in the neuroepithelium of the vomeronasal organ of larval *Xenopus laevis*. Purinergic Signal 10:327-36